STUDY OF *Leucaena leucocephala* SEED BIOMASS AS A NEW SOURCE FOR CELLULOSE

MARYAM HUSIN

FACULTY OF SCIENCE
UNIVERSITY OF MALAYA
KUALA LUMPUR

2019

STUDY OF *Leucaena leucocephala* SEED BIOMASS AS A NEW SOURCE FOR CELLULOSE

MARYAM HUSIN

THESIS SUBMITTED IN FULFILMENT OF THE REQUIREMENTS FOR THE DEGREE OF DOCTOR OF PHILOSOPHY

INSTITUTE OF BIOLOGICAL SCIENCES
FACULTY OF SCIENCE
UNIVERSITY OF MALAYA
KUALA LUMPUR

2019

UNIVERSITY OF MALAYA

ORIGINAL LITERARY WORK DECLARATION

Name of Candidate: **MARYAM HUSIN**

Matric No: **SHC140054**

Name of Degree: **DOCTOR OF PHILOSOPHY (EXCEPT MATHEMATIC & SCIENCE PHILOSOPHY**

Title of Project Paper/Research Report/Dissertation/Thesis ("this Work"):

STUDY OF *Leucaena leucocephala* SEED AS A NEW SOURCE FOR CELLULOSE

Field of Study: **BIOCHEMISTRY**

I do solemnly and sincerely declare that:

(1) I am the sole author/writer of this Work;
(2) This Work is original;
(3) Any use of any work in which copyright exists was done by way of fair dealing and for permitted purposes and any excerpt or extract from, or reference to or reproduction of any copyright work has been disclosed expressly and sufficiently and the title of the Work and its authorship have been acknowledged in this Work;
(4) I do not have any actual knowledge nor do I ought reasonably to know that the making of this work constitutes an infringement of any copyright work;
(5) I hereby assign all and every rights in the copyright to this Work to the University of Malaya ("UM"), who henceforth shall be owner of the copyright in this Work and that any reproduction or use in any form or by any means whatsoever is prohibited without the written consent of UM having been first had and obtained;
(6) I am fully aware that if in the course of making this Work I have infringed any copyright whether intentionally or otherwise, I may be subject to legal action or any other action as may be determined by UM.

Candidate's Signature Date:

Subscribed and solemnly declared before,

Witness's Signature Date:

Name:

Designation:

STUDY OF *Leucaena leucocephala* SEED AS A NEW SOURCE FOR CELLULOSE

ABSTRACT

Leucaena leucochephala is a tropical tree with many uses in which the application is primarily for wood production and the seeds for animal feed. The high growth rate and relatively abundant availability of *Leucaena leucocephala* make it suitable as a source for various applications such as production for energy, source of polysaccharides, livestock fodder, paper production, erosion control, and shade. Limited research has been conducted on *Leucaena leucocephala* seeds (LLS) due to more focus given to the wood parts for paper and pulp production. Therefore, the main objectives of this research are to optimize cellulose production with respect to the conditions used during the isolation process. Then, the feasibility of using cellulose as new source for the bioethanol application is evaluated. In general, lignocellulosic biomass is processed for bioethanol production through four major operations which are pretreatment process to remove hemicellulose and lignin, hydrolysis of cellulose or hemicellulose to produce sugar monomer, fermentation to convert sugars to ethanol, and separation or purification. The experimental result showed that boiling water under reflux can be considered as one of the cost effective and environmentally friendly methods to disrupt and remove some non-cellulosic compound. Isolation of cellulose by acid method is simple and fast compared to the alkaline method which is time consuming and requires bleaching step. Cellulose from LLS has been successfully isolated by using 80% acetic acid and 65% nitric acid to yield 33% cellulose. Microcrystalline and cellulose nanocrystals were further prepared from the LLS-cellulose via the acid hydrolysis method and yielded 71% and 27% respectively. The physicochemical and structural properties of the produced materials were characterized using Fourier-transform infrared spectroscopy (FTIR), morphology of the materials by field emission scanning electron microscopy (FESEM), cellulose crystallinity index (CI) by x-ray diffractometer (XRD), thermal stability behavior by

thermal gravimetric analysis (TGA), and differential scanning calorimetry (DSC). Based on the characteristics of micro and nano cellulose isolated, they could be used as precursors for other industrial applications such as fillers in bio composite. In the next step, the cellulose obtained was converted into glucose by dilute acid hydrolysis using sulphuric acid by varying the concentration, volume, and reaction time. Sugar composition was analyzed using the phenol-sulfuric acid method and pre-column derivatization HPLC techniques. The yield of glucose ranging from 70 – 85 % could be obtained from cellulose isolated from waste seeds of *Leucaena leucocephala*. Response surface methodology (RSM) was used for modelling and optimization of ethanol production from glucose obtained from LLS by *Saccharomyces cerevisiae*. Interaction of three independent variables, pH of media (4.0-5.5), volume of inoculumn (8-14 ml), and fermentation time (48-168 hr) in the batch fermentation was investigated. The optimization condition for bioethanol production from *Leucaena leucocephala* seeds was found with inoculum volume of 12.92 ml, pH of solution at 4.87, and fermentation time of 117.68 hr with predicted bioethanol yield of 22.18% and volume 9.89 ml.

Keywords: *Leucaena leucocephala*, seeds, cellulose, acid hydrolysis, bioethanol.

KAJIAN TERHADAP BIOJISIM BIJI BENIH *Leucaena leucocephala* SEBAGAI SUMBER BARU SELULOSA

ABSTRAK

Leucaena leucocephala adalah sejenis tumbuhan tropika yang mempunyai banyak kegunaan terutamanya bagi penghasilan produk berasaskan kayu dan makanan ternakan. Kadar pertumbuhan yang tinggi dan kewujudannya yang dominan menyebabkan *Leucaena leucocephala* sesuai digunakan sebagai sumber untuk pelbagai kegunaan antaranya penghasilan tenaga, sumber penghasilan polisakarida, makanan ternakan, penghasilan kertas, kawalan hakisan dan naugan. Kurang penyelidikan dijalankan ke atas biji *Leucaena leucocephala* (LLS) disebabkan terlalu banyak fokus diberikan kepada bahagian batang bagi penghasilan kertas dan pulpa. Sehubungan itu, objektif utama penyelidikan ini adalah untuk mengoptimumkan penghasilan selulosa bergantung kepada pembolehubah yang digunakan semasa proses pemencilan. Kemudian, kebolehlaksanaan selulosa sebagai sumber baharu untuk penghasilan bioethanol akan dinilai. Secara umumnya, biojisim lignoselulosa diproses bagi penghasilan bioethanol menerusi empat peringkat utama iaitu proses perawatan bagi menyingkirkan hemiselulosa dan lignin, hidrolisis selulosa dan hemiselulosa bagi menghasilkan gula monomer, fermentasi bagi menukarkan gula kepada etanol dan pemisahan atau penulenan. Keputusan kajian menunjukkan rawatan menggunakan air panas adalah menjimatkan dari segi kos dan mesra alam untuk menggangu dan menyingkirkan sebilangan bahan bukan selulosa. Pengasing selulosa mengunakan kaedah asid adalah mudah dan pantas berbanding dengan kaedah menggunakan alkali di mana ia memakan massa dan memerlukan langkah pelunturan. Selulosa yang dihasilkan daripada LLS telah dipencilkan dengan jayanya dengan mengunakan campuran 80% asid asetik dan 65% asid nitrik dengan peratus penghasilannya 33%. Lanjutan daripada itu mikrokristal dan nano selulosa telah dihasilkan daripada selulosa LLS menerusi kaedah hidrolisis dengan peratusan 71% dan 27% masing-masing. Ciri-ciri fisiokimikal dan struktur bagi produk yang telah dihasilkan

telah ditentukan menggunakan spektroskopi infra merah jelmaan fourier (FTIR) morfologi bahan-bahan menguna pancaran medan mikroskop pengimbas elektron (FESEM), indek pengkristalan selulosa mengunakan meter pembelauan x-ray (XRD), kestabilan sifat terma yang diukur oleh penganalisa permeteran graviti haba (TGA) dan permeteran kalori pengimbasan kebezaan (DSC). Beradasarkan sifat-sifat mikro dan nano selulosa yang telah dipencilkan, ianya sangat berpotensi digunakan sebagai asas bagi pelbagaian kegunaan industi seperti bahan pengisi dalam bio komposit, Kemudiannya, selulosa yang telah diperolehi telah ditukarkan kepada glukosa dengan hidrolisis asid cair menggunakan asid sulfurik pada pelbagai kepekatan, isipadu dan masa tindakbalas. Komposisi gula telah dianalisa menggunakan kaedah fenol-asid sulfuric dan teknik terbitan pra-kolum HPLC. Peratusan penghasilan glukosa di dalam julat antara 70-85% telah diperolehi daripada MCC yang telah dipencilkan daripada sisa biji *Leucaena leucocephala*. Akhir sekali, kaedah respon permukaan (KRP) digunakan untuk penghasilan etanol yang optimum daripada glukosa yang diperolehi dari LLS oleh Saccharomyces cerevisiae. Interaksi tiga pembolehubah dalam proses penapaian telah dijalankan iaitu pH media (4.0-5.5), jumlah inokulumn (8-14 ml) dan masa penapaian (48-168 jam). Kondisi optimum untuk penghasilan ethanol telah diperolehi pada jumlah inokulum 12.92 ml, pH larutan pada 4.87 dan masa fermentasi 117.68 jam, beserta jangkaan hasilan bioetanol 22.18% dan isipadu 9.89 ml.

Kata kunci: *Leucaena leucocephala*, biji benih, selulosa, asid hidrolisis, bioethanol.

ACKNOWLEDGEMENTS

In the name of Allah, the Most Gracious and the Most Merciful. Alhamdulillah, all praises to Allah for His blessings which enabled me to complete this thesis.First of all, I would like to express my utmost appreciation to my main supervisor, Dr. Zul Ilham Zulkiflee Lubes for his guidance, support, and motivating advice throughout my study. Very special thanks go to Dr. Rasadah Mat Ali for allowing me to use the facilities at Polysaccharide Research Lab, Forest Research Institute Malaysia (FRIM).

This study would not have been possible without the funding from the University of Malaya with the following grants, PG101-2015A. I would also like to acknowledge my sponsorship of study from Universiti Teknologi MARA (UiTM) Malaysia and MOE (Ministry of Education-High Education).

Special appreciation is dedicated to the laboratory staff from the Polysaccharide research lab, Natural Products Division, Forest Research Institute Malaysia (FRIM), especially Mr. Mohd Khair, Mrs. Nurul Nadiah, and Mrs. Suhaina for their valuable help and support on the completion my research work.

I also convey my thanks to all my colleagues and friends who gave me their words of encouragement and motivated me to finish my research. Not forgetting the members of Biomass Energy Lab, Fadhilah, Atiqurahman, and Idham Hakimi. There are many good memories with you all; thank you for everything.Words cannot express how thankful I am to my beloved family for always being my strength and inspiration. I could not complete this thesis without plentiful support from my husband, Abd Rashid Li.

TABLE OF CONTENTS

LIST OF FIGURES

LIST OF TABLES

LIST OF SYMBOLS AND ABBREVIATIONS

α	:	Alpha
β	:	Beta
ʎ	:	Lambda
θ	:	Theta
%	:	Percentage
°C	:	Degree celsius
°C/min	:	Degree celcius per minute
^{13}C	:	Carbon-13
µl	:	Microliter
µm	:	Micrometer
Adjusted R^2	:	Adjusted of coefficient of determination
AFEX	:	Ammonia fiber explosion
AFM	:	Atomic force microscope
ANNOVA	:	Analysis of variance
ASTM	:	American society for testing and materials
BNC	:	Bacterial nanocellulose
C	:	Carbon
Ca	:	Calsium
CCD	:	Centered composite design
C_6H_5OH	:	Phenol solution
CI	:	Crystallinity index
CLLS	:	Cellulose from mature seed of *Leucaena leucocephala*
cm	:	Centimeter
cm^2	:	Centimeter square
cm^3/min	:	Cubic centimeter per minute

CNN	:	Nanocrystalline cellulose
CNF	:	Cellulose nanofibrils
CNC	:	Cellulose nanocrystal
Cu	:	Copper
Da	:	Dalton
DF	:	Degree of freedom
DP	:	Degree of freedom
DSC	:	Differential scanning calorimeter
F	:	Feasible
Fe	:	Ferum
FESEM	:	Field emission scanning electron microscopy
FTIR	:	Fourier transform liquid chromatography
g	:	Gram
g/l	:	Gram per liter
g/Kg	:	Gram per kilogram
GPC	:	Gel permeation chromatography
HCL	:	Hydrochloric acid
HMF	:	Hydroxymethylfurfural
HPLC	:	High performance liquid chromatography
hr	:	Hour
H_2SO_4	:	Sulphuric acid
ICP	:	Inductively coupled plasma
K	:	Potassium
KBr	:	Kalium bromide
kGy	:	Kilogray
kV	:	Kilovolt

LLS	:	*Leucaena leucocephala* seeds
M	:	Molarity
mA	:	Miliampere
MCC	:	Microcrystalline cellulose
MCC-OELLS	:	Microcrystalline cellulose from residue of LLS after oil extraction
MCC-PELLS	:	Microcrystalline cellulose from residue of LLS after polysaccharide extraction
MFC	:	Microfibrillated cellulose
Mg	:	Magnesium
mg	:	Miligram
min	:	Minute
MLLS	:	Microcrystalline cellulose of *Leucaena leucocephala* seeds
ml	:	Mililiter
ml/min	:	Mililiter per minute
Mn	:	Manganese
mol/l	:	Mol per liter
MPa	:	Megapascal
MS	:	Mean square
MSLL	:	Mature seed of *Leucaena leucocephala*
N	:	Normality
Na	:	Sodium
$NaOCl_2$	:	Sodium chlorate
NaOH	:	Sodium hydroxide
NCC	:	Nanocellulose
NF	:	Not feasible
NFC	:	Nanofibrillated cellulose
NH_2CONH_2	:	Urea

NLLS	:	Nanocellulose from *Leucaena leucocephala* seeds
nm	:	Nanometer
NMR	:	Nuclear magnetic resonance
OELLS	:	Residue of LLS after oil extraction
P	:	Predicted value
PDA	:	Potato dextrose algae
PDB	:	Potato dextrose broth
PELLS	:	Residue of LLS after polysaccharide extraction
pKa	:	Acid dissociation constants
Predicted R^2	:	Predicted of coefficients of determination
R^2	:	Coefficients of determination
RLLS	:	Residual seed of *Leucaena leucocephala*
rpm	:	Revolutions per minute
RSM	:	Response surface methodology
SEM	:	Scanning electron microscope
SHF	:	Separate hydrolysis and fermentation
SPSS	:	Statistical package for the social sciences
SS	:	Sum of square
SSF	:	Simultaneous scarification and fermentation
T	:	Temperature
TAPPI	:	The Technical Association of Pulp and Paper Industry
TEM	:	Transmission electron microscope
TGA	:	Thermal gravimetric analysis
T_{max}	:	Maximum degradation temperature
V	:	Verification value
v/v	:	Volume per volume

wt%	:	Weight percentage
w/v	:	Weight per volume
w/w	:	Weight per weight
X_1	:	pH of solution
X_2	:	Inoculumn volume
XRD	:	X-ray diffraction
Y_1	:	Volume ethanol
Y_2	:	Concentration ethanol
Zn	:	Zinc

LIST OF APPENDICES

CHAPTER 1: INTRODUCTION

1.1 Background of study

Biofuels, generally represented by biodiesel and bioethanol, are liquid fuels derived from renewable biomass. The production of the first generation biofuels came from food-based feedstock such as sugar cane, sugar beet, corn, wheat, and oil seed rape, while the sources for the second and third generation are mostly non-edible and have substantial amount like agricultural residues, waste, algae, cellulosic materials, and lignocellulosic biomass (Chinwan & Pant, 2014). One of the main debates on bioethanol is the increasing production of the first generation bioethanol in relation to raising the food prices. Therefore, the utilization of lignocellulosic biomass as sustainable alternative substrates for bioethanol production has attracted more attentions.

Lignocellulose is the key structural element of plants and is found in roots, stalks, seeds, and leaves at various compositions. Generally, it is composed of three major components: cellulose (38–50%), lignin (15–30%), hemicellulose (23–32%), and a small amount of pectin, protein, extractives, and ash (Kopania *et al*., 2012). Cellulose and hemicellulose are the major components of plant biomass. Cellulose and hemicellulose are polysaccharides with long chains of monosaccharides linked by glycosidic bonds. Cellulose is made up of main glucose as its monomer, while the main sugar in hemicellulose is xylose, arabinose, mannose, and galactose. Cellulose is a renewable biopolymer resource that has high potential as a raw material for sustainable production which can be obtained abundantly in nature, is relatively cheap, and biodegradable (Duff & Murray, 1996; Kalia *et al*. 2011; Jose *et al*., 2014).

Cellulose can be extracted in different methods, many studies have been reported on the removal of hemicelluloses and lignin by using an alkaline solution such as sodium hydroxide (NaOH) and followed by bleaching (Bhattacharya *et al.*, 2008; Elanthikkal *et*

al., 2010; Chirayil *et al*., 2014; Le Normand *et al*., 2014). Bian *et al*. (2012) used sodium chlorite and potassium hydroxide. Nazir *et al*. (2013) employed a mixture of formic acid and hydrogen peroxide. This study has focused on using mixture of acid for isolation and purification of cellulose. Cellulose can be converted into sugar alcohol, oxygenated bio oil, and hydrocarbon by various chemical treatment methods and can be further utilized for the production of variety of valuable chemicals such as glucose, sorbitol, and Hydroxymethylfurfural (HMF) (Karim Ghani *et al.,* 2008). Cellulose is widely used in many aspects and industries such as food industry, pharmaceutical, paint, polymers, and more.

Due to the increasing demand in the market, studies and work to produce cellulose are still rapidly developing. Thus, in this study, isolation of pure cellulose from the uncommon plant source followed by the hydrolysis of their cellulose to glucose will be carried out. The cellulose hydrolyzates will further be fermented to bioethanol using *Saccharomyces cerevisiae*. Various sources of plant have been studied for isolation of cellulose and further used to produce microcrystalline cellulose (MCC) and nanocrystal, oil palm mass residue (Soom *et al*., 2009; Johar *et al*., 2012; Haafiz *et al*., 2013), jute (Jahan *et al*., 2011), banana plant waste (Elanthikkal *et al*., 2010), bagasse, and rice straw (El-Sakhawy & Hassan, 2007; Ilindra & Dhake, 2008; Nuruddin *et al*., 2011), wheat straw, corn stalks, dhaincha (Nuruddin *et al*., 2011; Mendes *et al*., 2015), kenaf (Wang *et al*., 2010), alfa (Trache *et al*., 2014), cotton stalks (El-Sakhawy & Hassan, 2007), soybean hull (Merci *et al*., 2015), tomato peel (Jiang & Hsieh, 2015), and pineapple leaf (Cherian *et al*., 2011). MCC is commercially available in different grades (purity and sizes) and has been used as a source for cellulose nanocrystal (CNN).

Hydrolysis of sugar from lignocellulosic biomass can be done by chemical and enzymatic methods; the yield varies depending on the type of biomass due to different cell wall compositions and structure, the type of monosaccharides and lignin present, and

the type of bonds between them. Extensive research has been completed on hydrolysis cellulose from rice straw, sugarcane bagasse, cotton cellulose, and corn stalk (Zhu *et al*., 2005; Punsuvon *et al*., 2008; Li *et al*., 2012; Yoon *et al*., 2014). Chemical hydrolysis method is the most common method used to break the β-1,4-glycosidic bonds of the cellulose structure by using different kinds of acids such as hydrochloric acid, sulphuric acid, hydrofluoric, and organic acids (Dussán *et al*., 2014). The interest toward acid hydrolysis for cellulosic materials for glucose conversion was applied in application in industrial production almost a century ago. Acid hydrolysis can be considered environmentally friendly because the formation of salt after neutralization can be separated by using alcohol and the alcohol used can further be recovered. The types of acid (e.g. sulphuric, hydrochloric, phosphoric) and salt (e.g. sodium chloride, sodium hydroxide) used will determine the types of salt formed. It can be sodium chloride, sodium phosphate or calcium sulphate. However, this salt needs to be removed from the sugar hydrolyzated because it acts as inhibitor during the fermentation process (Wei *et al*.,1982; Almagro *et al*., 2000; Shokoohi *et al*., 2015;). In addition, the work by Casey *et al*. (2013) reported that the growth of *Saccharomyces cerevisiae* and the ethanol yielded were more affected in the presence of chloride ion as compared to sulphate ion.

Recently, hydrolysis methods of cellulose to glucose using subcritical, hot compressed water, supercritical as well as combination of both have been intensively investigated and developed (Kamio *et al*., 2008; Cardenas-toro *et al*., 2014; Iryani *et al*., 2014) to increase the yield and reduce the time of hydrolysis processes. Despite the techniques proposed used green solvent and gave a high yield of glucose, they are not however practical to be industrialized because the reaction requires high temperature (normally above 150°C) and high pressure. The genus comprises about 32 different species of the family *Fabaceae* (Pandey & Kumar, 2013). It is available abundantly and distributed in most of the tropical areas of the world. Like other energy crops, *Leucaena leucocephala* consists of cellulose,

hemicellulose, and lignin (Jiménez *et al*., 2007; Feria *et al*., 2011). These compositions in biomass vary depending on the energy crops types and species due to genetic and environmental influences. Further, species of *leucaena* and cultivation factor (Chotchutima *et al*., 2013) will give a different chemical composition (Díaz *et al*., 2007), biomass productivity, and profitability (Mullen & Gutteridge, 2002).

An analysis of *Leucaena leucocephala* wood indicates that its main constituents are cellulose (40–47 %), hemicellulose (15-24%), and lignin (25-33%) (Saxena *et al*., 2009; López *et al*., 2010). Extensive research studies concerning the influence of plantation to the biomass yield (Al-Mefarrej *et al*., 2011; Chotchutima *et al*., 2013) and utilization of *Leucaena* as a raw material for pulping, energy crop, pharmaceutical product, and animal feeding have been done (López *et al*., 2008; Aderibigbe *et al*., 2011; Meena Devi *et al*., 2013). However, research on *Leucaena*'s varieties for its potential as a feedstock for energy purposes is less. Its biomass is being manipulated mainly for paper production. A variety of crops is currently being studied for biomass feedstock and energy production. Starch and sugar-based feedstocks have been proven successful for the production of bioethanol. The use of fruit seeds as a mainstream feedstock for bioethanol production is limited due to competition with food and feed. Therefore, due to increasing demand for both energy and food, the use of non-edible fruit seeds is an attractive starting material that can be utilized for bioethanol production.

1.2 Problem statement

Although the potential supply of lignocellulosic biomass is greater on woody plants than food crops, the main usage for bio-based chemical production is still based on the latter. When food crops with high sugar or starch such as sugarcane and corn are used, the total production cost will be high due to the high demand of these crops for food. The search for new alternative energy sources that are cheap, renewable, and do not create

environmental pollution has generated a great number of studies. Therefore, the supply of lignocellulosic biomass from non-food crop such as *Leucaena leucocephala* is essential. There are a few studies related to the seeds of this plant. Although the content of cellulose is not high in seeds compared to the wood, the amount of plant seeds is however considerably huge. The seed sources are sustainable and until now, no bioethanol production from this source has been reported. Studies associated to the uses of the seeds are more related to animal forages. *Leucaena leucocephala* seeds, which can be eaten by humans and animals but are not recommended for high consumption due to their toxic component, are known as mimosine (Aderibigbe *et al*., 2011). The seeds generally contain large amounts of protein, polysaccharides, and minerals. The oil content in *Leucaena leucocephala* seeds is the range 6% and 15% (Rao *et al*., 1984; Ahmed *et al*., 2009).

Cellulose isolated from biomass waste such as rice husk, oil palm residues, and sugarcane bagasse has been studied (Bhattacharya *et al*., 2008; Johar *et al*., 2012; Hafiz *et al*., 2014). Furthermore, water hyacinth (*Eichhornia crassipes*) and black grape peels (*Vitis vinifera L*.) have been evaluated as lignocellulosic feedstock for the production of sugar. However, such information is very limited for *Leucaena leucocephala* seeds (LLS). Ethanol production from LLS is a relatively new topic and therefore, the present study will investigate the potential of LLS as a source of cellulose and glucose for bioethanol.

In another aspect, the extraction of fruit and seed for commercial production such as juice, sauce, ketchup, puree, paste, or canned has commonly produced insoluble residual or waste (Kumar & Venkatesh, 2014). Sometimes, the amount of waste produced is higher than the amount being consumed. Seeds of *Leucaena leucocephala* have been evaluated for biodiesel and pharmaceutical products (Aderibigbe *et al*., 2011; Nehdi *et al*., 2014; Hakimi *et al*., 2017). Depending on the seeds, discarding this material generates

an environmental impact not only due to its toxicity such as *jatropha* (Parawira, 2010), but also due to the high produced volume. It is necessary to propose an adequate use for these cakes/residuals and one of the potential alternatives is by extracting the valuable products with high commercial values such monosaccharides and lignin. Thus, it can maximize the value derived from the biomass feedstock. The current practice of waste from fruit and seed extraction is utilized as animal feed. However, they can be also consumed for ethanol production (Izmirlioglu & Demirci, 2012).

1.3 Objectives of study

The current study aims to develop an efficient and feasible method for ethanol production from lignocellulosics. The finding of this research will help to create a new raw material to replace a sugar-based crop. In order to achieve this aim, various investigations have to be done to develop an effective utilization of *Leucaena leucocephala* seeds for bioenergy application as listed below.

1. To develop a simple and effective process to remove the non-cellulosic components for cellulose purification completely or partially.
2. To characterize properties of micro and cellulose nanocrystals produced from *Leucaena leucocephala* seeds.
3. To determine the influence of acid hydrolysis factors (acid concentration and reaction time) on the yield of glucose hydrolyzate produced from cellulose.
4. To optimize the production of bioethanol from glucose hydrolyzate using response surface methodology.

1.4 Scope of study

Leucane leucochephala can be one of the most potential sources of renewable energy to replace starch and agro-sugar feedstock. The advantages of using plant seeds of *Leucaena leucocephala* for energy production are the availability of feedstock, sustainable, non-food source, and high growth rate. This study aimed to develop effective processes to isolate pure cellulose from mature seeds of *Leucaena leucocephala* (MSLL) followed by disintegration to microcellulose and cellulose nanocrystals via acid hydrolysis. Pure cellulose was first isolated from mature seed of *Leucaena leucocephala* with a one-step treatment, 80% acetic acid 65% nitric acid mixture under reflux condition for 1 hr. The isolation method was adapted based on original procedures (Bian *et al*., 2000; Sun *et al*., 2004) with some modifications. Further, the cellulose as micro and nano were characterized by using various analyses to differentiate them. Cellulose, micro cellulose, and nano-cellulose obtained were analyzed to evaluate the applicability for glucose conversion. It will helpful to understand the applicability and effectiveness of glucose production from non-sugar source. Finally, the glucose derived from MSLS was used for conversion to bioethanol using fermentation. The study also included the optimization of glucose production from MSLS. Optimization will be done using the Response Surface Methodology (RSM) based on the Centered Composite Design (CCD) technique.

CHAPTER 2: LITERATURE REVIEW

2.1 *Leucaena leucocephala*

Leucaena leucocephala, belonging to the legume family of *Fabaceae*, is native to Southern Mexico and Northern Central America. It grows widespread throughout the tropic and subtropics. The genus *Leucaena* belongs to family *Fabaceae* and sub-family Mimosoideae and includes about 32 species. The three most important species of this genus are *Leucaena leucocephala* (Lam.) de Wit. or *Acacia leucocephala* (Lam.), *Mimosa leucocephala* (Lam.), and *Leucaena glabrata* (Rose) (Pandey & Kumar, 2013).

Leucaena is a fast growing tree which can be grown in all types of soils. It can rise up more than 20 m height in two to three years. Fruit is a pod of 12-14 cm long, turning brown with maturity and containing about 15-20 seeds (Nwokocha *et al*., 2012). Seeds are green when immature and turn dark brown with hard shining seed coat. The seeds are sustainable due to flowers; immature and mature pods are present on the tree at the same time. The plant is spread by scattered seeds, via birds, rodents, and cattle.

In Malaysia, it is commonly known as *Petai belalang*. In other places of the world, it is has various names such as horse tamarind, lead tree, *leucaena*, white lead-tree, white popinac, wild tamarind in English, and *kubabul* and *subabul* in India (Meena Devi *et al*., 2013; Pandey & Kumar, 2013). Other names include *ipil ipil*, *kariskis*, *palo-maria faux mimosa*, *kladingan*, *lamtoro, tagarai krathin*, and *to-bao*. Various parts of *Leucaena leucocephala* are widely used for a variety of purposes such as firewood, fiber, energy, cellulose pulp, and livestock fodder. Figure 2.1 shows the image of *Leucaena leucocephala*.

Figure 2.1: Image of *Leucaena leucocephala*.

Leucaena species is growing naturally in most tropical areas, abundantly available, a fast growing tree, and has sustainable resource. The tree can be used as a shade tree and prevention of slope failure (Normaniza *et al.*, 2008). In addition, almost all parts of this species can be utilized for marketable products such as feed, materials, chemicals, fuels, power, and heat. Nehdi *et al*. (2014) suggested that the large scale uses *Leucaena leucocephala* seed oil in the cosmetics and pharmaceutical industries. Linoleic acid form of fatty acid and antioxidant from the seed was reported to possess significant improvement to the cosmetic and pharmaceutical products. This is also corroborated by the work of Aderibigbe *et al.* (2011), who conducted experimental studies to identify the quality of lotion formulated from *Leucaena leucocephala* seed oil as one of the ingredients.

A recent study has revealed that *Leucaena leucocephala* seeds were used as substrates for solid state fermentation (Singh *et al*., 2014). In India, Thailand, and Indonesia, the young pods and seeds are eaten as a cooked vegetable or eaten raw as a salad. Further, leaves and seeds are used as one of the sources for livestock feeding. The seeds of

Leucaena leucocephala consist of hull (43.48–48.89%), endosperm (51.11–56.52%), and negligible germ (Nwokocha & Williams, 2012). The seeds' endosperm contain water soluble polysaccharides about 4–25% of a galactomannan (Nwokocha & Williams, 2012; Rahim *et al*., 2017) subjected to the efficiency purification process. The seeds are also found to contain anti-nutrient and toxic factors such as oxalic acid, phytic acid, tannins saponins, and haemagglutinins (Sethi & Kulkarni, 1994).

In addition, the various plant parts have been reported to contain protein (Singh *et al*., 2002; Kang *et al*., 2012), mimosine (Yeung *et al*., 2002), tocopherol (Nehdi *et al*., 2014) and condensed tannin (Abu Zarin *et al.*, 2016). The leaves and seeds have a toxic component (mimosine) that is not safe for extensive animal consumption. Several studied showed that different effect on consumption of *Leucaena leucocephala* in the animal diet in the ratio between to 5% to 40% dry weight depending on animal species (Zayed *et al*., 2018). The high growth rate and relatively abundant availability of *Leucaena leucocephala* make it suitable as a source for various applications such as production for energy, source of polysaccharides, livestock fodder, paper production, pulping and papermaking, erosion control, and shade. Table 2.1 shows *Leucaena leucocephala* suits a wide range of uses.

Table 2.1: Applications of *Leucaena leucocephala*.

Part	Isolation product	Findings	References
Seeds	Gum	The seed gum exhibit good quality and comparable to standard pharmaceutical binder.	Deodhar *et al*. 1998
		Leucaena seed gum can be used commercially as an adjuvant for pharmaceutical and non- pharmaceutical products.	Verma and Razdan, 2002
	Protein source	The inclusion of up to 50% *Leucaena* seeds, as protein source had no adverse effect on Dry Matter Intake (DMI), nutrient utilization, eating patterns, nitrogen balance and growth performance of lambs.	Singh *et al*. 2002
	Mimosine	Mimosine was found in all plant parts of *Leucaena* and the quantity of mimosine varied among the plant parts. In general, the young plant parts provided a greater amount of mimosine than the mature parts, except for the mature seeds.	Yeung *et al*. 2002
	Seed extracted (water, hot water and ethanol)	Mature seed extract showed the varying antioxidative activity, depending upon the type of extraction solvent and method of drying used	Benjakul *et al*. 2012
	Galactomannan	The yield of the water soluble polysaccharide from *Leucaena* seed was about 9% having with a molecular weight (Mw) $5.44 \pm 0.020 \times 10^5$ g/mol.	Nwokocha and Williams, 2012
		The yield of the water soluble polysaccharide from *Leucaena* seed was about 4% having a mannose/galactose ratio of 1.1.	Shirajuddin *et al*. 2015
	Methanol seeds extracted	The seed extract from *Leucaena leucocephala* exhibits antidiabetic and antioxidant activities by significantly decreasing the blood glucose level.	Chowtivannakul *et al*. 2016
	Oil	The study showed that *Leucaena leucocephala* seed oil extract had good pharmaceutical properties.	Aderibigbe *et al*. 2011
		Leucaena leucocephala seed oil has a good quality with a pleasant odor, showed a very high content of tocopherols and α-tocopherol content.	Nehdi *et al*. 2014

Table 2.1, Continued

Part	Isolation product	Findings	References
Bast/branch wood	Cellulose pulp	*Leucaena diversifolia* grown for 2 years was found to be the most suitable choice for obtaining pulp and paper among the five *Leucaena* varieties examined.	López *et al*. 2011
		Leucaena leucocephala has proved a suitable raw material for hemicellulose derivatives and a solid phase for producing cellulose pulp.	Feria *et al*. 2012
	Energy	The autohydrolysis of *Leucaena leucocephala* K366 provides industrially useful liquor due to its contents in xylose, xylo-oligomers and various other compounds. Also, its autohydrolysis solid phase can be used to obtain other chemicals or directly burnt for energy production.	Feria *et al*. 2011
		Bio-oil derived from pyrolysis of the *Leucaena leucocephala* trunks were mainly composed of methoxy phenol derivatives, acetophenone and dicarboxylic acids.	Payormhorm *et al*. 2013
Leaves	Animal fodder	*Leucaena leucocephala* leaf could be used as a protein source, while the combination of *Leucaena leucocephala* leaf and *cassava* could enhance the voluntary feed intake, nutrient digestibility and rumen fermentation in swamp buffalo fed.	Kang *et al*. 2012
		Supplementation of *Leucaena* leaf pellet resulted in the improvement of nitrogen balance and microbial nitrogen supply.	Hung *et al.* 2013
	Mimosine	Soxhlet extraction by using water as a solvent gave more mimosine extract compared using ethyl acetate.	Ilham *et al*. 2015
	Condensed tannins	The condensed tannins extracted from *Leucaena leucocephala* hybrid-Rendang can be used to discover the bioactive natural product that may serve as a leads in the development of new pharmaceuticals in food and as potent antimicrobial and cytotoxic agent.	Abu Zarin *et al*. 2016

2.2 Lignocellulose sources

Feedstocks for bioethanol production from biomass are classified into three categories of agricultural raw material: simple sugars or sucrose-containing feedstock, starch, and lignocellulose. Among these materials, lignocellulose is the most promising feedstock due to its availability, low cost advantage, and it lessens the conflict in the use between food and energy.

Lignocellulose is a complex carbohydrate polymer that mainly consists of cellulose, hemicellulose, and lignin. The composition of these compounds varies from one biomass to another depending on their source such as maturity, origin, and species (Table 2.2). Cellulose, the major constituent of all plant materials, is a linear and homopolymer composed of repeating sugar units of glucose linked by β-1,4 glycosidic bonds (Mood *et al.*, 2013).

Cellulose and hemicelluloses are sources of carbohydrate polymer bonded together with lignin that form a complex structure. Hemicellulose is a highly branched polymer that consists of heteropolymer of D-xylose, D-glucose, D-arabinose, D-mannose, and D-galactose. Lignin is cross-linked phenolic polymers and is tightly bound in the cell wall along with cellulose and hemicellulose. Syringyl, guaiacyl, and p-hydroxy phenol are the main units of a lignin macromolecule (Watkin *et al*., 2015).

Lignocellulosics are processed for bioethanol production through four major operations: pretreatment process to remove hemicellulose and lignin, hydrolysis of cellulose or hemicellulose to produce sugar monomer, fermentation and separation or purification. Pretreatment is the most important step to maximize the cellulose yield. It decreases the crystallinity of cellulose and enhances the biodegradability of cellulose during hydrolysis with increased yields of monomeric sugars.

Table 2.2: Analysis of lignocellulosic material feedstocks.

Part	Material	Percentage (%)		
		Cellulose	**Hemicellulose**	**Lignin**
Shell	Almond	27.0	27.0	27.2
	Coconut	24.2	24.7	34.9
	Kukui nut	14.6	12.3	60.1
	Macadamia nut	26.9	17.8	40.1
	Pecan	5.6	3.8	70.0
	Walnut	21.0	18.8	32.7
Wood	Alder	32.3	23.5	24.8
	Birch	35.7	25.1	19.3
	Eucalyptus	43.0	13.2	25.3
	Leucaena	40.8	15.0	26.9
	Oak	34.5	18.6	28.0
	Pine	42.1	17.7	25.0
	spruce	41.1	20.9	28.0
Residue	Corncob	26.3	25.2	16.3
	Garlic	24.3	6.9	8.5
	Rice hull	30.9	16.8	35.9
	Sunflower seed hull	26.7	18.4	27.0
	Oat hull	48.4	16.1	16.2
	Sugarcane bagasse	40.2	24.3	22.3
Other	bamboo	39.5	17.6	25.2

2.3 Cellulose

Cellulose is natural fibers consisting of a linear chain of several hundreds to over ten thousand β-glucose units' chain with the formula $(C_6H_{10}O_5)_n$. Commonly, the size of cellulose represents a degree of polymerization (DP), which varies from plant materials and isolation methods, for example around 10,000 glucopyranose units in wood and 15,000 in cotton (Frone *et al*., 2011). Cellulose can be found in different parts of plant such as bast, seed, leaf, straw, grass, and wood. The amount of cellulose in plant varies depending on the species, origin, maturity, and extraction process. Figure 2.2 shows the chemical structure of cellulose that consists of intramolecular and intermolecular hydrogen bonding networks. These hydrogen bonds result in low solubility of cellulose in solvent (Sun *et al*., 2004).

Although cellulose is the main composition in plant, it can be obtained from other sources such algae, tunicate, and bacterial. Tunicate is the marine animal, which can only produce cellulose. Iwamoto *et al.* (2009) have studied the elastic modulus of single microfibril from tunicate (*Halocynthia papillosa*). They found that tunicate's microfibrils gave elastic modulus similar to natural cellulose crystals obtained from plant material. Meanwhile, bacterial cellulose has been studied by many researchers due to its different mechanical properties, non-toxicity, high porosity, and low density compared to plant cellulose (Martínez-Sanz *et al*., 2011; Vasconcelos *et al*., 2017). Moreover, cellulose from bacteria has high purity and does not consist of any other non-cellulosic components such as lignin and hemicellulose (Castro *et al*., 2011). These features make bacterial cellulose to have the potential to be used in biomedicine (Shah *et al*., 2013; Hu *et al*., 2014) and as reinforcement material (Roman and Winter, 2004; Hirai *et al*., 2009).

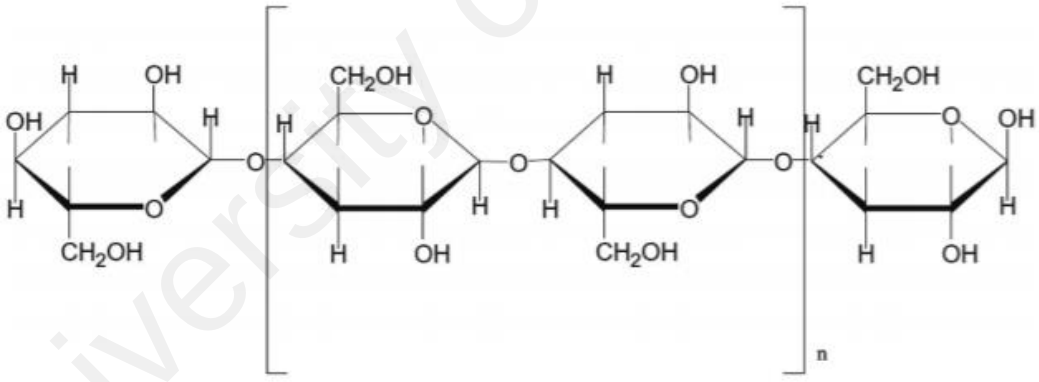

Figure 2.2: Chemical structure of cellulose.

Crystallinity of cellulose depends on the composition of amorphous and crystals. Four different crystalline cellulose allomorphs have been reported to be known as Celluloses I, II, III, and IV. The difference in polymorphs is subjected to cell dimensions, geometry, chain orientation, and polarity. The existence of these polymorphs have been identified by X-ray diffraction and nuclear magnetic resonance spectroscopy (^{13}C NMR) (Sun *et al*., 2005). Cellulose type 1 is a common form in nature. Cellulose I consists of two allomorphs, cellulose α and β. Meanwhile, Celluloses II, III, and IV were obtained

through a variety of treatments from Cellulose I. In addition, Cellulose I when exposed to strong alkali solution generates Cellulose II. Further, Cellulose III is found by treatment of Cellulose I or Cellulose II with liquid ammonia. Cellulose IV was prepared by heating Cellulose III (Goldberg *et al*., 2015). Cellulose can further be processed into microfibril and nano whisker. At present, cellulose production is mostly developed from wood biomass chemical processing.

2.4 Method of cellulose isolation

In recent years, there has been a significant interest in cellulose fibres isolation from various sources. Cellulose isolation normally involves three important steps: extraction with organic solvent removal of fats, oils, resins, waxes, and other soluble organic compound; bleaching to remove lignin; and treatment with strong alkaline solution to remove hemicellulose. Many pretreatment processes have been reported for cellulose isolation (Rabemanolontsoa & Saka, 2016; Seok *et al*., 2016). Pretreatment methods have been employed to disrupt the structure, to hydrolyze, solubilize, and for removal of lignin, hemicellulose, and other products (Balat, 2011; Duque *et al*., 2017; Karimi & Taherzadeh, 2016; Qing *et al*., 2017).

2.4.1 Physical treatment

Physical treatment is referred to as size reduction using mechanical comminution processes through milling, chipping, or grinding. It is usually considered as the first step of pretreatment method. The main advantage of physical treatment includes no production of toxic materials as by product or chemical used. It helps to increase the surface area of biomass, thus enhancing the enzymatic digestibility. Furthermore, it is also capable of decreasing the degree of polymerization and crystallinity of lignocellulose. The combination of physical pretreatments and other pre-treatment is frequently used, which could give a better result than individual (Kumar & Sharma, 2017).

Physical process can be categorized into process known as milling and irradiation. Ball milling and wet disk milling are commonly used to mill lignocellulosic biomass into fine powder. Nevertheless, the choice of the milling process depends on the condition of lignocellulose material either wet, dry, or both. For example, the ball mill can be used for either dry or wet materials, hammer mill for dry materials, and colloid mill only for wet materials (Taherzadeh & Karimi, 2008).

The drawbacks of milling process include high energy requirement and incapability to remove the lignin which acts as inhibitor for enzymes and cellulases. Milling can significantly reduce the particle size; however, use of very small particles may not be desirable due to higher energy consumption. Previous works reported that the energy consumption of mechanical comminution is closely related to the final particle size of lignocellulosic materials (Mani *et al*., 2004). In other words, the smaller the screen size, the higher the specific energy for grinding biomass samples. Irradiation technology such as electron beam, gamma rays, and microwaves has also been commonly used for changing the properties of polymers. Irradiation induces a chain–cleavage mechanism by changes in the microstructural crystallinity of the substrates. Driscoll *et al.* (2009) studied the relationship between radiation dose and cellulose fiber degradation. The crystallinity of the microcrystalline cellulose was reduced from 87% to 45% with molecular weight reduced from 82,000 Da to 5000 Da at high electron beam (1000 kGy). In another study done by Shin *et al*. (2012), it was shown that the cellulose content of the kenaf fiber obtained by electron beam irradiation treatment at 300 kGy was higher than that of the non-irradiated kenaf fiber's. However, the irradiation methods are not practical to be used in the industrial application because they are expensive and have difficulties. Treatment with high electron beam is a considerably environmentally benign method; however, the application limits to the presence of lignin, crystallinity, and density of lignocellulose material (Taherzadeh & Karimi, 2008).

2.4.2 Chemical treatment

The isolation of cellulose fibres requires the removal of other components such as lignin, hemicellulose, and pectin from the biomass. Chemical pretreatment technologies applying numerous reagents have been studied. Generally, in this method, a dried biomass is immersed in acids or bases solution under specific temperatures for a period of time. The treated biomass is filtered to separate the solid substrate from the liquor.

Various sources of plants have been studied for isolation of cellulose which can further be used to produce microcrystalline cellulose (MCC) and nanocrystal such as oil palm mass residue (Johar *et al*., 2012; Soom *et al*., 2009), jute (Jahan *et al*., 2011), banana plant waste (Elanthikkal *et al*., 2010), bagasse, rice straw (El-Sakhawy & Hassan, 2007; Ilindra & Dhake, 2008; Nuruddin *et al*., 2011), wheat straw, corn stalks, dhaincha (Nuruddin *et al*., 2011), kenaf (Wang *et al*., 2010), alfa (Trache *et al*., 2016), cotton stalks (El-Sakhawy & Hassan, 2007), soybean hull (Merci *et al*., 2015), tomato peel (Jiang & Hsieh, 2015), and pineapple leaf (Cherian *et al*., 2011). The idea of extracting cellulose from unused agricultural residues or lignocellulosic waste is aligned with the current interest towards waste minimization and waste to wealth concept.

The production of cellulose from lignocellulosic biomass requires pretreatment step to remove undesired hemicelluloses and lignin which act as protective barrier to cellulose. Alkaline treatment such as sodium hydroxide (NaOH) has been studied by many researchers. In their experiments, oven-dried banana fibers were treated with different concentrations of NaOH (2% - 5%) at 80°C -100°C for 2-4 hr (Elanthikkal *et al*., 2010; Henrique *et al*., 2013; Mandal & Chakrabarty, 2011). Fahma *et al*. (2010) treated oil palm empty-fruit-bunches with 6 wt.% potassium hydroxide (KOH) solution at 20°C for 24 hr. On the other hand, Nazir *et al.* (2013) employed a mixture of formic acid and hydrogen peroxide method. Recently, Jiang and Hsieh (2015) reported that the isolation of cellulose

in tomato peels by sodium chlorite/potassium hydroxide gave slightly higher yield of 13.1% cellulose compared to 10.2–11.3% cellulose from sodium hydroxide/hydrogen peroxide process. The disadvantages of this method are the time consuming and involves bleaching procedure. The bleaching treatment was performed to break down the phenolic compounds present in lignin, to remove the by-products, and to whiten the pulp. Sodium chlorite is frequently applied for delignification process in the isolation of cellulose from wood, which can form toxic compound such as chlorinated organic compounds (Nazir *et al*., 2013). The chlorinated compounds may give effect to the environmental after the disposal such as accumulate in food chains.

Many researchers have focused on sugarcane bagasse and corn stover pretreatment for bioethanol production (Liu *et al*., 2018). A mixture of acetic acid and sulphuric acid was used to enhance the digestibility of sugarcane bagasse. Pretreatment was carried out by reacting the sugarcane bagasse in an acid solution (1% (w/v) sulfuric acid and 1% (w/v) acetic acid and heating up to 190°C for 10 min. The results showed that the hemicellulose was removed around 90% and the cellulose loss during pretreatment was less than 15%, which corresponded to the amorphous fraction (Jackson de Moraes Rocha *et al*., 2011). Sun *et al.* (2004) have proposed a one-step treatment of sugarcane bagasse with an 80% acetic acid and 70% nitric acid mixture. Their study showed that treatment produced high purity of cellulose with relatively free of lignin and hemicelluloses. In addition, these methods reduced the loss of cellulose as compared to alkaline method which required two steps. Another study investigated on rice straws that were treated by two different treatments, NaOH solution and thermal steam explosion. They found that NaOH treatment gave lower cellulose yield (Boonterm *et al.*, 2016). Another treatment used combination steam explosion with ionic liquid. In their work, these authors used 2% hydrogen peroxide aqueous solution with low-flux ozone blowing for bleaching (Jiang *et al.*, 2011). The drawback for the use of ionic liquids in biomass pretreatment includes

relatively large amounts of ionic liquid impurities that reacted with cellulose even after intensive washing (Gericke *et al*., 2012). Overall, each method has different result related to the amount and quality of cellulose. The choice of methods for cellulose isolation depend on the final target.

2.4.3 Physicochemical treatment

Pretreatment techniques have been widely studied to process various biomass conditions in an effort to enhance lignin removal and increase the efficiency. In physicochemical pretreatment, parameters such as pressure and temperature are introduced in the presence or absence of a chemical. In a similar way for chemical pretreatment, lignin and hemicellulose are removed and cellulose structure is disrupted. The common techniques of physico-chemical pretreatments include steam explosion, ammonia fibre explosion, carbon dioxide explosion, hydrothermal, and wet oxidation. Among these techniques, the steam explosion pretreatment is the most commonly investigated (Han *et al*., 2010; Xu *et al*., 2010; Zhang *et al*., 2008; Mu *et al*., 2014; Boonterm *et al*., 2016).

Steam explosion involves the break-down of molecules by pressure-saturated steam within (20–50 bar) at high temperature (160–270°C) for several seconds to several minutes. Then, the pressure rapidly reduces to atmospheric pressure, which causes the lignocellulosic materials to be exploded and as part of hydrolysis. Steam explosion is one of the most cost-effective in terms of energy consumption (Ferro *et al*., 2015). However, partial destruction of cellulose, incomplete degradation of lignin, and the production of inhibitory compound are the disadvantages (Zhang *et al*., 2008; Sun *et al*., 2016). Ammonia fiber explosion (AFEX) involves pretreatment of biomasses with ammonia; it is similar like steam explosion, moderate temperature (60–120°C), and high pressure (≈ 2 MPa) and followed by a sudden release of pressure. AFEX is a promising pre-treatment

process with several advantages such as mild reaction temperature; however, high cost of liquid ammonia makes it unpractical (Haghighi Mood *et al*., 2013).

2.5 Cellulose micro and nanoscale isolation

Cellulose can be further disintegrated to micro and nano size by chemical and physical methods. These micro and nano can be produced from various materials are high in cellulose. MCC is obtained from purification and partially depolymerized cellulose and is usually prepared by treating alpha cellulose with an excessive amount of mineral acids (Xiang *et al*., 2016). Nanocellulose (NCC) is obtained from concentrated acid hydrolysis of MCC.

The most investigated sources of materials for the obtainment are wood (Kushnir *et al*., 2015), agricultural residues (Da Silva *et al*., 2010; Kopania *et al*., 2012), leaf fibers (Istirokhatun *et al*., 2015; Santos *et al*., 2018), and the shell of fruits (Neto *et al*., 2013; Frone *et al*., 2017). The micro and nano cellulose have received much attention due to high mechanical strength and stiffness. In addition, it is renewable, biodegradable, non-toxic, and biocompatible.

2.5.1 Microcrystalline cellulose

Commercial MCC is produced from wood and cotton. These sources are used as cellulose feedstock, this leads to competition among many areas such as furniture, pulp and paper industries, building products, as well as the combustion of wood for energy and the employment of cotton for textile industry (Trache *et al*., 2016). Therefore, the options are turned to non-woody cellulose such as herbaceous plants, grass, aquatic plants, agricultural crops, and their by-products. MCC is characterized by a high degree of crystallinity in a range from 55%–80% depending on the origin of the cellulosic sources and processing parameter (Chuayjuljit *et al*., 2010) and the width is in the range of 10–

50 μm. The application of MCC is diverse, it has a high potential to be used in many industrial sectors areas such as pharmaceutical, food, cosmetics, and polymer composites industries. MCC powder has been used as a binder and filler in polymer composites as reinforcement agent and medical capsules (Levis & Deasy, 2001; Islam *et al*., 2017).

Even though MCC can be produced from any material that is high in cellulose, the extraction of MCC from different sources is relevant since it dictates the overall performance of MCC. The structure and features of MCC vary with the origin of cellulose and the hydrolysis conditions applied, such as the temperature and time of hydrolysis procedure, nature and concentration of acid as well as the fiber-to- acid ratio that play important roles in the particle size, morphology, crystallinity, thermal stability, and mechanical properties of MCC (Xiang *et al*., 2016). Several studies on the isolation of MCC from cellulosic materials have been conducted using different approaches, Merci *et al*. (2015) obtained MCC from soybean hull using sodium hydroxide (NaOH), followed by extrusion with sulfuric acid (H_2SO_4). Haafiz *et al*. (2013) produced MCC from oil palm with empty fruit bunch pulp using acid hydrolysis reaction with 2.5 mol/l hydrochloric acid (HCl). El-Sakhawy and Hassan (2007) isolated MCC from agricultural waste using acid hydrolysis reaction with 2.5 mol/l sulphuric acid and hydrochloric acid, while Kalita *et al*. (2013) used 4% sodium hydroxide, followed by bleaching with sodium hypochlorite and hydrogen peroxide and finally using acid hydrolysis with 2.5 N. These studies showed that HCl is most frequently used as acid hydrolysis to prepare MCC and differs in the pretreatment method.

2.5.2 Nanocellulose

Nanocellulose, which can be produced by different methods from several lignocellulosics that affect their dimensions and functions, is generally used to describe cellulosic materials with a dimension in the range of nanometer. In addition, there are three main subcategories that classify nanocellulose, which are (1) cellulose nanocrystals (CNC) with synonyms such as cellulose (nano) whiskers, nanocrystalline cellulose, and rod-like cellulose microcrystals; (2) cellulose nanofibrils (CNF), which can also be referred to as nanofibrillated cellulose (NFC), microfibrillated cellulose (MFC), and cellulose nanofibers; and (3) bacterial nanocellulose (BNC) (Abdul Khalil *et al*., 2014; Brinchi *et al*., 2013). Further, the standardization of the terminology (Standard Terms and Their Definition for Cellulose Nanomaterial WI 3021) was proposed by the Technical Association of the Pulp and Paper Industry (TAPPI) and the International Organization for Standardization (ISO) and the term "nanocellulose" is used only for nano-scaled fibrils (Gómez *et al*., 2016), which can be applied to materials with at least one dimension less than or equal to 100 nm and could be perceived as nanomaterial (Mondal, 2017).

The type of nanocellulose produced is determined by the processing conditions. Generally, CNC is rod-like or needle-like cellulose crystals with a dimension of 5-70 nm and 100-250 nm in length (Mariano *et al*., 2014; Oun & Rhim, 2016). The length and width of cellulose whiskers obtained from various sources are listed in Table 2.3. It is produced by strong acid hydrolysis to remove non-cellulosic components and most amorphous cellulose from the source materials. Meanwhile, CNF is commonly produced by mechanical pressure, which involves high-pressure homogenization before and/or after chemical or enzymatic treatment. CNF is characterized as long, high aspect ratio, flexible, and entangled long nanofibrils. Therefore, it is not so easy to determine the length of CNF with microscopic techniques because nanofiber forms network like the structure as shown in Figure 2.3.

Acid hydrolysis is commonly used for the extraction of nanocellulose from various types of plant's fiber sources. Strong sulfuric acid, hydrochloric acid, and combination of them have been used to hydrolyze the glucosidic bond in cellulose (Julie Chandra *et al*., 2016). During acid hydrolysis, the amorphous part of cellulose is more accessible compared to the crystalline part. Various hydrolysis parameters have been studied such as concentration, reaction time, reaction temperature, and solid to acid ratio, which determine the effect of the morphology and properties of nanocellulose produced (Siqueira *et al*., 2010).

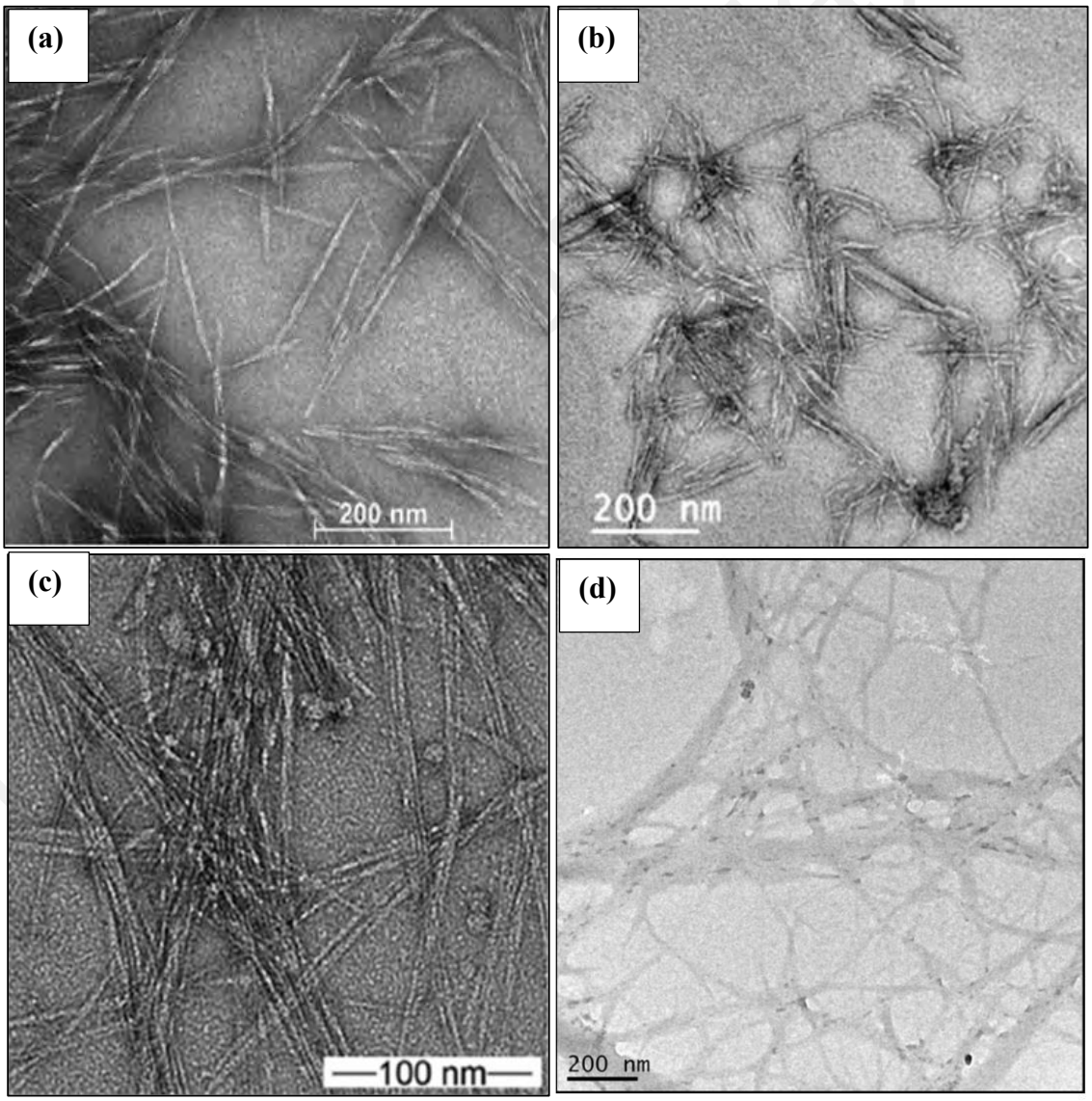

Figure 2.3: Example of transmission electron microscopy images showed the cellulose nanocrystals (CNC) (a) elephant grass (b) pistachio shells and nanofibrillated cellulose (NFC) (c) banana peel (d) H*elicteres isora*. Adapted from Santos *et al*., 2008; Chirayil *et al*., 2014; Marett *el al*., 2017.

Deepa *et al*. (2015) found different diameter of nanocellulose ranging from 10-25 nm produced from different types of raw material. It showed that the shape, size, and surface properties of the nanocellulose are generally influenced by the source and hydrolysis conditions. Meanwhile, Fahma *et al*. (2010) and Mendes *et al.* (2015) investigated the effect of hydrolysis time on the structure and properties of nanocellulose. They discovered that the hydrolysis time affected the properties of nanocellulose such as crystallinity, degree of polymerization, particle size, and thermal stability. Mondal (2017) stated that nano dimensions, quality, and yield of nanocellulose would depend on the source of lignocellulosic biomass when the same method of extraction is applied. These statements are in accordance with those reported by Abraham *et al.* (2011). They found the quality and yields of nanocellulose derived from pineapple biomass are better than the nanocellulose extracted from banana and jute stem (Abraham *et al.*, 2011).

2.5.3 Structure and properties of cellulose material

Morphology of microcellulose and nanocellulose has been studied using microscopy techniques, such as scanning electron microscopy (SEM), field-emission scanning electron microscopy (FESEM), atomic force microscopy (AFM), and transmission electron microscopy (TEM). Microscopic techniques analysis provide useful information on how the image of fibril looks like (needle, rod, twist, chiral helixes); individual or entangled fibers. The ribbon-like morphologies show microfibrils twisted with a width of 20–70 nm can often be observed in bacterial nanocellulose (Castro *et al*., 2011). Commonly, cellulose nanocrystal isolated from plant sources exhibit rod-like shape, needle-like shape, or spherical shape (Neto *et al.*, 2013; Gómez *et al*., 2016; Ferreira *et al*., 2018). Further, microscopic techniques are used to determine the diameter and length of individual particles. However, the length of nanocellulose is very difficult to determine from TEM images because nanofibrils are overlapped with each other and there are difficulties in identifying both ends (Chirayil *et al*., 2014; Deepa *et al.*, 2015).

Crystallinity of cellulose can be measured using different techniques such as x-ray diffractogram (XRD), solid-state ^{13}C NMR, Raman spectroscopy, and Fourier-transform spectroscopy (FTIR). Crystallinity represents the relative amount of crystalline cellulose present in cellulose and has also been used to identify changes in cellulose structures after each stage of treatments (Bhatnagar & Sain, 2005; Zhao *et al*., 2007; Rahimi Kord Sofla *et al.*, 2016).

Table 2.3: Examples of the length (L) and diameter (D) of nanocellulose from various sources obtained by different techniques.

Type	Source	Diameter	Length	Method	References
CNC	Coconut husk	6 nm	80-500 nm	64 wt% H_2SO_4; 45°C; 120 min -180 min	Rosa *et al*. 2012
	Oil palm biomass	< 10 nm	>100 nm	64% H_2SO_4;40ºC; 60 min	Haafiz *et al.* 2014
	Groundnut shells	5 to 18 nm	67-172 nm	65 wt% H_2SO_4; 75 min;45°C	Bano and Negi, 2017
	Waste cotton cloth	3 to 35 nm	28-470 nm	Mixed solution of H_2SO_4 (98 wt%), HCL (37 wt%)	Wang *et al*. 2017
	Cotton linter	12 nm	177 nm	60 wt% H_2SO_4; 45°C; 60 min	Morais *et al*. 2013
CNF	Water hyacinth	25 nm	NA	Cryocrushing and sonication	Thiripura Sundari and Ramesh, 2012
	Banana peel	13-17 nm	264-589 nm	high-intensity ultrasonication	Tibolla *et al*. 2014
	Arecanut husk	< 10 nm	NA	viagrinding and homogenization	Julie Chandra *et al*. 2016
	Bamboo	2–30 nm	NA	Ultrasonication	Xie *et al.* 2016
	Pinecone	5- 25 nm	>1000 nm	Mechanical grinding	Rambabu *et al*. 2016

The crystallinity value varies depending on the selection of measurement techniques in the following order: XRD height method > XRD amorphous subtraction > XRD peak deconvolution > NMR C4 peak separation (Park *et al.*, 2010). The simplest and frequently used method to measure crystallinity is XRD using peak height method developed by Segal and coworkers (Segal *et al*., 1959) the calculation is based on the ratio of height of the 002 peak and height of the minimum (I_{AM}) between 002 and peak 101 as shown in Figure 2.4. Fourier-transform infrared spectra are useful in identifying the chemical changes of chemical compositions of lignocellulose material after and before any treatment or modification. FTIR has been intensive in cellulose identification, used to obtain information of chemical changes, and includes the effectiveness of pretreatment (chemical, physical, and biological) on a removal of hemicellulose and lignin components. Typical FTIR spectra of cellulose consist of two regions at high wavenumbers (2800–3500 cm^{-1}) and low wavenumbers (500–1700 cm^{-1}) (Haafiz *et al*., 2013). The most important peak to investigate cellulose component is peak 1430 cm^{-1}, indicated to crystallized cellulose I, peak at 1420 cm^{-1}, assigned to amorphous cellulose and crystallized cellulose II, and peak at 1426 cm^{-1}, referred to mixture of crystallized cellulose I and amorphous cellulose (Colom & Carrillo, 2005; Bian *et al*., 2012). Another important peak is at 893- 900 cm^{-1}, specific for glycosidic linkages between glucose units (Elanthikkal *et al*., 2010; Fahma *et al*., 2010; Haafiz *et al*., 2014; Deepa *et al.*, 2015).

Thermogravimetric analysis (TGA) and differential scanning calorimetry (DSC) are frequently used to study the thermal properties of cellulose as a filler or reinforcement in polymer composite. TGA provides information on thermal degradation temperature, moisture content, and thermal stability, while DSC has been used to measure the melting temperature and crystallization temperature of cellulose materials.

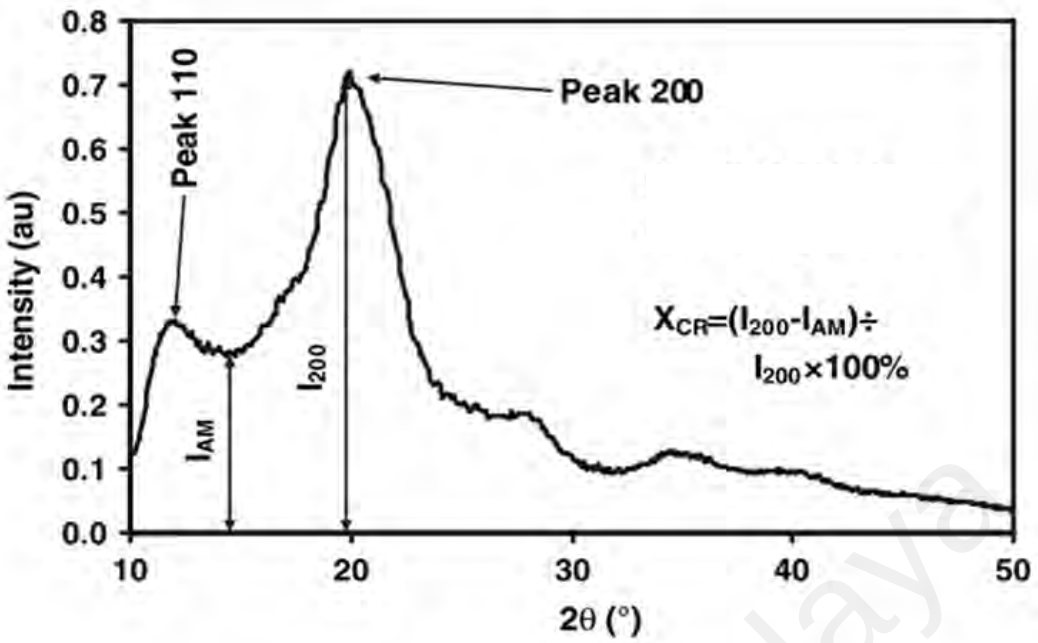

Figure 2.4: Crystallinity determination using peak height method. Adapted from Cheng *et al.*, 2007.

According to Yang *et al*. (2006), thermal degradation profile of lignocellulose material shows four steps degradation which are the water loss occurred below 220°C, hemicellulose decomposition between 220 - 315°C, breakage of glycosidic linkage of cellulose between 315-400°C, and followed by lignin decomposition at above 400°C. The chemical structure of lignocellulosic material determines its thermal decomposition. Hemicellulose is easy to hydrolyse due to its random amorphous structure. Cellulose constitutes a very long polymer of glucose unit and has crystalline structure which is very strong and resistant, while lignin has a very high molecular weight, thus very high thermal stability, and is difficult to decompose (Kim *et al*., 2006; Yang *et al*., 2006). The TGA curves of MCC and NCC generally show two degradation stages that correspond to the removal of water within the cellulose at the region between 60°C and 140°C and the second stage concerns the dehydration, decarboxylation, depolymerization, and decomposition of glycosyl units in cellulose (Trache *et al*., 2016).

2.6 Hydrolysis of cellulose for conversion of glucose

Many studies have been reported on the conversion of cellulose to glucose using acid hydrolysis, enzymatic hydrolysis, and in ionic liquid (Table 2.4). The purpose of each hydrolysis process is to break the beta glycosidase bonds of cellulose into glucose (Figure 2.5). Furthermore, acid hydrolysis is the most extensive study in facilitating the acid hydrolysis process. Acid hydrolysis is generally composed of two forms: dilute acid hydrolysis that is generally lower than 10% (w/w) and concentrated acid hydrolysis above 10% w/w (Kumar *et al*., 2015). Further, dilute acid hydrolysis is accomplished in two different conditions, which are generally at high temperature (T > 160°C) and low temperature of T ≤ 160°C (Kumar *et al*., 2015).

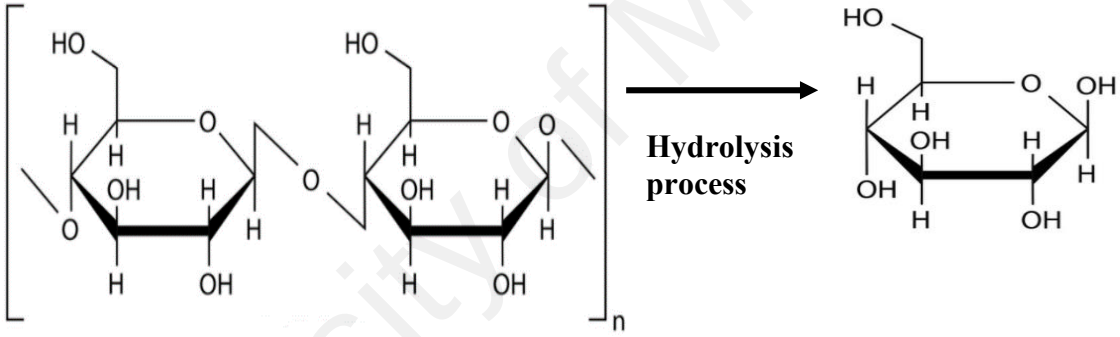

Figure 2.5: Hydrolysis process.

Research on cellulose acid hydrolysis of biomass still continues, although cellulose degradation using acid hydrolysis is a common practice in the industries (Wang *et al*., 2014). The optimum condition of acid hydrolysis of biomass has been reported by previous researcher by using 0.4% sulfuric acid at 215°C, which yielded 70% of glucose (Saxena *et al*., 2009). A similar finding was also reported by Dussán *et al*. (2014) whereby the maximum extraction of glucose from cellulose sugarcane bagasse was not more than 71% using hydrolysis condition of 2% of H_2SO_4 at 155ºC for 10 min. Further, small amount of degradation glucose product produced was 5-hydroxymethylfurfural and furfural.

Table 2.4: Hydrolysis methods for cellulose hydrolysis.

Hydrolysis Method	Advantages	Drawback
Acid	Less expensive	Equipment corrosion.
	Achieving high activity.	Inconvenient for separation and recycling.
Enzymatic	Highly selective.	Many enzymes are costly.
	Environmentally friendly.	Sensitive to operating condition, such as pH, temperature and pressure.
Ionic Liquid	Good performance in dissolving cellulose.	Many ionic liquid are expensive.
		The recovery of the ionic liquid is a highly energy consuming process.

In contrast, high glucose yield of 85% from yellow poplar was obtained using a simulated countercurrent shrinking-bed reactor system by applying 0.07% (w/w) H_2SO_4 and 225°C (Torget *et al*., 2000). Siqueira *et al*. (2013) determined the effect of lignin composition to the cellulose hydrolysis. The cellulose conversion is higher when the lignin composition decreases. Kumar *et al*. (2015) applied a two-stage sulphuric acid hydrolysis of sugarcane bagasse, 8% at first stage, and 40% at the second stage at temperature 100°C and 80°C respectively. Glucose was produced only at the second stage, with approximate yield of 65%.

Hutomo *et al*. (2015) compared the cellulose hydrolysis with glucose using two different acids. Based on their study, sulphuric acid gave higher glucose yield compared to hydrochloric acid. In another study, Wijaya *et al.* (2014) evaluated the effect of crystallinity on cellulose degradation of differently categorized biomasses (hardwood, softwood, and non-woody biomasses). They reported that the lowest crystallinity gave high glucose yield. Morales-delaRosa *et al*. (2014) used batch reactor to optimize acid hydrolysis of cellulose to increase glucose yield and minimize the levunic acid. Their

variables were temperature between 120°C to 220°C, acid concentration ranging from 0.2 to 2.5 mol/l, acid strength ranging from 4.8 to 6.6, and types of cellulose (fibrous and microgranular). They summarized that high glucose yield can be obtained at moderate reaction temperature with low acid concentration; strong acid (pKa < 0).

Another acid frequently used for acid hydrolysis is phosphoric acid. Gámez *et al*. (2006) treated sugarcane bagasse with phosphoric acid in autoclave at 122°C, which resulted in high glucose yield of 6% at condition of 300 min and 3.2 g/l phosphoric acid. In a different study using the same acid, Orozco *et al*. (2007) conducted acid hydrolysis using microwave reactor. They found the highest glucose yield at reaction time of 3–5 min with 7.5% acid concentration. Lenihan *et al.* (2010) also treated potato peels with phosphoric acid using pilot batch reactor. This optimum sugar yield of 82.5% was obtained at 135°C and 10% (w/w) acid concentration, by which 98% from the total sugar was glucose.

A combination of acid hydrolysis and enzymatic hydrolysis was applied by Amiri and Karimi (2013) to enhance cellulose degradation. Initially, cellulose was treated using dilute-acid hydrolysis for glucose production and the residual solid from the acid hydrolysis was enzymatically hydrolyzed. The proposed method successfully produced high yield of glucose of 95.4%. In a different investigation, Hegner *et al.* (2010) explored the hydrolysis of cellulose using Nafion SAC 13 and ferric chloride supported on amorphous silica. They obtained 11% yield of conversion cellulose to glucose at temperature of 190°C.

Recently, research focus on the application of ionic liquid as a solvent for cellulose degradation has also gained considerable interest due to high yield of glucose (Morales-delaRosa *et al*., 2012; Zhuo *et al*., 2015; Hsu *et al*., 2017). Dilute acid hydrolysis is a preferable process because it does not require acid recovery, where ionic liquid is needed.

Thus, this makes the ionic liquid application for cellulose hydrolysis expensive (Sun *et al*., 2013; Kumar *et al.,* 2015; Liu *et al.*, 2017).

The enzymatic methods for cellulose degradation have advantages due to their selectiveness to specific reaction and no formation by-products which can disturb the next subsequent process. Conversely, enzymatic hydrolysis of cellulose has been observed as not practical to be industrialized due to high cost of enzymes and the hydrolysis process occurs at a slow rate (Sasaki *et al*., 2012). Thus, the optimum yield of glucose is affected by many factors, which are commonly the investigated reaction conditions (concentration, time, temperature). Nevertheless, lignocellulose composition, pre-treatment method, type of acids, and device configuration are also among the contributing factors (Kabyemela *et al*., 1997; Torget *et al*., 2000; Dussán *et al*., 2014).

2.7 Ethanol as biofuel from biomass

More countries are shifting towards renewable energy to reduce reliance on fossil fuel. Among the renewable energy sources, biomass has attracted major intentions and is abundantly available around the world besides also having a diversity of biomass source. It can be used as feedstock for many applications such as for the production of chemical, fuels, materials, cosmetics, and pharmaceutical. Recently, the production of biofuels such as biodiesel and bioethanol from energy crops has been a major research focus (Atabani *et al*., 2013). Presently, several countries such as the United Kingdom, Sweden, and Finland are already cultivating energy crop which can be utilized as lignocellulose feedstock. In Europe, energy crops like *Leucaena leucocephala*, *miscanthus*, willow, reed canary grass, and poplar have been intensively studied to be used in the production of pulp and paper, biofuels, and bio-based products (Demirbas *et al*., 2009; Sindhu *et al*., 2016; Zabed *et al*., 2017). Due to economic reasons such as price volatility as well as legislative and regulatory mandates, more countries are expected to use and cultivate

energy crop as a source of raw material for fuels and chemicals. The choice depends on several factors such as its availability, environmental benefits and high yield biomass, and also low production cost for large-scale cultivation.

Biofuels produced from lignocellulose biomass such as agricultural waste or forestry material are particularly desirable because they avoid conflict resources from the production of food crops. Lignocellulose feedstock comprises carbohydrates and substantial amounts of lignin that can be transformed into wide range of products such as power generation, transportation fuels, and various chemical compounds and materials. Therefore, lignocellulose feedstock can be used in large biorefinery process, which is similar to petroleum refinery as illustrated in Figure 2.6.

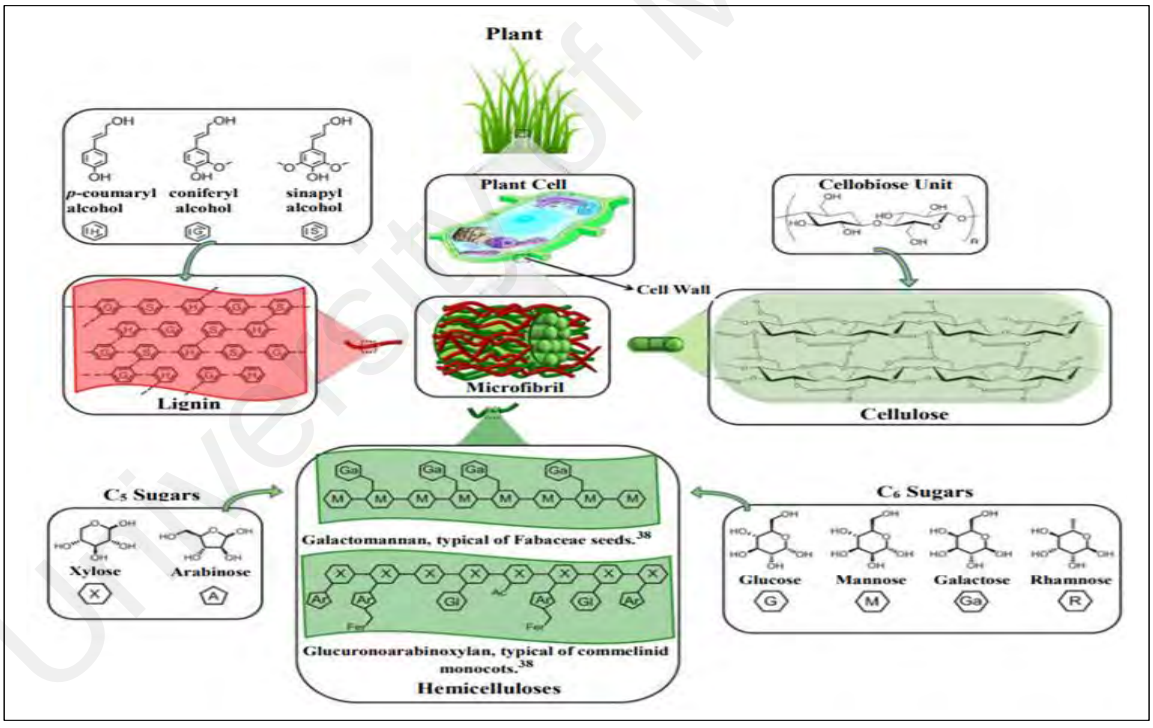

Figure 2.6: The composition and structure of lignocellulose. Adapted from Isikgor and Becer, 2015.

Therefore, several studies have been carried out concerning the effect of plantation to the wood quality. Nevertheless, studies related to the effect of plantation on the seed quality have not been performed. The seeds or fruits of plants also have the potential to become sources for various applications, since the lignocellulose compositions for some species are similar and higher than wood. Additionally, the composition of these compounds varies from one plant to another depending on their sources such as maturity, origin, and species (Table 2.5).

Table 2.5: Lignocellulose composition of seed/fruit from various biomass.

Biomass material	Cellulose (%)	Hemicellulose (%)	Lignin (%)	References
Mango	55.0	20.6	23.9	Henrique *et al*. 2013
Melon shell	42.1	19.5	1.1	Pius *et al.* 2014
Soy hull	48.2	24.0	5.8	Neto *et al*. 2013
Rubber	25.8	66.4	ND	Hassan *et al*. 2014
Oat hull	36.7	34.8	19.4	Skiba *et al*. 2017
Plum	No data available			Frone *et al.* 2017
Tamarind	No data available			González-Hernández *et al*. 2012

2.7.1 Conversion of biomass to ethanol

Bio-ethanol is commonly produced by fermentation of sucrose, molasses, or glucose extracted from starch crops and sugar crops such as sugar cane, corn, wheat, sorghum, and potatoes. Yeast or bacteria are responsible for transforming diverse mixtures of biomass monosaccharides such as glucose, mannose, and galactose, xylose, rhamnose, and arabinose into ethanol (Sudiyani *et al*., 2013; Taherzadeh & Karimi, 2015). The widely studied yeast for sugars fermentation is *Saccharomyces cerevisiae* because it accepts a wide range of pH. However, it is anable to utilize pentose sugars (Kuhad *et al*., 2010; Tesfaw & Assefa, 2014; Gupta & Verma, 2015). Recently, many studies have

investigated the production of ethanol from biomass because it is cheap, renewable, abundant, and does not compete with food production. However, it is required to have more steps than the conversion of starch due to composed mixture of carbohydrates polymer (lignin, cellulose, and hemicellulose). Pretreatment is required to ensure maximum usage of cellulose and hemicellulose. These components are further converted into hexose and pentose sugars through acid and enzymatic hydrolysis and can efficiently be used for ethanol fermentation. Fermentation can be done either by separate fermentation of individual sugar or fermentation of both pentose and hexose sugars. In addition, hydrolysis and fermentation processes can be achieved by separate hydrolysis and fermentation (SHF) or through simultaneous saccharification and fermentation (SSF).

SHF is a conventional method that allows the hydrolysis process to firstly yield sugars and followed by the fermentation. The main advantage of this method is that each process can be controlled and optimized. In SSF, hydrolysis and fermentation are located in a single reactor, in which enzyme and yeast are also put together in the same reactor. Gupta *et al*. (2009) suggested that SHF gives better efficiency of ethanol production. SHF is commonly preferred than SHF because it produces better rates, yields, and concentrations of ethanol (Wyman *et al*., 1992; Dahnum *et al*., 2015). In addition, SHF process can minimize the production of inhibitor during sugar conversion because the glucose formed in solution will immediately be converted to ethanol (Sasikumar & Viruthagiri, 2008; Wyman *et al*., 1992). In contrast with SHF, one problem associated with SSF is the different optimum temperatures of hydrolysis and fermentation process (Sasikumar & Viruthagiri, 2008).

Various biomass sources have been studied for bioethanol conversion. Different pathways for the conversion of different feedstock are being studied. The most investigated pathways to produce bioethanol are acid pretreatment, delignification, and enzymatic hydrolysis to produce sugar and fermentation to bioethanol. Kuhad *et al*.

(2010) extracted hexose sugar hydrolysate from *Lantana camara* and fermented using *Saccharomyces cerevisiae,* which gave the ethanol yield to obtain 17.7 ± 0.96 g/l with yield of 0.48 g/g for 16 hr. Similarly, Gupta *et al*. (2009) isolated cellulose from *Prosopis juliflora* (Mesquite) and produced 18.52 g/l of ethanol with corresponding yield of 0.49 g/g. Hoşgün *et al.* (2017) used alkaline pretreatment, enzymatic hydrolysis, and fermentation and produced 40.71% of 37.73 g/kg biomass.

2.7.2 Response surface methodology (RSM)

Response surface methods consist of a group of empirical techniques devoted to the evaluation of relations existing between a cluster of controlled experimental factors or test variables. Their responses are measured according to one or more selected criteria. The main advantage of using RSM is that there will be a huge reduction in the number of experiments needed to evaluate multiple variables and their interactions, thus indicating that the RSM is less laborious and is more time consuming than normal experiments (Mohammadi *et al.*, 2016).

The optimal conditions of the factors or test variables are obtained by solving the regression equation and also by analysing the response surface contour plots. Response surface methodology is an empirical modeling technique and is used to estimate the relationship between a set of controllable experimental factors and observed results (Gomes *et al*., 2011). Central composite design (CCD) is a very efficient design tool for fitting second-order polynomial models and is therefore selected for this study. The CCD is optimized for fitting quadratic models and thus, the number of experimental points in the CCD is sufficient to test the statistical validity of the fitted model and the lack of fit of the model (Ghosh *et al*., 2012).

The conventional optimization method is one-factor-at-a-time. This method is not preferable due to its difficulty to conclude interactions of each factor (Esfahanian *et al*., 2013). RSM is a useful technique for modeling and determining the optimal process conditions for hydrolysis and fermentation process. Many studies have been done using RSM for various substrates (Wang *et al*., 2006; De Lima *et al*., 2010; Habeeb *et al*., 2016). Sasikumar and Viruthagiri (2008) reported the optimization of process conditions for the production of ethanol from pretreated sugarcane bagasse. The successfully produced maximum ethanol concentration was 32.6 g/l for substrate concentration of 180 g/l of sugarcane bagasse at the optimized process conditions of temperature 35°C, pH 5.5, and 72 hr in aerobic batch fermentation. Uncu and Cekmecelioglu (2011) fermented the mixed carbohydrate components of kitchen wastes to ethanol. They obtained the optimum conditions of ethanol production using a commercial dry baker's yeast *Saccharomyces cerevisiae* and were respectively assessed by response surface methodology. Esfahanian *et al.* (2013) evaluated two different models for optimization, response surface methodology (RSM), and artificial neural network (ANN). They reported that prediction by ANN was almost similar to RSM. Further, they found that the optimum conditions of 32°C, pH 5.2, and glucose concentration of 50 g/l produced ethanol concentration of 16.2 g/l.

CHAPTER 3: METHODOLOGY

3.1 Material

3.1.1 Solvents and chemicals

The chemicals used in this work were of analytical grade and obtained from Fluka Chemicals and Sigma-Aldrich. The acids used were 2.5 M hydrochloric acid (HCl), 72% sulphuric acid (H_2SO_4), 80% acetic acid (CH_3COOH), and 65% nitric acid (HNO_3). The chemicals used were sodium chlorite ($NaClO_2$), Dimethyl suphate (Me_2SO_4) sodium hydroxide (NaOH), 2 % phenol solution (C_6H_5OH), 3% uranyl acetate solution, 0.05% sodium azide, dextran standard, potassium bromide powder (Kbr) and urea (NH_2CONH_2). The solvents used were toluene, methanol, ethanol, acetonitrile, and dimethyl sulfoxide.

3.1.2 Plant material

Mature fruits of *Leucaena leucocephala* were collected at Forest Research Institute Malaysia (FRIM) between October 2015 and April 2016. The mature seeds (LLS) were separated from their pods manually. The seeds were dried and ground into powder using an industrial blender (Waring BB155 3/4 HP, USA).

Figure 3.1: Image of mature seeds of LLS.

3.2 Characterization for seed

The chemical characterizations were determined in triplicate based on the following standard: alcohol: toluene (TAPPI T204 cm-07), holocellulose (Wise *et al*., 1946), α-cellulose (Ritter 1929), klason lignin (TAPPI T222 om-02), moisture content and ash content adapted from ASTM D 2974-87.

3.2.1 Alcohol toluene solubility

The alcohol toluene solubility was conducted according to TAPPI T204 cm-07 (2007). Alcohol toluene solubility was conducted to measure the waxes, fats, resins, and oils, and certain other ether extractives using soxhlet extraction apparatus. Approximately six grams of dried LLS were added to the cellulose extraction thimble and placed in a soxhlet extraction chamber. A mixture of ethanol and toluene with a ratio of 2:1 was prepared and transferred to the round bottom flask. The mixture was heated for four to five hr to provide a boiling rate which was not less than 24 cycle extractions. After the extraction was completed, the extract in the flask was collected from the apparatus and evaporated the solvent to near dryness *in vacuo* at 45°C using rotary evaporater. The extract was transferred to the weighing dish and oven-dried at 105 ± 2°C, cooled in a desiccator, and weighed until a constant weight was obtained. The test was conducted in triplicates. The formula used to calculate the alcohol–toluene solubility content is as follows:

$$\text{Alcohol-toluene solubility (\%)} = \frac{W_2}{W_1} \times 100 \qquad (3.1)$$

Where;

W_1 = Weight of dried sample LLS
W_2 = Weight of dried sample after extraction

3.2.2 Holocellulose content

Holocellulose content was determines according to Wise *et al*. (1946). About Six grams of dried sample LLS (extractive free) were added into a conical flask. Then, the sample was treated with a mixture of 450 ml distilled water, 0.6 ml of cold glacial acetic acid, and three grams of sodium chlorite ($NaClO_2$). This mixture was placed into a water bath at temperature around 70°C for five hours and stirred constantly. Cold glacial acetic acid and $NaClO_2$ were added to the sample at every one-hour interval. The extract was cooled and filtered and followed by washing with cold water to remove ClO_2 from the extract. The filtered extract was transferred to the crucible and oven-dried at 105 ± 2°C, cooled in a desiccator, and weighed until a constant weight was obtained. The test was conducted in triplicates. The formula used to calculate the holocellulose content is as follows:

$$\text{Holocellulose (\%)} = \frac{W_3}{W_2} \times (100 - W_1) \qquad (3.2)$$

Where;

W_1 = Alcohol –toluene extractive (%)
W_2 = Weight of dried LLS (extractive free)
W_3 = Weight of dried sample in crucible

3.2.3 α-Cellulose

A-cellulose content was determined according to Ritter (1929). A two-gram dried holocellulose sample was treated with 50 ml of 17.5% sodium hydroxide (NaOH). The solution was stirred using magnetic stirrer for 30 min. Then, 50 ml of distilled water was added to the reaction mixture and left for 5 min. The solution mixture was filtered and washed with 50 ml of 8.3% NaOH, and followed by 50 ml of 10% acetic acid. Lastly, it was washed with hot water until it was free from acid. The filtered sample was transferred to the crucible and oven-dried at 105 ± 2°C, cooled in a desiccator, and weighed until a constant weight was obtained. The test was conducted in triplicates. The formula used to

calculate the α-cellulose content is as follows:

$$\alpha\text{-cellulose (\%)} = \frac{W_3}{100 \times W_2} \times W_1 \quad (3.3)$$

Where;

W_1 = Holocellulose content (%)
W_2 = Weight of dried holocellulose sample
W_3 = Weight of dried sample in crucible

3.2.4 Klason lignin content

The klason lignin content was conducted according to TAPPI T222 cm-02 (2002). A one gram of dried LLS sample (extractive free) was added to 15 ml of 72% cold sulphuric acid. This mixture was placed into a water bath at temperature around 20°C for two hours and stirred constantly. The reaction of mixture was terminated by adding 345 ml distilled water which diluted the concentration of the sulphuric acid to 3% and autoclaved at 121°C for 30 min. Solids were separated from aqueous solution by filtration. The filtered sample (lignin) was transferred to the crucible and oven-dried at 105 ± 2°C, cooled in a desiccator, and weighed until a constant weight was obtained.

$$\text{Klason lignin (\%)} = \frac{W_3}{W_2} \times (100 - W_1) \quad (3.4)$$

Where:

W_1 = Alcohol –toluene extractive (%)
W_2 = Weight of LLS
W_3 = Weight of dried sample in crucible

3.2.5 Moisture content

The moisture content was conducted according to ASTM D 2974-87 (1987). Approximately five grams of LLS were weighted and placed into a crucible. The sample was dried for 17 hr in the drying oven at 103 ± 3°C. The sample and crucible were weighted and drying was continued until the constant weight was reached. Then the

sample was cooled, the sample plus the crucible were re-weighted, and the weight of dried sample was recorded. The formula used to calculate the moisture content is as follows:

$$\text{Moisture content (\%)} = \frac{\text{Initial mass} - \text{oven dried mass}}{\text{Oven dried mass}} \times 100 \quad (3.4)$$

3.2.6 Ash content

The ash content was conducted according to ASTM D 2974-87 (1987). Empty porcelain crucible was ignited in the muffle furnace at 750 ± 25°C for a minimum of 4 hr. The crucible was cooled in the desiccator and weighed. About 2 grams of LLS were weighed into the porcelain crucible and placed in the muffle furnace at 575 ± 25°C for 5 hr. The sample and crucible were cooled and weighed. The sample was placed back in the muffle furnace until the constant weight was reached. The formula used to calculate the ash content is as follows:

$$\text{Ash content (\%)} = \frac{W_2}{W_1} \times 100 \quad (3.5)$$

Where;

W_1 = weight of dried sample
W_2 = weight of ash

3.2.7 Elemental analyzer

The parameters analyzed were Carbon (C), Hydrogen (H), Sulphur (S), and Oxygen (O) content. The weights of dry samples used were 2.5-3.0 mg. Elemental compositions were performed using a Perkin-Elmer 2400 Series II CHNS/O analyser.

3.2.8 Inductively couple plasma (ICP)

The mineral content or elemental analysis of the sample solutions was performed using the PerkinElmer Optima 7300 DV ICP-OES instrument (PerkinElmer, Inc. Shelton, CT, and USA). Eight elements were selected to determine their composition in LLS. These elements are magnesium (Mg), potassium (K), sodium (Na), ferum (Fe), manganese (Mn), copper (Cu), zinc (zn), and calcium (Ca).

3.2.8.1 Sample preparation

Wet digestion methods with combination of acid mixtures were used for elemental analysis to increase the solubility and chemical degradation of sample matrices in solution (Kuboyama *et al*., 2005). About 2 mg of three samples were weighed. Then, 3 ml of nitric acid and 9 ml of hydrochloric acid were added to all samples. The samples were heated for a few hours on the hot plate until the samples digested. After cooling, 10 ml of distilled water was added to the sample and mixed. The residue was filtered and diluted to 50 ml with distilled water. The standard solutions of elements for calibration procedure were produced by diluting a stock solution of 1000 mg/l and about five different concentrations of standard element solutions were prepared.

3.3 Preparation of cellulose from matured seed of *Leucaena leucocephala*

3.3.1 Pretreatments

Isolation of cellulose from lignocellulosic biomass requires pretreatment steps to remove undesired hemicelluloses, lignin, and others which act as protective barrier to cellulose. The common pretreatment methods employed are chemical treatment using acid and alkaline. Acetic acid-nitric acid mixture was chosen for the preparation of cellulose. Isolation of cellulose using alkaline treatment was also studied to compare the effectiveness of the removal of non-cellulosic material. Both treated samples were

analysed using fourier-transform infrared spectroscopy even though a new method was employed in this study which is known as hot water treatment to investigate the effect on LLS surface morphology and chemical structure.

3.3.1.1 Hot water treatment

The removal of primary and secondary metabolites was done according to Duarte *et al*. (2011) with some modifications. About two hundred grams of LLS were weighted and two liters of distilled water were added. The mixture was boiled under reflux at 95°C - 100°C and for 2 hr. At the end of extraction, the water extract was filtered through a cotton cloth. The filtered product was boiled again with new distilled water and the process was repeated for 3 times. The filtration aqueous extract was discarded and the insoluble residues were collected and dried in the oven at 60°C and stored for FTIR and FESEM analyses. Further, the residue of LLS (RLLS) was used for cellulose purification using acid as described in procedure 3.3.2.1.

3.3.2 Cellulose isolation

3.3.2.1 Mixture of acetic-acid-nitric-acid

The isolation method was adapted based on the original procedures described by Sun *et al*. (2004) with minor modifications. The dried insoluble residues of RLLS were treated in a mixture of 80% of acetic acid and 65% of nitric acid using a ratio of 5:1. The ratio of solvent-to-LLS has a high significance to the physical appearance of the cellulose (color and size of fibrils). The solution was heated at 90 °C for 1 hr under reflux. Then, the solution was cooled at room temperature and filtered. The insoluble whitish residue was washed repeatedly with distilled water until the pH of the washing distillate water became pH 5-6. After that, the residue (cellulose) was dried in the oven. The mass of dried cellulose was measured. Appendix A showed the steps involved for the cellulose isolation.

3.3.2.2 Alkaline and bleaching method

Non-polar compounds such as oil, fats, and waxes were removed from the LLS by soxhlet extraction. The LLS (200 g) were weighed and placed inside the cellulose timble. The timble was loaded into the chamber of the soxhlet extractor and a mixture of ethanol and benzene (1:2 v/v) was placed in a distillation flask. The extractor and distillation flask were connected together and placed on the heating mantle. Then, it was heated to reflux for 48 hours. After the extraction was completed, the ethanol benzene mixture extract was discarded and the solid LLS that remained in the thimble was collected and dried in the oven at 103 ± 2°C for 24 hr.

The isolation method was adapted based on the procedures described by Elanthikkal *et al*. (2010) and Henrique *et al*. (2013). The dewaxed LLS (100 grams) was treated four times with 2 liters of 1 M sodium hydroxide aqueous solution for 4 hr at 80°C under mechanical stirring and washed several times with distilled water until the NaOH was completely removed. Then, it was dried at 40°C for 24 hr in an air-circulating oven. After that, the bleaching treatment was done to whiten the sample. It was performed by treating the sample with 5% NaOCl at 30°C for 3 hr. After this treatment, the sample was washed with deionised water until pH of 7 was reached.

3.4 Preparation of microcellulose

The acid hydrolysis of MSLL-cellulose was conducted according to a method described in the literature (Chuayjuljit *et al.*, 2010; Haafiz *et al.*, 2014) and based on a classic method (Battista, 1950). The prepared cellulose was hydrolysed with 2.5 M hydrochloric acid under reflux for about 1 hr at 90°C-100°C and the ratio of cellulose over solvent used was 1:20. The hydrolysed cellulose was filtered through cotton cloth and washed repeatedly with distilled water until it was free from acid. The solid residue (MCC) was dried in the oven at 105°C and stored in a desiccator until further evaluation was carried out. The MCC obtained after drying was snowy-white in appearance.

3.5 Preparation of cellulose nanocrystals

A few attempts had been made to produce nanocellulose from cellulose LLS as shown in Appendix B. Different reaction time and speed of mechanical stirrer were used to ensure the success of nanocellulose produce. Cellulose nanocrystal (CNN) was prepared using acid hydrolysis method. Cellulose isolated from LLS was used as a raw material for preparation of microcellulose and nanocellulose.

3.5.1 Isolation of cellulose nanocrystal

Nanocrystalline cellulose was prepared by following the procedure outlined by Jiang and Hsieh (2015). The acid hydrolysis of cellulose fiber was accomplished with 64 wt % sulphuric acid at an acid-to-cellulose ratio of 10 ml/g. The hydrolysis reaction was conducted at 45°C under constant stirring for 1 h. The reaction was stopped by adding 4–5 times cold distilled water based on the volume of the reacting mixture. The nanocellulose suspension was centrifuged at 10,000 rpm for 10 min to obtain a precipitate. This process was repeated until the pH of the suspension was around 5. The solid suspension was then dialyzed against distilled water for several days until the pH became constant using dialysis tubing with a 3000 molecular weight cut off. The experimental set up as shown in Figure 3.2. The nanocellulose suspension was then sonicated with Ultrasonic Liquid Processors S4000. It was done by immersing it in ice bath to avoid heat-up for 5 min at 40% amplitude as to disrupt the large cellulose aggregates. Subsequently, the suspension was stored in a refrigerator at 4°C and designated as cellulose nanocrystal.

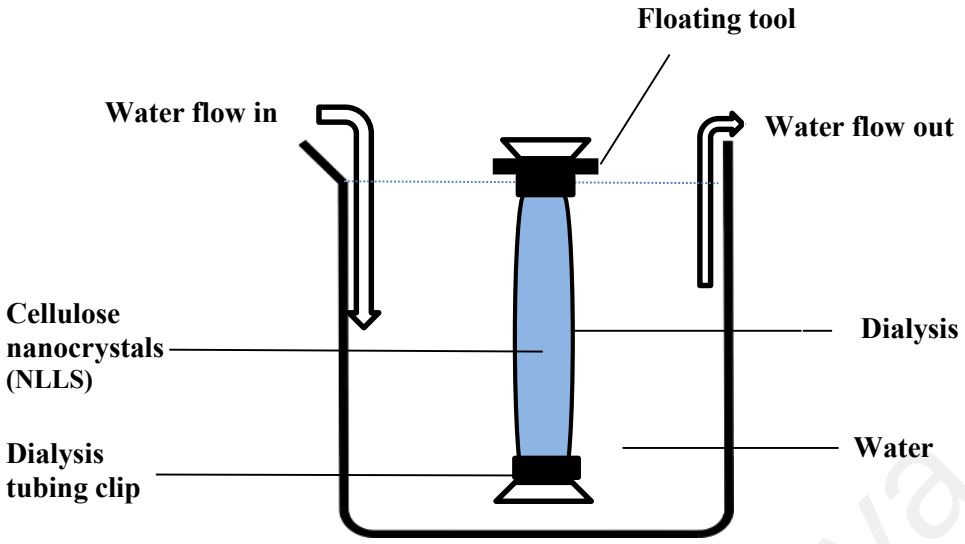

Figure 3.2: Dialysis process using dialysis membrane.

3.6 Characterization of cellulose material

A few tests were conducted to characterize the prepared cellulose and microcellulose such as fourier-transform infrared spectroscopy, thermal gravimetric analysis, differential scanning calorimeter, field emission scanning electron microscopy, gel permeation chromatography, and x-ray diffraction.

3.6.1 Field emission scanning electron microscopy

Field emission scanning electron microscopy was carried out using JEOL JSM-7600F. A small amount of the LLS, cellulose, and MCC samples were prepared by dispersing dry powder on double-sided conductive adhesive tape. The FESEM micrographs were obtained to study the surface morphology and crystallite size of each sample.

3.6.2 X-ray diffraction

Diffraction patterns of the samples were performed with an x-ray diffractometer (X'Pert PRO MD PANalytical). XRD patterns were recorded in the 2θ range of 10-90° with an automated X–ray using CuK α radiation as the beam source (λ=1.5418 Å) and a scan rate of 1.5° min^{-1}. The operating voltage was 35 kV and tube current was equal to

30 mA. The crystallinity index (CI) of the samples was determined according to the Segal empirical formula (Segal *et al*., 1959):

$$CI(\%) = \frac{I_{002} - I_{AM}}{I_{002}} \times 100 \quad (3.6)$$

Where CI is the crystallinity index, I_{200} is the maximum intensity of the peak at 2θ = 22.6°, and I_{AM} is the lowest intensity of the amorphous measured between the plane 100 and 200 at about 2θ = 18-19°.

3.6.3 Fourier transform infrared spectroscopy

Fourier transform infrared spectroscopy was recorded using a Perkin-Elmer Spectrum 100 IR spectrophotometer. Ultrathin pellets were prepared by mixing 2 mg of each sample (LLS, cellulose, and MCC) with potassium bromide (KBr) powder. ID Spectra of all samples were recorded in the range of 4000-450 cm^{-1} to analyse the difference in the functional groups present.

3.6.4 Thermal gravimetric analysis

A Netzsch thermogravimetric analyzer (TG209 F3 Tarsus model) was used to study the thermal behaviour of the samples. Each sample (10.0 ± 1.0 mg) was analysed from 30-900°C at a rate of 10 °C/min under a nitrogen atmosphere with a gas flow of 80 cm^3/min.

3.6.5 Gel permeation chromatography

Gel permeation chromatography was used to determine the molecular weight of samples. About five grams of soluble cellulose sulfates were dissolved in 5 ml distilled water, and then the solutions were filtered using 0.45 µm syringe. The samples were labelled as CLLS, MLLS, and NLLS respectively. The molecular weights of the samples

were determined using Ultrahydrogel 2000 column gel permeation chromatography. The sample was injected and eluted with 0.05% sodium azide solution at a flow rate of 1.5 ml/min. At the same conditions, a series of dextran standards with different molecular weights from 11600, 23800, 48600, 148000, and 273000 Da were used for plotted standard calibration curve (molecular weight of dextran standards versus elution time). Dextran standards were prepared by weighting 2 mg each and dissolving in 2 ml distilled water. Then, the solutions were filtered using 0.45 μm syringe and were injected to the column of gel permeation chromatography.

3.6.5.1 Conversion of non-soluble cellulose to soluble cellulose

Soluble cellulose was prepared by a slight modification of the method used by *Han et al.* (2008). Six grams of dried of material were dissolved in 100 ml of dimethyl sulphate containing 48 g of urea (8 M). Then, mixture of Me_2SO (100 ml) and concentrated H_2SO_4 (10 ml) were prepared by thorough mixing and the mixture was added drop-wise to cellulose-Me_2SO-urea solution with stirring. The solution was heated to 100°C in a water bath with stirring for 6 hr. The solution was diluted in 2 liters of distilled water and then dialyzed against water for 5 days using dialysis tubing with 3000 molecular weight cut off for 5 days to remove unreacted micro particulate cellulose. The remaining solution in the dialysis membrane was then concentrated in vacuo using rotary evaporator (Eyela model SB-651, Tokya, Japan). The dried cellulose sulphate was kept for gel permeation chromatography analysis. The apparatus for conversion of cellulose sulphate was set up as shown in Figure 3.2.

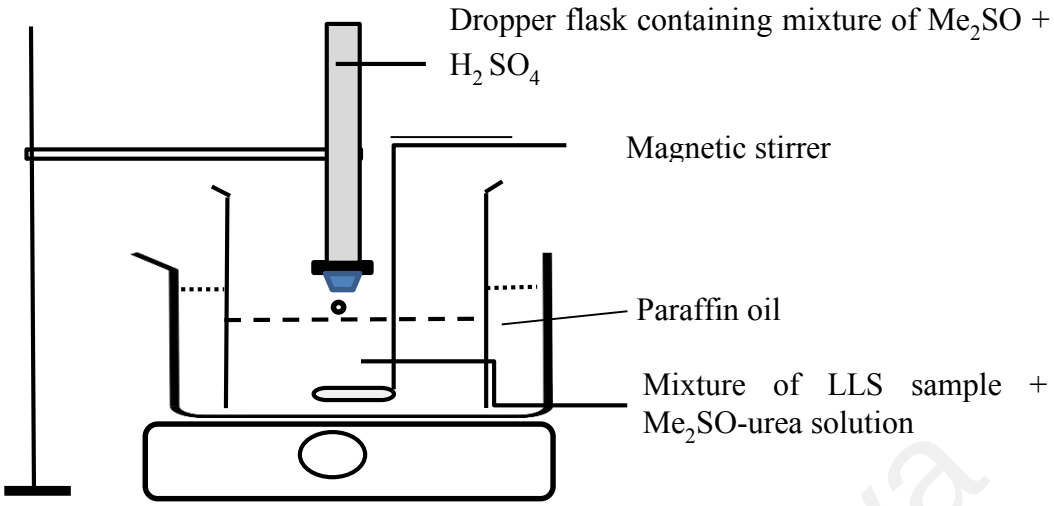

Figure 3.3: Conversion of cellulose sulphate.

3.6.6 Characterization techniques for cellulose nanocrystals

The characterization procedure used for nanocellulose is the same as characterization procedure for cellulose and microcellulose. However, there are two additional tests required for characterization cellulose nanocrystals sample, which are transmission electron microscopy and particle analyzer analysis.

3.6.6.1 Transmission electron microscopy

The morphologies of cellulose nanocrystals from LLS were examined by transmission electron microscopy (TEM). Transmission electron micrographs images were obtained using a TEC-NAI T12 FEI (Germany). A drop of diluted cellulose nanocrystals in aqueous suspension was deposited on a Cu microgrid (200-mesh) and the grid was negatively stained with a 3% (w/w) solution of uranyl acetate and dried at room temperature. The sample was observed at 80 kV. The dimensions of the whiskers were determined using digital image analyses (Image J). Around 30-50 nanocrystal particles were randomly selected to determine the average length and diameter respectively.

3.6.6.2 Particle analyzer

Particle size of nanocellulose was measured using dynamic light scattering (DLS, Zetasizer Nano S90, and Malvern). About 2 mg of dried nanocellulose was weighted and dissolved in 5 ml dimethyl sulfoxide at the ratio of 1:50 (v/v) and ultrasonicated for 30 min (Morais *et al*., 2013).

3.7 Production of glucose

Glucose was produced from cellulose, microcellulose, and cellulose nanocrystals to identify the carbohydrate content. As the main component of lignocelluloses, cellulose is a biopolymer consisting of many glucose units connected through β-1,4 glycosidic bonds. Conversion of cellulose to glucose requires acids such as HCl and H_2SO_4 for breakage of β-1,4 glycosidic, hence resulting in sugar molecule glucose.

3.7.1 Acid hydrolysis

Acid hydrolysis method was adapted on procedure by Morales-delaRosa *et al*. 2014 and Casey *et al*. 2013, with a modification. About 100 mg samples were weighed and placed in 50 ml schott glass bottles. Cold 72% sulphuric acid was added; 3 ml to each sample and stirred thoroughly for about 1 min. Then, 17 ml of distilled water was added to the reaction mixture in order to decrease the concentration of H_2SO_4 to 2 M and autoclaved at 121°C for 2 hr. After the reaction was completed, the hydrolysates were cooled and neutralized using 4 M sodium hydroxide until the pH reached 7.0. Neutralization process caused the formation of the by-product (formation of salt known as sodium sulfate) in the hydrolysate solution. The hydrolysate (sugar) was separated from the sodium sulfate salt by the addition of organic solvent. The salt was filtered and the filtrate containing sugar was dried, weighed, and stored in cold room.

3.7.2 Glucose analysis

The dried hydrolysate product (sugar) was analysed using UV Visible Spectroscopy and High Performance Liquid Chromatography (HPLC). These tests were conducted to identify the purity of the isolated materials in terms of the carbohydrate content and monosaccharide compositions respectively.

3.7.2.1 Ultraviolet spectrophotometer

Total carbohydrate or monosaccharides content in the sample was estimated using the phenol-sulfuric acid method as described by Khamlue *et al*. (2012). This method is based on the original procedures described by Dubois *et al.* (1956).

(a) ***Preparation of sample***

About 100 mg of dried hydrolysates were dissolved in 100 ml distilled water. Next, 10 ml volume of solution was placed into test tubes and 1 ml of 2% phenol solution was added. Then, 5 ml of concentrated sulphuric acid was added rapidly. The solution was systematically mixed in an incubating shaker for 30 min at 30°C. The mixture was then analysed under UV absorbance at ʎ max 490 nm using UV-Vis spectrophotometer (Thermo Fisher Scientific UV–Vis spectrophotometer-model Evolution 300) in triplicates for every tested sample. The amount of carbohydrate content in cellulose hydrolysates was determined and expressed as percentage of glucose.

(b) ***Preparation of standard glucose***

External calibration glucose standards were performed for the quantification of total carbohydrate contents. Stock solution of glucose 100 ppm was prepared by accurately weighing 100 mg of glucose standard. The glucose was dissolved in 30 ml distilled water and then transferred into 100 ml volumetric flask. The distilled water was added until reaching the volume of the volumetric flask. From the glucose stock solution, about five

different concentrations of standard glucose solutions were prepared. Then, 1 ml of 5% phenol solution and 5 ml of concentrated sulphuric acid were added to the series of glucose standard prepared. The mixture was then analysed under UV absorbance at 490 nm using UV-Vis spectrophotometer (Thermo Fisher Scientific UV–Vis spectrophotometer-model Evolution 300) in triplicates for each sample.

3.7.2.2 High performance liquid chromatography

HPLC analysis was performed using a Series LC-10A HPLC system (Shimadzu, Kyoto, Japan) equipped with refractive index detector (RID-10A). Sugars were separated on an aminopropylsilyl column (Agilent) (250 mm 4.6 mm, 5 µm particle size). All samples were filtered through 0.45 µm whattman filter paper. HPLC analysis was carried out by isocratic elution using acetonitrile mixture: distilled water (80: 20, v/v) at a flow rate 0.6 ml/min, oven temperature maintained at 40°C, and injection volume of 5 µl. A mixed standard solution was prepared by dissolving the standard compound of rhamnose, xylitol, arabitol, fructose, glucose, and sucrose in unionized water and diluted to a series of solution to obtain the standard calibration curves.

3.8 Production of bioethanol from cellulose

In this study, microcellulose from LLS was used as a feedstock for the production of ethanol. The microcellulose material was first converted to glucose by acid hydrolysis and then fermented with yeast. Response surface methodology was used in the design of experiments and analysis of results to evaluate the role of some fermentation parameters in affecting ethanol productivity by *Saccharomyces cerevisiae*. Response surface methodology was used to determine the optimum condition for bioethanol production from microcellulose LLS. The experimental design and statistical analysis used was performed by using MINITAB 17.

3.8.1 Preparation of inoculum culture of Saccharomyces *cerevisiae*

Saccharomyces cerevisiae that was used in this study was obtained from commercial baker yeast, Mauripan brand. About 1 g of yeast was added in 15 ml of distilled water. Active culture for inoculation were produced by growing the yeast in potato dextrose algae (PDA) and potato dextrose broth (PDB) with constant shaking at 60 rpm, 30°C and for 24 hr.

3.8.2 Design of experiment

The effect of inoculum volume, pH substrate, and reaction time on glucose conversion was studied using a Central Composite Design (CCD) of response surface methodology (RSM). Table 3.1 shows the central composite design. The optimal conditions determined from the design analysis were validated experimentally by three replicates run. The independent variables used in this study are initial pH (x_1), volume of inoculum (x_2), and fermentation time (x_3). The ranges of independent variables were designated by (-1) and (+1) respectively and were fixed based on literature survey (Al-Judaibi, 2011; Izmirlioglu & Demirci, 2012; Turhan *et al*., 2010).

Table 3.1: Level of the test variables used for design of experiment.

Variables	Unit	-α	Low (-1)	High (+1)	+α
pH	-	4	4.5	5.5	6
Inoculum volume	ml	8	10	14	16
Time	hr	48	78	168	168

The test variables values listed in Table 3.1 were then applied to MINITAB Software Version 17 to obtain the experimental design. Table 3.2 shows 20 runs of experiment with a combination of test variables.

Table 3.2: Experimental design according to central composite design for production ethanol from glucose hydrolysate.

Run	Factor 1 :pH, (x_1)	Factor 2: Volume, (x_2)	Factor 3: Time, (x_3)
1	4.50	10.00	78.00
2	5.50	10.00	78.00
3	4.50	14.00	78.00
4	5.50	14.00	78.00
5	4.50	10.00	138.00
6	5.50	10.00	138.00
7	4.50	14.00	138.00
8	5.50	14.00	138.00
9	4.16	12.00	108.00
10	5.84	12.00	108.00
11	5.00	8.63	108.00
12	5.00	15.36	108.00
13	5.00	12.00	57.55
14	5.00	12.00	158.45
15	5.00	12.00	108.00
16	5.00	12.00	108.00
17	5.00	12.00	108.00
18	5.00	12.00	108.00
19	5.00	12.00	108.00
20	5.00	12.00	108.00

3.8.3 Fermentation of cellulose hydrolysate

Fermentation experiments were performed in sterile 100 ml Erlenmeyer flasks. Each flask was filled with 100 ml of glucose from LLS (prepared by dissolving 10 g cellulose hyrolysate). The pH value of each flask was adjusted according to the required experimental conditions as shown in Table 3.2. Then, the yeast suspension was transferred to each flask as stated in Table 3.2. Fermentation process was carried out on incubated shaker at 60 rpm and 27°C at different incubation periods from 57 to 158 hr as

shown in Table 3.2. After each fermentation was completed, the fermented products were distilled and the distillate product was collected at temperature ranging from 75°C–80°C (boiling point ethanol = 78.3°C) and recorded as volume of ethanol.

3.8.4 Analysis of bioethanol

Bioethanol produced from the fermentation of glucose hydrolyzate was identified using Gas Chromatography (GC-FID) supplied by Agilent Technologies 6890N and equipped with Flame Ionization Detector with capillary column. The analyses were performed under the following chromatographic conditions: the oven detector was set to 115 ºC, the carrier gas (nitrogen) with a flow of 4.8 ml/min, and the injection volume of samples was 2 µl (Lin *et al*., 2013). The standard calibration curve was prepared using ethanol (99.9% purity). A series of volume of ethanol was pipetted (0.5 ml, 1.0 ml, 1.5 ml, 2.0 ml, and 3.0 ml) into a 10 ml volumetric flask. Then, the volumetric flask was marked up to volume with distilled water. The graph area of the peaks against percent ethanol was plotted and used for ethanol calculation. The ethanol yield was calculated using the following equation and formulae below. Refer Appendix C1 and Appendix C2 for detail calculation:

$$C_6H_{12}O_6 \longrightarrow 2\,(CH_3CH_2OH) + CO_2$$

$$\text{Yield of ethanol (\%)} = \frac{\text{Actual ethanol yield}}{\text{Theoretical ethanol yield}} \times 100 \qquad (3.7)$$

CHAPTER 4: RESULTS AND DISCUSSION

4.1 Characterization of mature seed of *Leucaena leucochephala*

Lignocellulosic biomass is composed of one or a mix of plant parts such as seeds, cones, stems, leaves, and bark. As discussed in Chapter 2, compositional and physical properties of plants and their parts' different fractions vary widely; thus, in order to use a new potential lignocellulosic, the chemical characterization and compositional analysis of LLS need to be carried out. The quality of the LLS is determined by proximate analyses, ultimate analysis, and multicomponent compositions. Lignocellulosic biomass has large variations in terms of moisture contents and ash yield characteristics determined by proximate analyses. The moisture content in biomass is normally measured as air-dried and oven-dried basis and varies in the interval of 3% – 63% depending on the types of biomass (Vassilev *et al*., 2010; Orozco *et al*., 2014). Thus, biomass can be categorized into high and low moisture content biomass. High moisture content of biomass materials is essential to facilitate the drying process for a better control of the process of variables in energy conversion. According to Oliveira and Franca (2009), biomass with high moisture content is more appropriate for a fermentation process, whereas low moisture content is more suitable for thermochemical processes such as combustion, pyrolysis, or gasification.

The moisture and ash content of LLS is around 12%. This is in agreement with Sethi and Kulkarni (1994), who found the amount of moisture in two varieties of *Leucaena* seeds in the range of 10% - 15%. It has been reported that the physical properties such as length, width, and thickness of the seeds affect the moisture in the range of 4.75% – 19.57% for *jatropha curcas* (Garnayak *et al.*, 2008). The same finding was also reported for watermelon seeds (Koocheki e*t al*., 2007) small amount of ash around 4% produced at combustion temperature 550°C by which the yield did not differ much from that of

Meena Devi *et al*. (2013), who found ash content of *Leucaena leucocephala* seeds at 3.7%. Meanwhile, Sethi and Kulkarni (1994) discovered ash content in two varieties of *Leucaena* seeds in the range of 6%-14%. Vassilev *et al*. (2010) revealed that ash yield is influenced by the composition, abundance, and origin of the biomass constituents; thus, it should be interpreted together with the genesis of constituents in biomass. The low ash content is preferred because it does not create any major problems such as slagging and deposit formation during the thermal process (Vassilev *et al*., 2010; Thiagarajan *et al*., 2013).

Table 4.1: Characteristics of LLS.

Parameter	Value (%)	Component	Weight (wt%)
Moisture	12±0.26	C	44.4
Ash	4.2±0.55	H	6.1
Holocellulose	51.9±2.34	N	4.7
α-cellulose	27.5±1.56	S	0
Lignin	16.9±1.43	O	44.8

The proportions of C, H, N, S, and O in the biomass are depending on the species of biomass, growing condition, and geographical situation of the region. Table 4.1 gives an elemental analysis of LLS. Among all these elements, carbon (C) and oxygen are the highest among most biomasses with approximately 44%. According to Vassilev *et al*. (2010), the C content in biomass varies in the range of 42% – 57% and decreases in the following order: woody biomass > agricultural by-products and residues > herbaceous and agricultural biomass > straws > grasses. Ragland *et al*. (1991) showed that the C content of softwood biomass was 50%-53% and hard wood biomass in the range of 47%-50%. In addition, the amount of C varies depending on the amount of lignin and extractives present in the biomass (Ragland *et al*., 1991).

The cellulose content of LLS was around 28%, which indicated that LLS is a suitable material to be used as substrate for cellulose production. Cellulose content of LLS was higher in the present study compared to the reported values (Singh *et al*., 2002) with 16.5%. The amount of cellulose was in agreement with Sun and Cheng (2002), which reported that the amount of cellulose in nut shell was in the range of 25% - 30%. The cellulose content in LLS is approximately similar to the results from oilseed rape, olive husk, and legume straw (García *et al.*, 2016), and higher than in fruit wastes such as oranges, bananas (Orozco *et al*., 2014), mangoes leaves (Sun & Cheng, 2002), and melon seeds (Pius *et al.*, 2014) but lower than that from soy hulls (Flauzino *et al*., 2013), potato peel (Lenihan *et al*., 2010), *jatropha* seed husk (Thiagarajan *et al*., 2013), and rice straw (Binod *et al*., 2010).

The composition of lignin depends on the type of material and it varies widely from different hardwood, softwood, and agricultural residues (Taherzadeh & Karimi, 2015; Wahab *et al*., 2013). Watkins *et al*. (2015) reported that alfalfa fibers yielded the highest lignin content of 34% followed by pine straw, wheat straw, and flax fibers with lignin contents of 22.65%, 20.40%, and 14.88% respectively. In this study, the lignin content in LLS was 16.9%. Unlike cellulose and hemicellulose, lignin needs to be isolated because it cannot produce monosaccharides by hydrolysis. Lignin acts as a binder with cellulose and hemicellulose; thus, the relatively low lignin content is required, which means that it is easy to treat and fractionate in releasing carbohydrates for fermentation. However, Yoon *et al*. (2014) reported that lignocellulosic biomass generated less fermentation inhibitors such as furans and formic acid than the delignified biomass such as pure cellulose or holocellulose under the same reaction condition.

Biomass also contains a small content of inorganic species or minerals, such as magnesium, zinc, calcium, and sodium. as a result of nutrients uptake during its growth. Mineral matter in LLS consists mostly of salts of potassium, calcium, and magnesium

and other elements are present in lesser amounts. The trend of the mineral content in the seeds of LLS as shown in Figure 4.1 was in a descending order of K > Ca > Mg > Fe > Na > Mn > Cu. According to Ragland *et al*. (1991), the content of mineral in biomass varies in between and within species, soil types, and growth rate. In an analysis of the effects of inorganic species, Pang *et al*. (2015) found some minerals such as Ca and Na that decreased the catalytic conversion of cellulose to ethylene glycol.

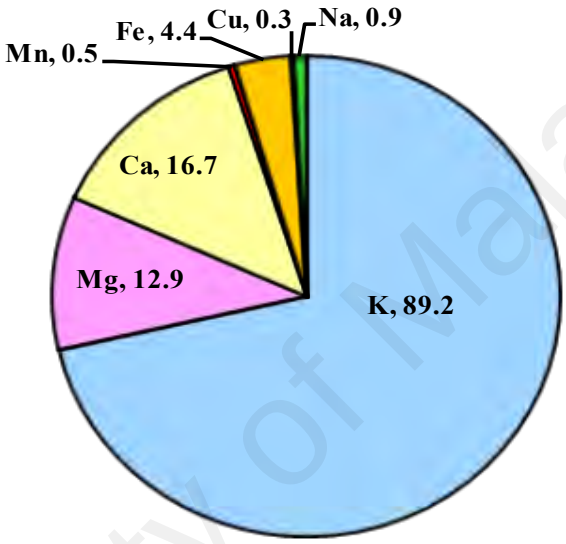

Figure 4.1: Composition the inorganic species in LLS (unit in mg/L).

4.2 Preparation of cellulose from LLS

Leucaena leucocephala seeds consist of mainly lipid, protein, and carbohydrates. Carbohydrates, particularly polysaccharides, can be exploited by various industries. This study presents the extraction of cellulose from LLS to increase the value and efficient utilization of the seeds. Successful cellulose isolation depends on the pre-treatment stage. The aims of pretretament are to break down the lignin that covers the outer wall layer of lignocellulose material, increase pore size, and reduce cellulose crystallinity by opening up the crystalline structure. Different pre-treatment methods have been reported to remove the non-cellulosic components; it can either be physical or chemical as well as combination of both as proposed and applied (Mosier *et al*., 2005; Zhu *et al*., 2005;

Punsuvon *et al.*, 2008; Taherzadeh & Karimi, 2015). Pre-treatment has been viewed as one of the most expensive processing steps in cellulosic biomass; therefore, this study aimed to develop simple and cost-effective processes to completely or partially remove the non-cellulosic components.

4.2.1 Effect of hot water treatment

The purpose of treatment using hot boiling water prior to acetic acid-nitric acid extraction is to remove any primary metabolites such as soluble and insoluble polysaccharides, protein, and acid soluble lignin from the LLS. Several secondary metabolites such as amino acids, tannins, and saponin are expected to be removed from LLS as well. To reduce the process costs related to pre-treatment, non-cellulosic material of LLS was removed by treatment with boiling water at 100°C under reflux for 1 hr, 2 hr, and 3 hr. The aim of this study was to scrutinize the effect of boiling time on the pattern of FTIR spectra (structural changes). Figure 4.2 shows the FTIR spectra of the LLS and cellulose produced from the residue treated at different boiling reaction times. All spectra at different boiling times showed similarity, which demonstrated that their functional groups are also similar.

There were two noticeable peaks at high wavenumbers, the peaks at 3334 cm^{-1} and 2914 cm^{-1} of all samples were associated with hydroxyl groups (OH) and CH_2 groups of cellulose (Chirayil *et al.,* 2014). The appearance of peak at 1643 cm^{-1} was related to the absorption of water due to strong interaction between cellulose and water (Sun *et al.*, 2004; Johar *et al*., 2012). Meanwhile, the peak alocated at 1113 and 1059 cm^{-1} of all samples was attributed to the C-O-C glycosidic linkage and the C-O-C pyranose ring skeletal vibration (Fahma *et al*., 2010; Mandal & Chakrabarty, 2011; Kalita *et al*., 2013). The small peak at 897 cm^{-1} was associated with C-H anomeric specific for β-glycosidic linkages (Haafiz *et al*., 2004).

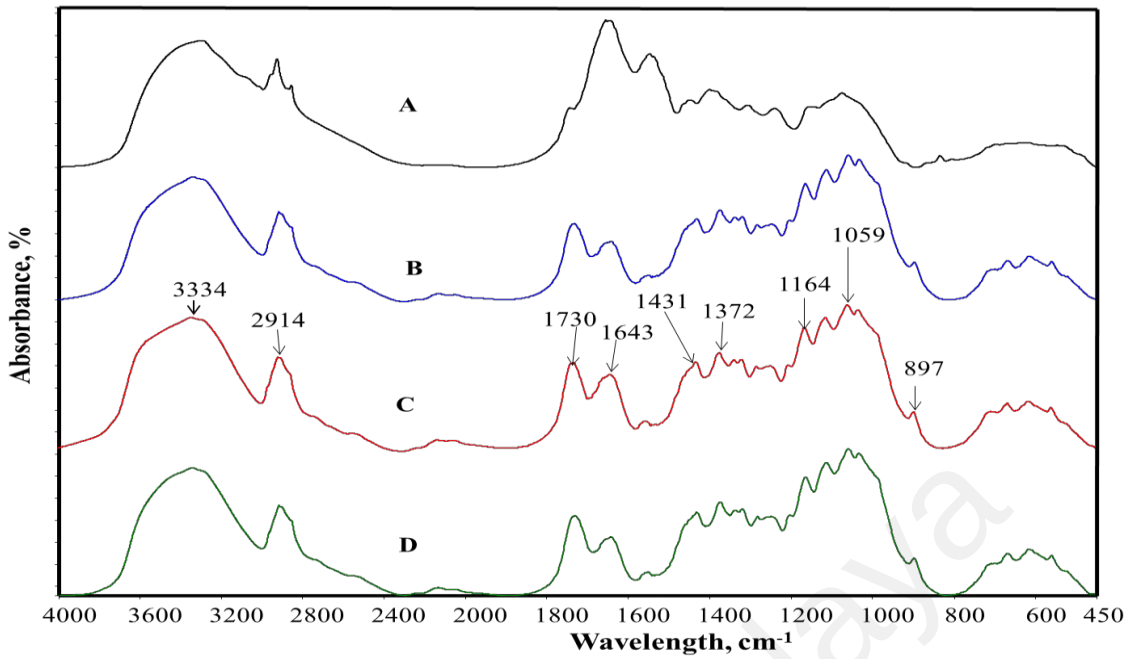

Figure 4.2: IR spectra of the (A) LLS and (B) 1 hr boiling treatment (C) 2 hr boiling treatment (D) 3 hr boiling treatment.

Second derivative FTIR was used to help identify the discrepancy between all spectra. It is suitable to identify the chemical constituents and to compare the effectiveness of treatment. In this study, the second derivative FTIR in the region 1800-1000 cm^{-1} was observed as shown in Figure 4.3 to investigate some overlapped absorption peaks and the effectiveness of treatments. A significant reduction in the intensities of the bands was around 1746 and 1511 cm^{-1}, corresponding to the acetyl or uronic ester groups of hemicellulose and C=C bonds in the aromatic rings in lignin respectively (Elanthikkal *et al*., 2010; Le Normand *et al*., 2014). Another band around 1600 cm^{-1} that was associated with the aromatic ring present in lignin (Mandal & Chakrabarty, 2011) was getting gradually lost when the boiling time increased. The peak at 1049 cm^{-1} in all cellulose samples was due to ether linkage from lignin or hemicellulose that disappeared while it caused an increase in intensity for the peaks at 1031 and 1075 cm^{-1} (Chirayil *et al.,* 2014; Orozco *et al*., 2014).

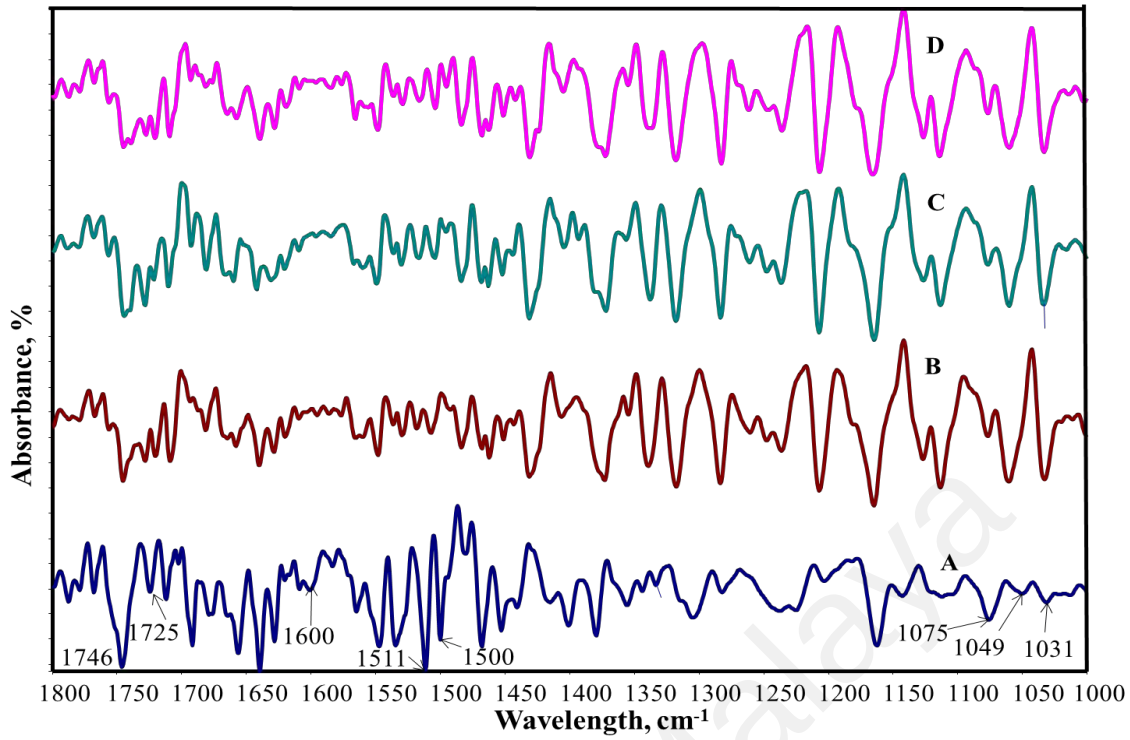

Figure 4.3: Second derivative IR spectra in the range of 1800 – 1000 cm^{-1} of the (A) LLS and (B) 1 hr boiling treatment (C) 2 hr boiling treatment (D) 3 hr boiling treatment.

Figure 4.4 shows the FESEM images of raw LLS and residue of LLS after hot water treatment. The image of raw LLS showed smooth surfaces with compact fibril packing, which typically contain hemicellulose, cellulose, lignin, and other elements (inorganic components). Relative composition was obtained by EDX data, hence revealing that the highest element in the LLS structure is carbon and oxygen. Other elements present in minor percentage are potassium, sodium, magnesium, sulfur, and calcium as shown in Appendix E. After treatment with boiling water under reflux for 2 hr, the image showed that there were changes in the surface of raw LLS.

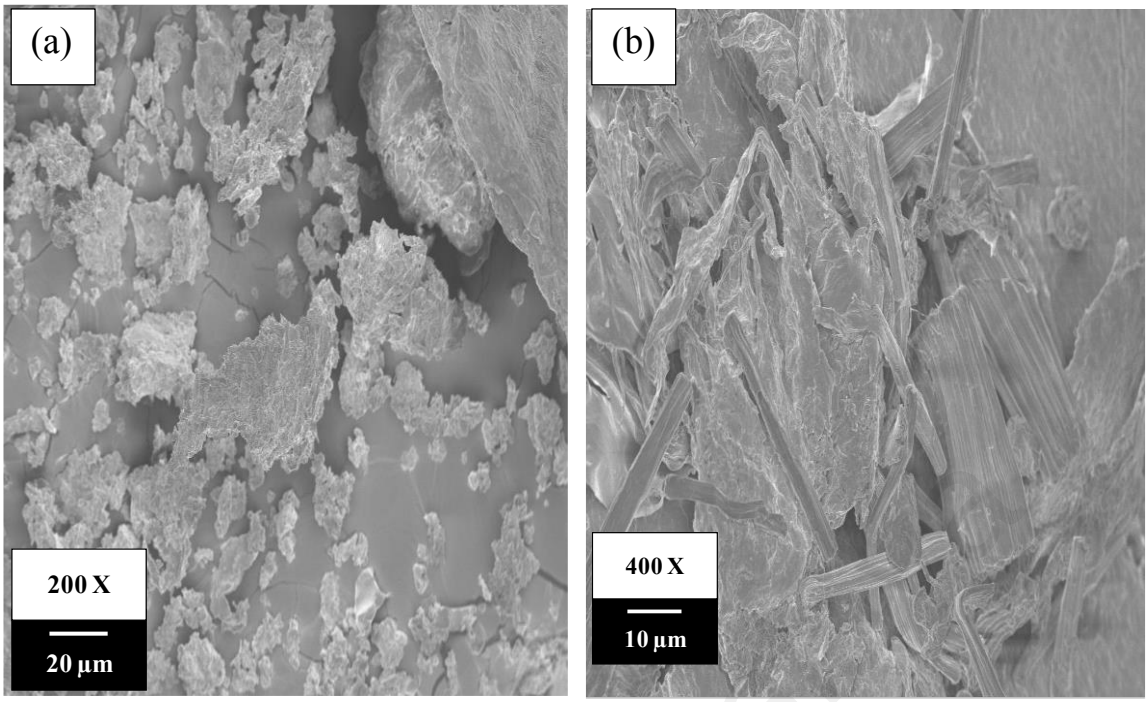

Figure 4.4: FESEM images of (a) raw LLS and (b) residue of LLS after hot water treatment.

In summary, the boiling water under reflux can be considered as one of the cost effective, environmentally friendly, and effectively pre-treatment methods for removal of some non-cellulosic materials such as wax, protein, and soluble hemicellulose.

4.2.2 Comparison of cellulose prepared from acid and alkaline method

Alkaline treatment is a commonly used method and is widely investigated for removal of non-cellulosic materials. Although the alkaline method is a preferable method; however, it still has some disadvantages as discussed in Chapter 2. Thus, in order to compare the impacts of different isolation methods on cellulose preparation, alkaline method was performed. The cellulose obtained was evaluated for its chemical composition by Fourier-transform infrared spectroscopy (FTIR).

The spectra of isolated cellulose obtained from acid and alkaline treatment (Figure 4.5) showed characteristics of cellulose, which had two main fragments at 2900-3500 and

700–1800 cm^{-1}. The typical absorption bands associated with the cellulose were around 3400, 2900, 1430, 1370, 1113, and 897 cm^{-1}. Similar IR pattern of cellulose was obtained by other researcher when isolating cellulose and micro cellulose from agricultural waste (Uesu *et al*., 2000; Johar *et al*., 2012; Merci *et al.*, 2015). Under the investigated condition, the variation of cellulose isolation method had little or no impact on the structural changes of cellulose.

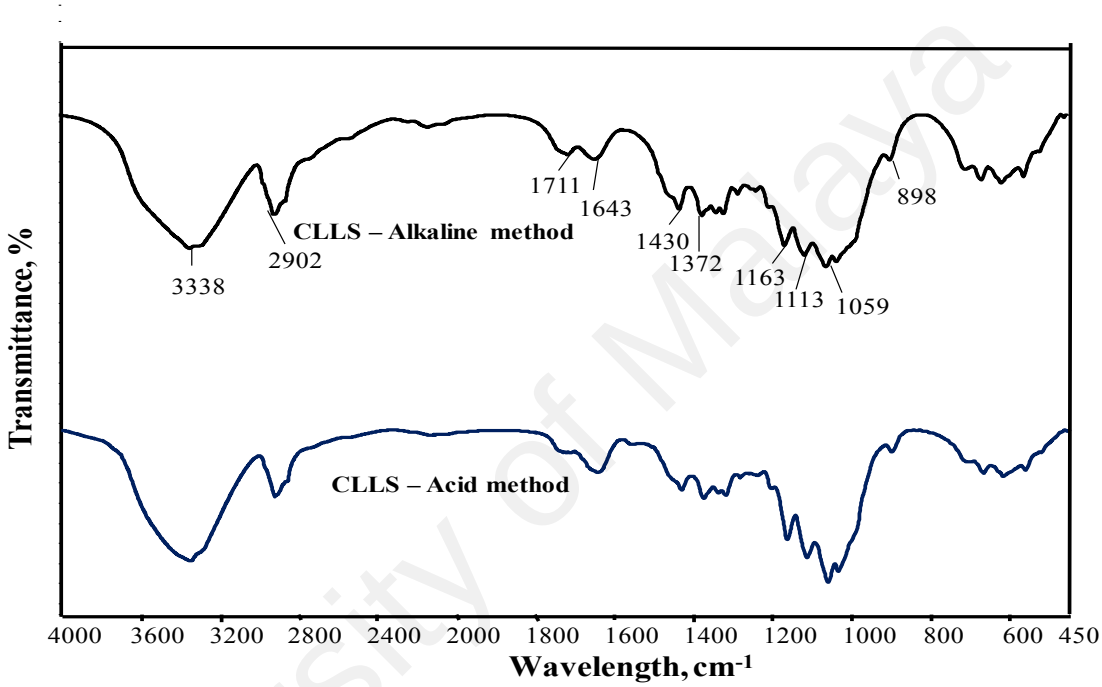

Figure 4.5: FTIR spectra of cellulose produced from alkaline and acid method.

4.3 Characterization of cellulose and microcrystalline cellulose

The yield of LLS-cellulose (CLLS) extracted from LLS was 33% (dry mass) compared to cellulose yield found in mango seeds, which was 29% (Henrique *et al*., 2013) using alkaline treatment method and 30.73% for rice straw by ionic liquid extraction (Jiang *et al*., 2011). After the purification process, the percentage of yield of micro cellulose LLS (MLLS) obtained from CLLS was 71% (dry mass).

4.3.1 Fourier transform infrared spectroscopy

The IR spectra of the CLLS and MLLS are shown in Figure 4.6. The spectra of CLLS and MLLS showed almost identical peaks, indicating that their functional groups were not distinctively different. However, the prominent peak at 1732 cm^{-1} in the spectrum CLLS can be associated with the presence of lignin and hemicellulose. According to several authors, this peak indicates either acetyl or uronic ester groups in hemicellulose or the ester linkage of carboxylic group of the ferulic and p-coumaric acids lignin (Elanthikkal *et al*., 2010; Johar *et al*., 2012; Chirayil *et al*., 2014; Le Normand *et al*., 2014). Almost no similar peak was present in the FTIR spectra of the MLLS. The peaks at 1242 cm^{-1} for CLLS were associated with the C-O out of plane stretching vibration of the aryl group in lignin (Mandal & Chakrabarty, 2011). The appearance of a peak around 1337 in all samples was related to the bending vibration of the C-H and C-O bonds in the cyclic ring of sugar moiety.

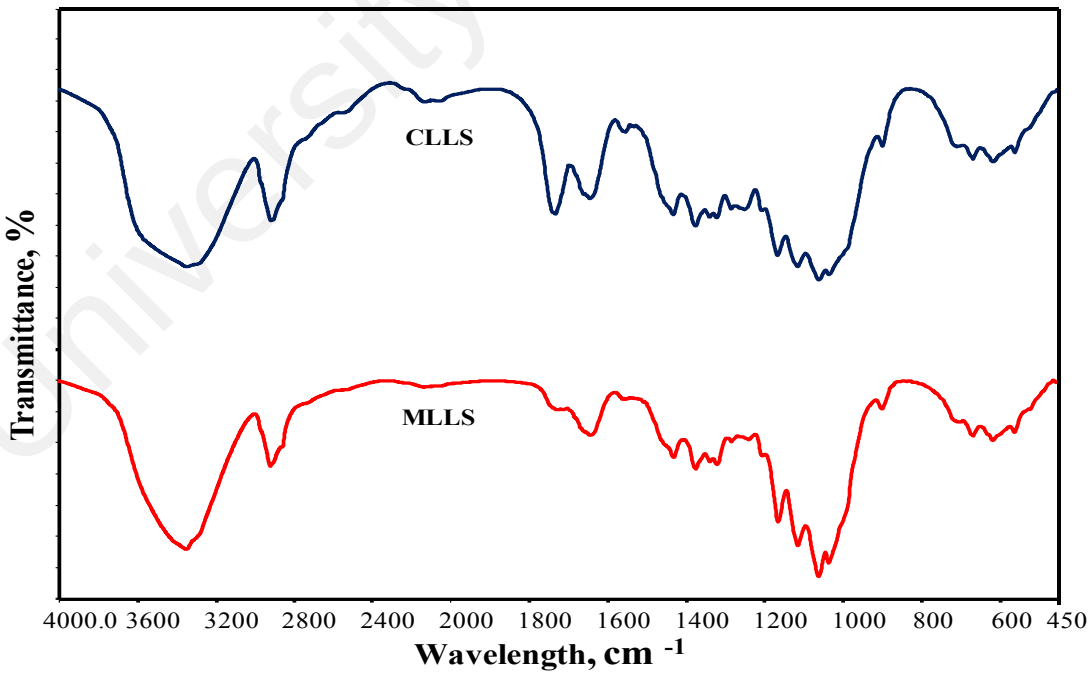

Figure 4.6: Comparison IR spectra of CLLS and MLLS.

The absorption bands at 1430 cm^{-1} and 898 cm^{-1} were observed in CLLS and MLLS. The band that is associated with a symmetric CH_2 bending vibration at 1430 cm^{-1} is called as the crystallinity band and the increase in its intensity demonstrates higher degree of crystallinity (Kalita *et al*., 2013; Trache *et al*., 2014; Shankar & Rhim, 2016). On the other hand, the peak at 897 cm^{-1} is originated from β-glycosidic linkages between glucose units in cellulose (Sun *et al*., 2004) and the intensity will decrease when the crystallinity of the sample increases (Soom *et al*., 2009).

FTIR spectrum of MLLS showed a decrease in intensity for both the crystallinity bands compared to CLLS, which suggested that the crystallinity index cellulose fibrils decreased during the hydrolysis process and this observation will be confirmed by XRD analysis. Higher crystallinity in CLLS can further be confirmed by the increase in intensity of the absorption band from 2916 cm^{-1} to 2917 cm^{-1}, which is associated with C-H stretching (Kalita *et al.*, 2013). The peak range of 3306-3349 cm^{-1} of all samples was associated with intermolecular and intramolecular O-H stretching vibration band. The peaks at 1060 cm^{-1} and 1639 cm^{-1} were detected in all samples due to the C-O-C pyranose ring skeletal vibration and OH bending of absorbed water (Mandal & Chakrabarty, 2011; Kalita *et al*., 2013). In addition, the peak at 1112 cm^{-1} is known as the ring breathing band that corresponds to C-C. Field emission scanning electron microscopy.

4.3.2 Field emission electron microscopy

The FESEM micrograph of CLLS and MLLS are presented in Figure 4.7 and also Appendix F. The surface morphology of CLLS and MLLS obtained comprised individual fibres and a few bundle forms. It was observed that there were more individual fibres obtained in LRRS-MCC due to destruction of fibre bundles during acid hydrolysis. The diameters of individual fibre of MLLS prepared based on acid hydrolysis was around 5-

10 µm, which was similar or lower than other plant fibres as reported by others (Wang *et al*., 2010; Jahan *et al*., 2011; Nuruddin *et al*., 2011).

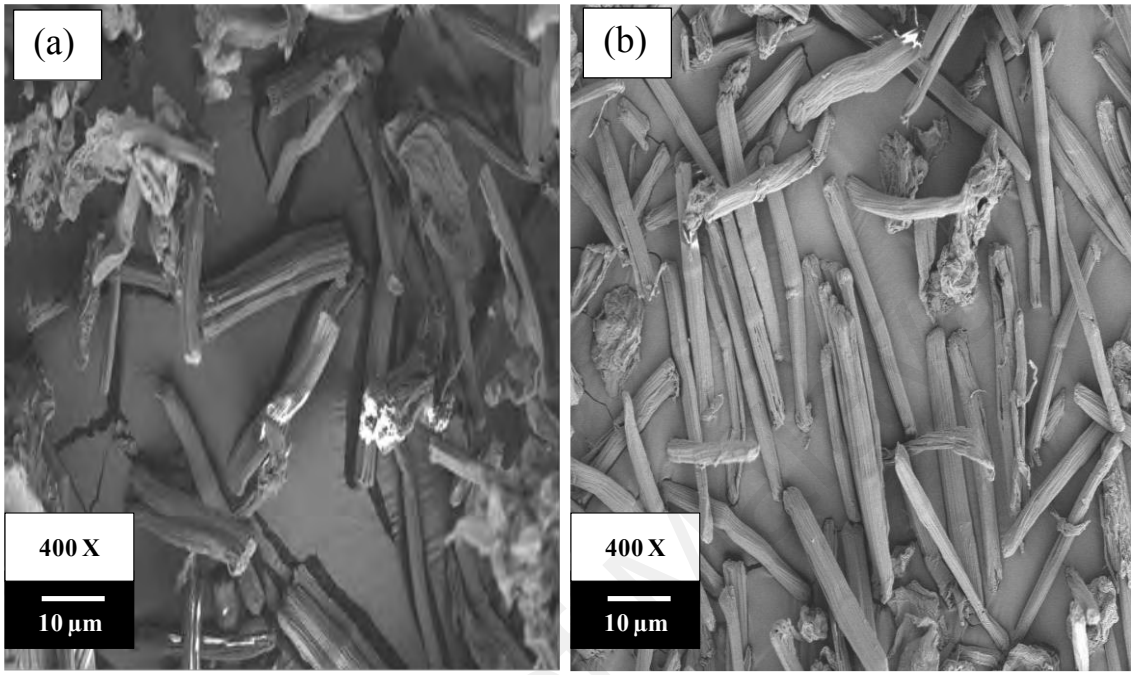

Figure 4.7: FESEM micrograph of (a) CLLS and (b) MLLS.

MCC products, which are derived from wood, have been produced by various manufactures and are available on the market. The distribution of particle size and moisture content of MCC produced are influenced by the selection of drying techniques (Thoorens *et al*., 2014). Commonly, commercial MCC is manufactured by spray drying. However, spray drying parameters have the tendency to affect MCC properties, hence resulting in possible different grade of MCC (Gamble *et al*., 2011).

4.3.3 X-ray diffraction

Biomass crystallinity estimation is very important in order to give the researcher information about the digestibility of the sample. At present, there are four techniques that can be used to determine the crystallinity index (CI) of the materials which are XRD, solid state 13C NMR, infrared spectroscopy, and Raman spectroscopy. XRD has widely been applied to obtain the CI even though there are limitations mentioned by several

authors (Park *et al*., 2010; Poletto *et al.*, 2014). Image based on Figure 4.8 indicates the presence of cellulose type 1 with absence of the doublet located at main diffraction peak (22.6°). Qualitatively, the peak intensity of CLLS appeared to be higher than MLLS and LLS, which showed that the CLLS was more crystalline than others. CI of the CLLS was reduced after being converted to cellulose micro fibrils (MLLS from 57.5% to 80.3% respectively), thus indicating that MLLS structure is more rigid than CLLS. High crystallinity materials are suitable to be used in biocomposite processing.

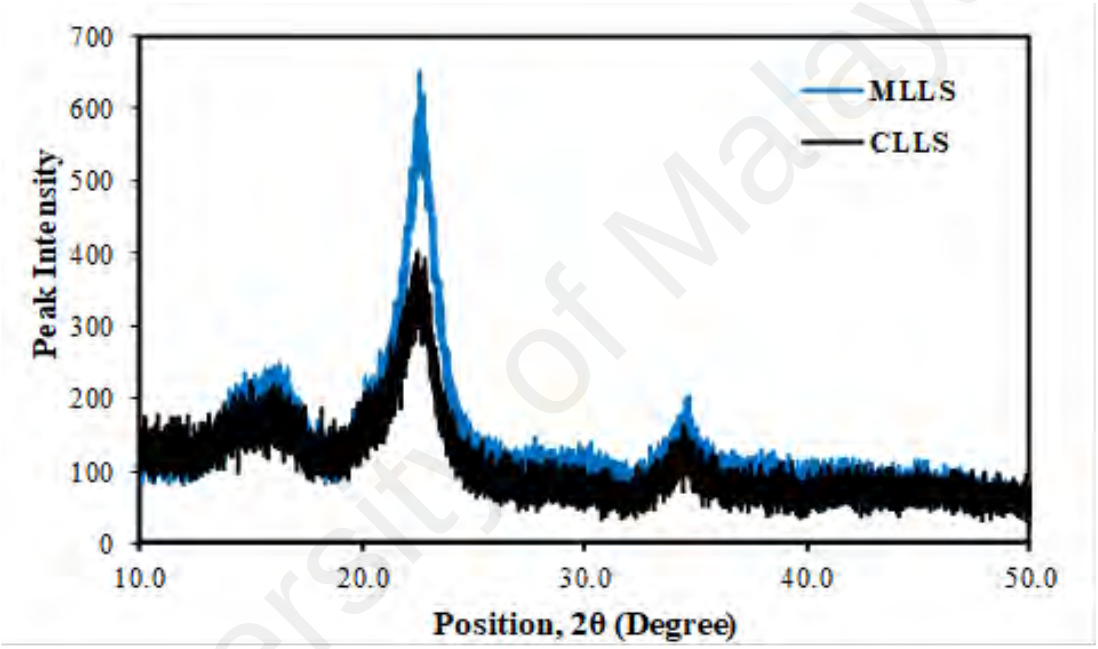

Figure 4.8: X-ray diffraction patterns of the CLLS and MLLS.

4.3.4 Thermal gravimetric analysis

Data from Thermo gravimetric analysis (TGA) is very useful to evaluate the thermal stability of natural fibres in order to be used in bio composite processing. The mixing process of bio composite (polymer matrix and natural fibers) occurred at high temperature, which was above 200°C; thus, the degradation profile of the lignocellulosic materials must be identified. Figure 4.9 and Figure 4.10 show the TGA and DTG behaviors. The initial stage of all samples known as the drying stage occurred at temperature ranging from 29 – 120°C. Many studies reported that at the initial stage, the

weight loss was due to water evaporation in the cellulose (Mandal & Chakrabarty, 2011; Johar *et al*., 2012; Trache *et al*., 2014). The rate of temperature for water evaporation depends on the original moisture content of the sample. LLS shows three important degradation steps, which are regarded as degradation of hemicellulose, cellulose, and degradation of lignin. It was reported by Yang *et al.* (2007) that the degradation temperature for hemicellulose and cellulose occurred at 220 – 315°C and 315 – 400°C respectively. The degradation of lignin slowly occurred at temperature ranging from ambient to 900°C; thus, the decomposition was overlapped in between hemicellulose and cellulose. A similar profile was reported for fibres from wood (Park *et al*., 2010).

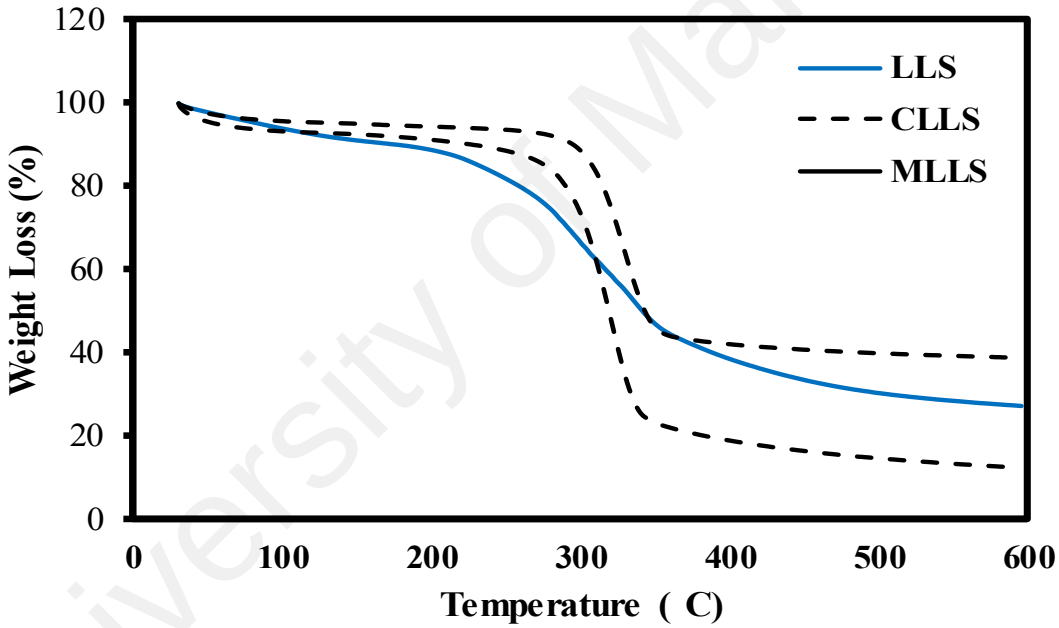

Figure 4.9: TGA behavior of the CLLS and MLLS.

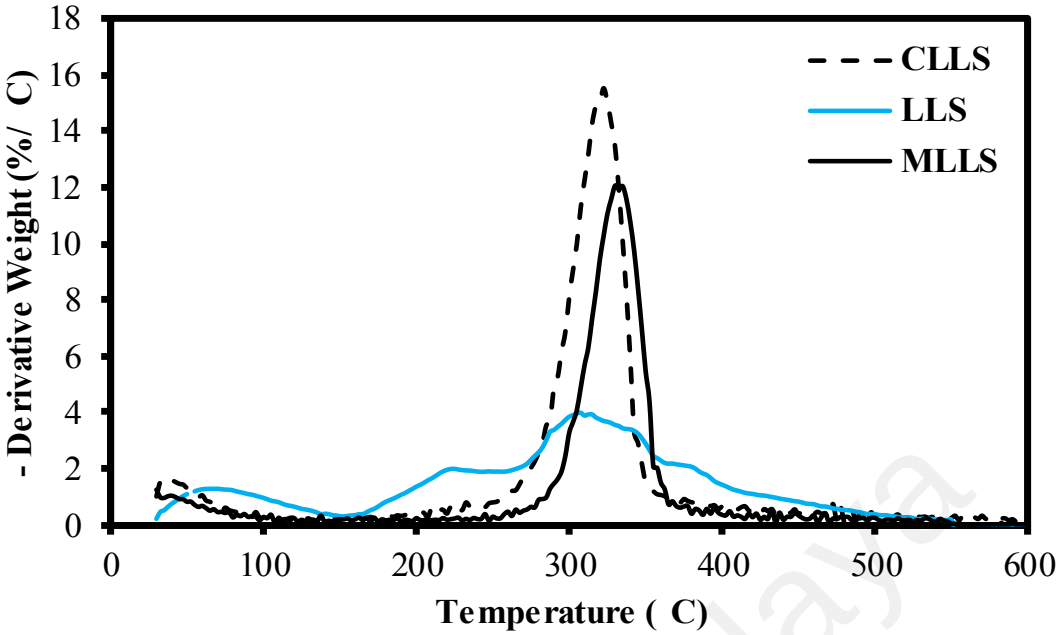

Figure 4.10: DTG curves of LLS, CLLS and MLLS.

The decomposition peaks where the maximum mass loss occurred for CLLS and MLLS were at 320.8°C and 329.5°C respectively. Higher degradation peak of MLLS than CLLS might be due to the difference in the degree of crystallinity (García *et al*., 2016) or reduction of molecular weight (Mandal & Chakrabarty, 2011), while the degradation pattern for CLLS and MLLS obtained were found to be similar to the patterns of jute and oil palm biomass (Fahma *et al*., 2010; Jahan *et al*., 2011; Haafiz *et al*., 2013). It can be predicted that the presence of hemicellulose, lignin, and other non-cellulosic constituents which decompose at low temperatures helps to cause early onset of degradation of the LLS. Thus, the removal of all these non-cellulosic materials helps to rise in the onset temperature of degradation. The thermal degradation data onset temperature and maximum degradation temeperature (T_{max}), and the residual weight at 600°C are listed in Table 4.3. Further heating until 600°C revealed that weight loss and residual weight of MLLS was higher than CLLS. This result is due to the higher amount of crystalline domains cellulose in MLLS which are intrinsically flame resistant (Mandal & chakrabaty, 2011; Trache *et al*., 2014).

Table 4.2: Thermo gravimetric parameters for the thermal degradation processes of CLLS and MLLS.

	Degradation Peak Temperature (°C)		
Samples	**Onset (°C)**	**T_{max} (°C)**	**Residual Mass (wt%)**
MLLS	325	320.8	38.7
CLLS	319	329.5	12.8

4.4 Characterization of cellulose nanocrystals

Nanocellulose has raised a great interest and been applied in many fields such as pharmaceutical, biomaterial, textiles, and others (Chen *et al*., 2014; Jose *et al*., 2014; Lin & Dufresne, 2014; Othman, 2014). Cellulose consists of crystalline and amorphous regions; its composition depends on source of the original cellulose. For that reason, diverse lignocellulosic sources are used as sources for the generation of nanocellulose. Additionally, different approaches have been employed to prepare nanocellulose where its properties and applications are influenced (Palme *et al*., 2016). The yield of nanocellulose prepared from CLLS was 27%. Bondeson *et al.* (2006) isolated nanocellulose from microcrystalline cellulose by hydrolysis in 63.5 wt% sulfuric acid at 45°C for 2 hr and the yield of their nanocellulose product was only 30%. Further, Lu *et al*. (2016) stated that the cellulose nanocrystal produced through hydrochloric acid hydrolysis tends to give low yield of 20%, which is probably due to disintegration of amorphous regions and degradation of crystalline parts during hydrolysis.

4.4.1 Morphology analysis

There are many interesting features that constitute cellulosic materials; a few examples include unique morphology, biodegradability, and high strength. Consequently, they are useful in various fields such as biomedical, energy, environment, and reinforcement in polymer matrix. However, there is a need for the

production of larger quantities of cellulose in industrial application, which demands the production capacity to be optimized. FESEM micrographs in Figure 4.11a show that the aggregation of cellulose was broken down after acid second hydrolysis process and further reduction in diameter or size of fibrils. The nanocellulose prepared by the acid hydrolysis exhibited a rod-like shape and individualized. It also shows that the nanocellulose was aggregated with each other (Figure 4.11b). Similar result has been reported by Morais *et al.* (2013).

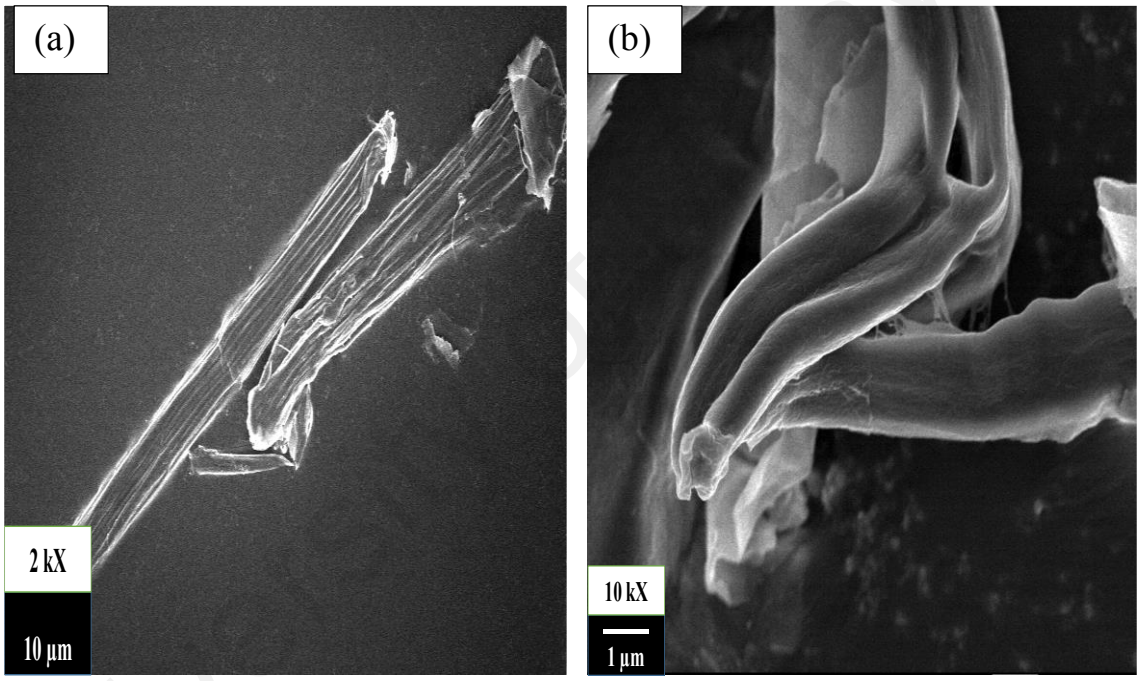

Figure 4.11: FESEM micrograph (a) individual particle of nanocellulose (b) agglomeration of nanocellulose.

4.4.2 Transmission electron microscopy

The TEM image of nanocellulose from LLS is shown in Figure 4.12. These images show individual long fibers and attached together, which had a diameter in the range of 2–11 nm. The length cannot be measured precisely because it is difficult to discriminate the both ends of the nanoparticle. Nevertheless, the TEM images predicted these cellulose nanofibrils in the range of 200 nm – 300 nm in length. Therefore, the aspect ratio of the

nanocellulose from LLS is expected to be too high in the range of 70 – 90 nanometer. This is also corroborated by Chirayil *et al*. (2014), which showed that the structure of the fibrils were associated with one another. Similar findings were also reported by previous studies (Henrique *et al*., 2013; Deepa *et al*., 2015). High aspect ratio (L/D) obtained from the previous studies reported on garlic straw residues (Kallel *et al*., 2016), *Syngonanthus nitens* (Siqueira *et al*., 2010), and spruce bark (Le Normand *et al.*, 2014). The aspect ratio reported in the literature for cellulose nanocrystal varies from plant material and process. Deepa *et al.* (2015) observed that the morphology and size of the nanocellulose vary in different sources. On the other hand, Rosa *et al*. (2010) studied the effects of preparation conditions, such as bleaching and hydrolysis time on the dimensions of cellullose nanowhiskers. They observed that there was no major difference in the aspect ratio measured from different conditions of preparation. In addition, the dimension of the individual fiber was close to the value reported for cellulose nanocrystal isolated from spruce bark (Le Normand *et al*., 2014). Nanocellulose with high aspect ratio is a good criterion to be used as a filler in biocomposite (Kallel *et al*., 2016; Marett *et al*., 2017) it helps to improve the mechanical strength of the material.

Large fiber bundle was also observed in the TEM samples. Typically, laterally aggregated fiber was observed from the TEM images, which formed a network due to high specific area and strong hydrogen bonds established between the nanoparticles. The morphological results obtained by microscopy were similar to those of other reports that extracted cellulose nanocrystals from different sources such as mango seeds (Henrique *et al.*, 2013), tomato peel (Jiang & Hsieh, 2015), and banana peel (Tibolla *et al.,* 2017).

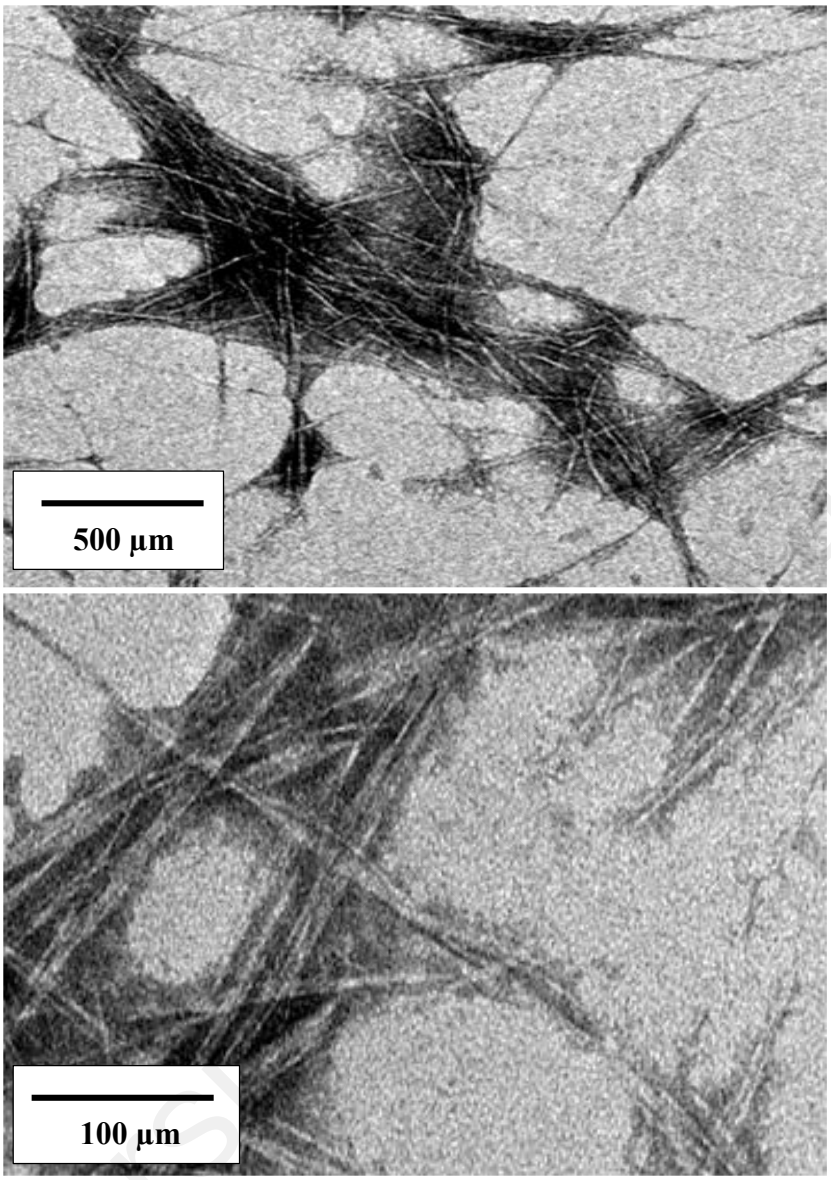

Figure 4.12: TEM micrographs of nanocellulose.

4.4.3 Particle analyzer

The particle size distribution of nanocellulose was not uniform and resulted in two regions: 97.5% of the particles were around 136.9 nm and 2.5% were around 4302 nm. Similar finding was also reported from the isolation of cellulose nanoparticles from other sources by acid hydrolysis (Morais *et al*., 2013; Mendes *et al*., 2015). The particle size distributions measured by particle size analyser are not similar with the TEM result. It was reported that nanocellulose diameter that varies from 10 nm to 80 nm and length ranging from 100 nm to 1000 nm (Kallel *et al*., 2016; Marett *et al.*, 2017).

4.4.4 FTIR analysis

Figure 4.13 shows the FTIR spectra of nanocellulose-LLS obtained from two stages acid, indicating the changes in chemical composition of the fibers. The most distinct absorption peak was observed on the cellulose at 1730 cm^{-1} and was attributed to the C=O stretching vibration of the acetyl and uronic ester groups of lignin and/or hemicellulose (Jonoobi *et al*., 2011). Another significant peak was noticed at 1551 cm^{-1}, as present only in cellulose due to the C=C stretching in lignin. These peaks disappeared in the spectra of nanocellulose-LLS, which indicated the removal of lignin and hemicellulose residues during the second step of acid hydrolysis. Additional absorbance band at 1203 cm^{-1} appeared in the spectra as an indication of sulphate groups that were introduced during the second step of acid hydrolysis, attributing to S=O vibration (Xie *et al*., 2016). Besides these, the spectra of all samples showed typical absorption band and were similar to the characteristics of nanocellulose extracted from other sources (Deepa *et al*., 2015; Ditzel *et al*., 2017; Smyth *et al*., 2017).

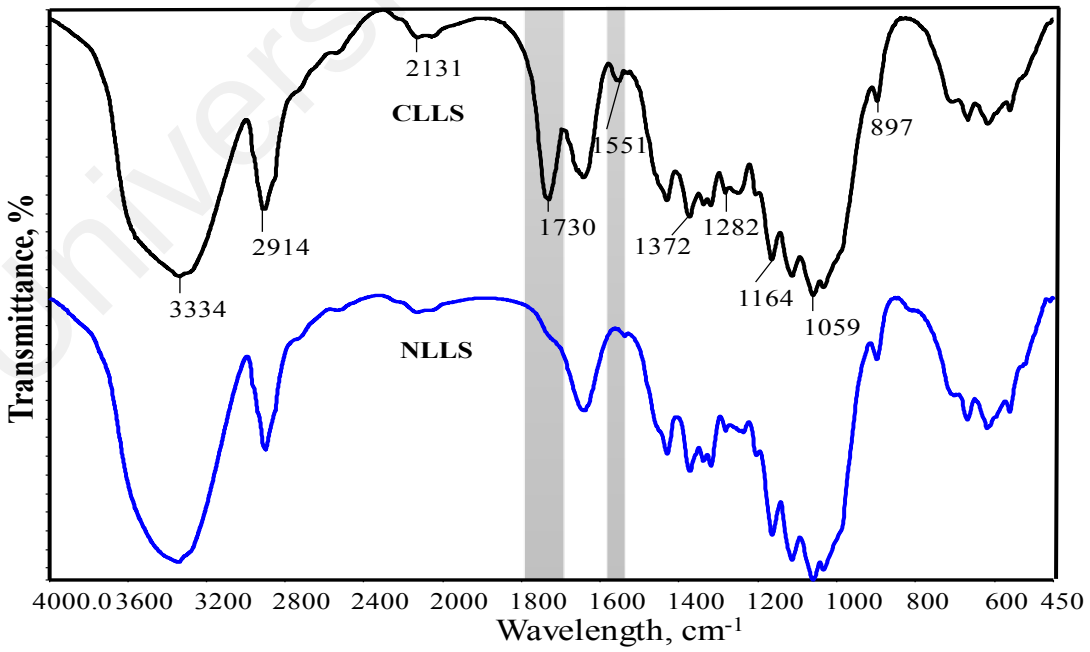

Figure 4.13: IR spectra of NLLS in comparison with CLLS various stages of processing.

4.4.5 Thermal stability

Figure 4.14 illustrates two stages of decomposition of both CLLS and NLLS. A small weight loss in the region of 30°C-100°C was related to the vaporisation and removal of bound water in the cellulose (Chirayil *et al.*, 2014). The degradation profiles of the cellulose showed major differences from nanocellulose.

DTG curve showed maximum degradation of cellulose at 320.8°C and nanocellulose at 273.6°C (Figure 4.14b). The cellulose nanofibrils from matured seeds of *Leucaena leucocephala* showed lower decomposition of temperature than their cellulose. Several authors have mentioned about the reduction in thermal degradation of nanocellulose correlated to the presence of sulfate groups during sulphuric acid hydrolysis (Mandal & Chakrabarty, 2011). A similar finding was reported by Jiang and Hsieh (2015) in the isolation of nanocellulose from tomato peels. Moreover, the remaining residues of NLLS at 600°C were higher as compared to the cellulose with 17.26 wt% and 12.80 wt% respectively. This is probably due to the formation of sulphate group on the surface of the nanocellulose whereby it acted as flame-resistant at high temperature (Jiang & Hsieh, 2015; Phanthong *et al*., 2016). In addition, García *et al.* (2016) reported that high crystallinity is related to high thermal degradation.

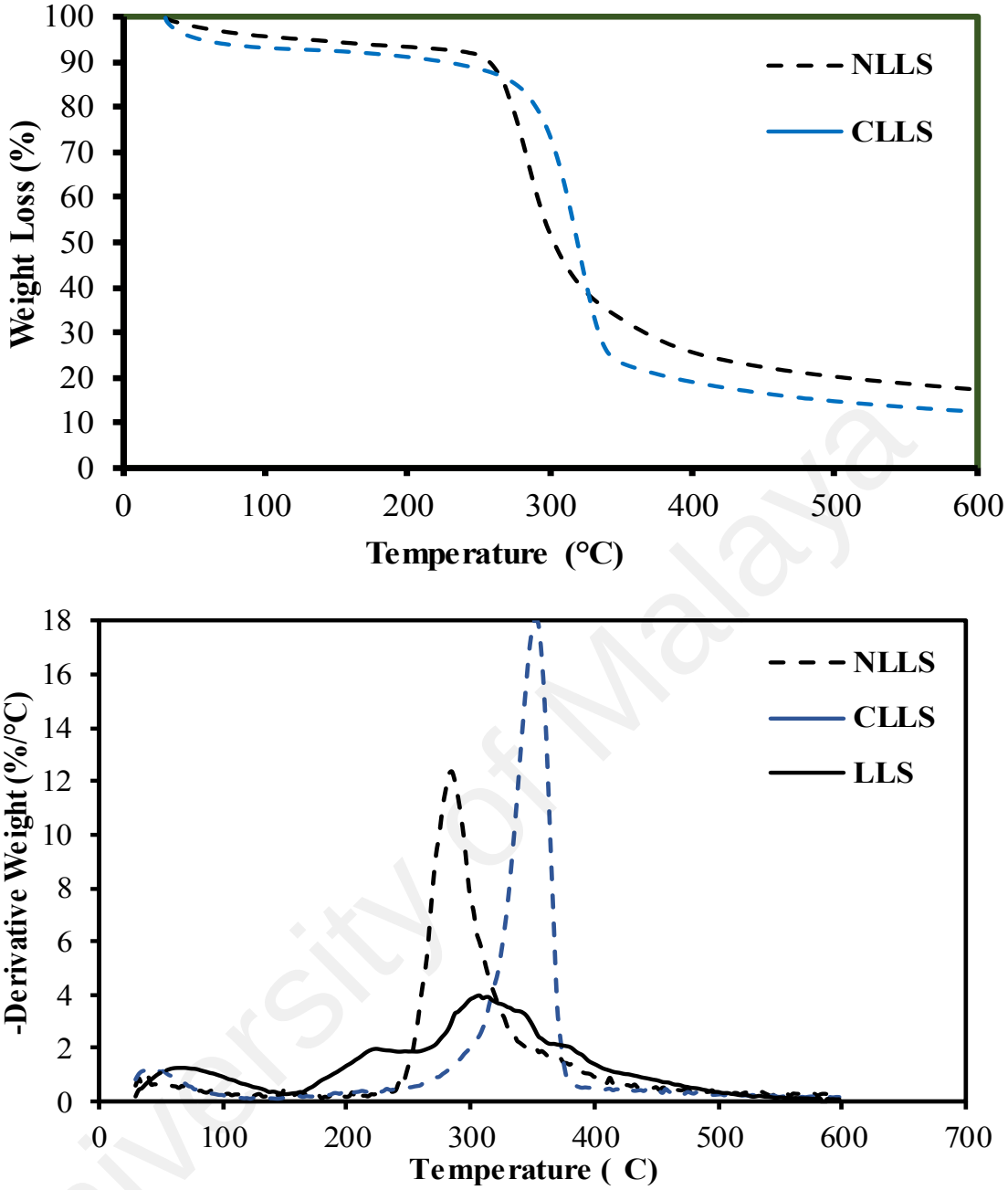

Figure 4.14: Comparison of (a) TG and (b) DTG curves of CLLS and NLLS.

4.4.6 X-ray diffraction

The XRD patterns of cellulose and nanocellulose were illustrated in Figure 4.15. LLS showed the characteristic of cellulose type I, with peak intensity of the 0 0 2 lattice plane located at 2θ = 22.6° and intensity of the amorphous cellulose at the position of 2θ = 18.2°. Crystallinity for cellulose was calculated to be 57.5% and 75.9% for nanocellulose. These data were interrelated by FTIR spectra; the high amount of non-cellulosic components' contents in cellulose decreased the crystallinity (Reddy & Rhim, 2014). An

increase in the crystallinity of nanocellulose is related to increase in the rigidity of the cellulose structure, which may relate to the removal of the amorphous materials. Further, it is important to increase the mechanical properties of polymer nano-composite. Marett *et al*. (2017) demonstrated that the addition of 5 wt% CNCs isolated from pistachio shells led to an increase in the modulus of elasticity; however, the result obtained was lower than the composites made with commercially available CNCs due to differences in terms of crystallinity.

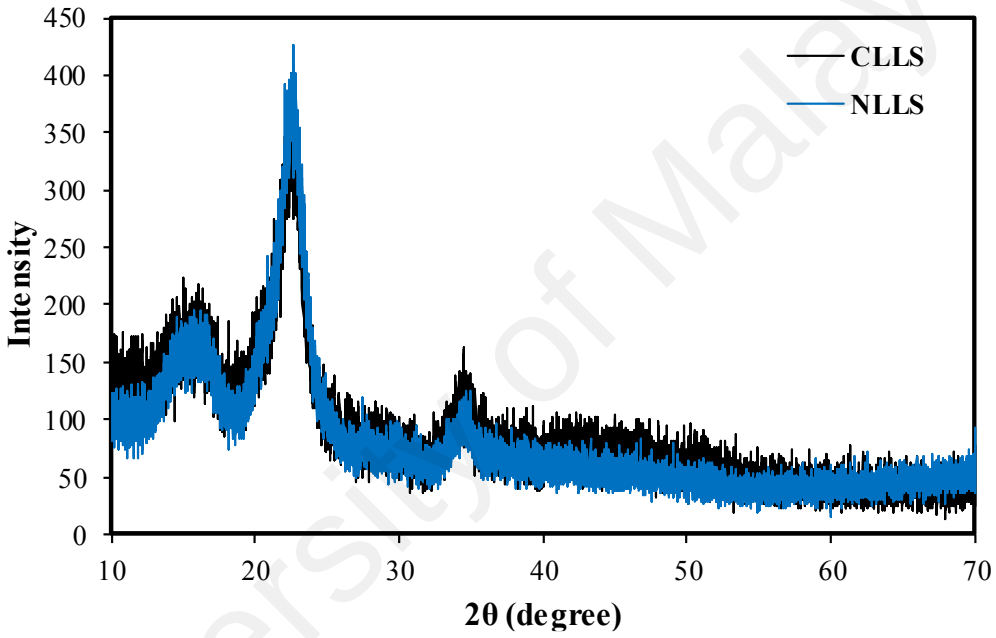

Figure 4.15: X-ray diffraction patterns of the LLS and NLLS.

The crystallinity observed for NLLS was found to be slightly higher than the one nanocrystals extracted from other agricultural residues such as bagasse, rice straw, and cotton stalks (Marett *et al.*, 2017). Other studies have reported on the following crystallinity indices for nanocrystalline cellulose extracted from lignocellulosic materials such as pistachio shells, CI = 68% (Marett *et al*., 2017), kelp, CI = 69.4% (Liu *et al*., 2017), and pinecone, CI = 79.5% (Rambabu *et al*., 2016). Haafiz *et al.* (2014) and Chirayil *et al*. (2014) obtained high crystallinity nanocrystals from microcrystalline cellulose derived from oil palm biomass and isora fiber, with crystallinity of 88% and 90%

respectively. The nanocellulose had a broad crystallinity depending on many factors such as the extraction methods and characterization techniques; as in the literature by which the range was from 64% to 91% (Park *et al*., 2010; Rambabu *et al*., 2016; Marett *et al*., 2017).

4.4.7 Gel permeation chromatography

The determination of the degree of polymerization of cellulose is commonly based on two techniques either via viscometry or Gel permeation chromatography (Trache *et al*., 2016). Gel permeation chromatography is a technique that provides detailed information about molecular weight distribution and relative molecular weight of the cellulose polymers. Figure 4.16 shows the GPC chromatogram of CLLS and NLLS. Calculation of molecular weight is shown in Appendix D. Both celluloses were converted to water soluble cellulose sulphates in order to facilitate the determination of the molecular weight of particular cellulose using GPC and water as a carrier solvent.

The single peak detected at retention time of 8.5 minutes for both samples indicated that the product was pure cellulose. The peak observed was adjacent to the cellulose peak at retention time of 9.2 minute and associated with the peak of carrier solvent (Alliet, 1967). The results revealed that the molecular weight of cellulose decreased after the second step of acid hydrolysis from 14 111 Da to 1081 Da, which reflected its thermal stability (Mandal & Chakrabarty, 2011). In addition, the degree of molecular weight reduction also depends on the hydrolysis conditions (Thoorens *et al*., 2014). During the hydrolysis process, due to chain breakage, the molecular weight of NCC decreases compared to that of the original cellulose's.

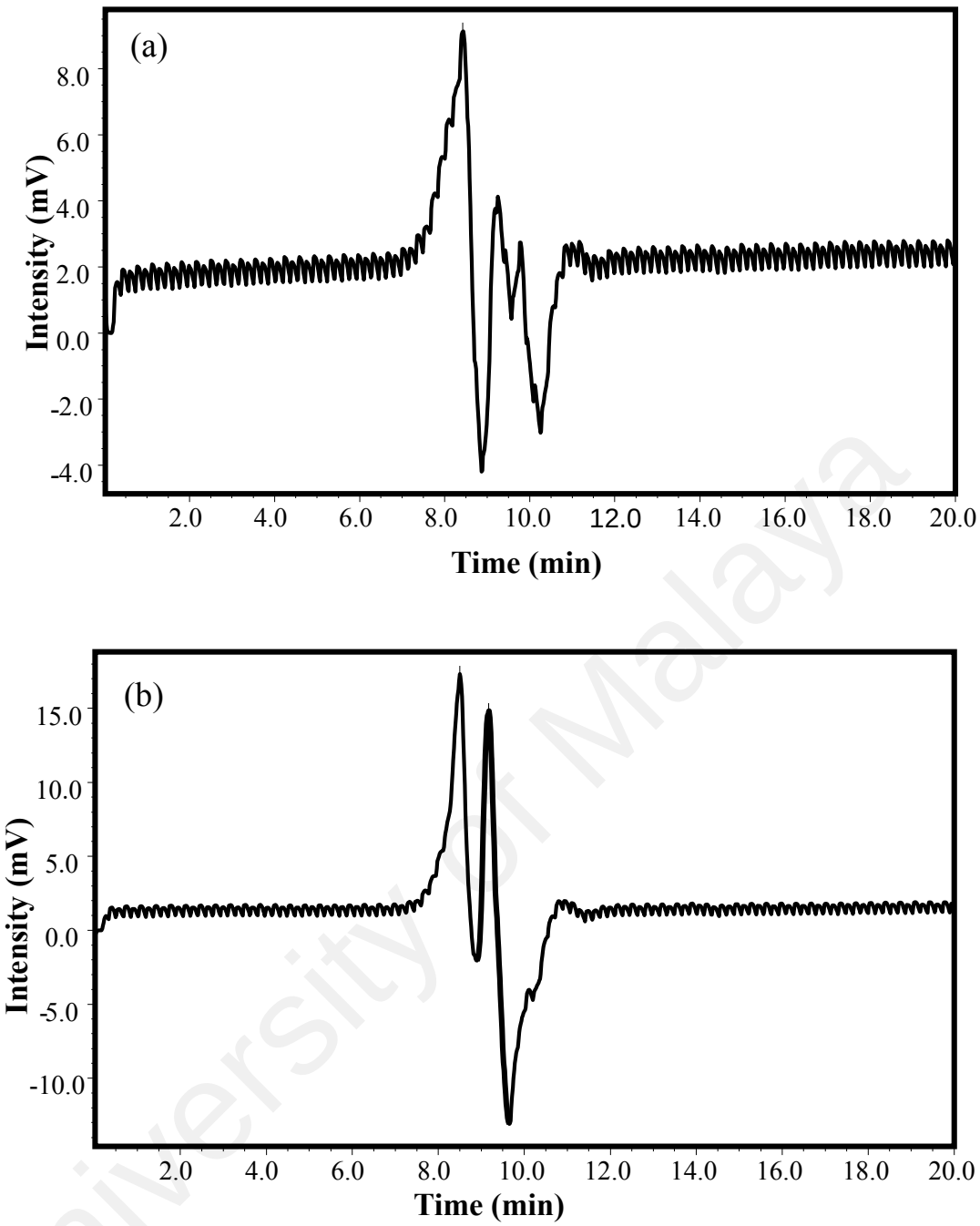

Figure 4.16: GPC of (a) CLLS and (b) NLLS.

4.5 Summary of characterization for CLLS. MLLS, and NLLS

FTIR, XRD and TGA are useful tool to investigate the purity of the prepared sample. Table 4.3 Summarized the experimental results of TGA, XRD and FTIR for CLLS, MLLS, and NLLS Chemical composition determination, morphological investigation, infrared spectroscopy, thermal gravimetric, and X-ray diffraction analyses confirmed the removal of non-cellulosic materials. The chemical treatments induced an increase of the

crystallinity index for microcrystalline cellulose from 57.5% to 80.3 %, but contrary with the cellulose nanocrystals which showed reduced crystallinity index. As anticipated, microcrystalline cellulose exhibit enhanced thermal stability than that cellulose nanocrystal.

TEM micrograph is a well-established in studying detailed morphology of nanostructures. It appears that the cellulose nanocrystals show individual long fibers and attached together, which had a diameter in the range of 2–11 nm. The particle analyser analysis have given supporting evidence for the formation of nanocellulose, which indicate that majority of the hydrolyzed particles lie in the nano range.

The result strongly shows that the cellulose, microcrystalline cellulose, and cellulose nanocrystals sample obtained from *Leucaena leucocephala* has great potential to be used in many field. It can be concluded from these results that the produced microcrystalline cellulose exhibited better thermal properties than cellulose nanocrystals, making them has great potential applications in reinforced-polymer composites.

Table 4.3: Summary of the experimental results for TGA, XRD and FTIR analysis.

Analysis	Materials		
	Cellulose (CLLS)	**Microcrystalline Cellulose (MLLS)**	**Cellulose Nanocrystals (NLLS)**
TGA			
T_{on} (°C)	325.2	307.8	265.4
T_{max} (°C)	320.8	329.5	273.6
Residual mass (%)	12.43	38.67	17.26
XRD			
Crystallinity (%)	57.5	80.3	75.9
FTIR (Peak Assignment, cm^{-1})			
OH groups	3334	3344	3348
CH_2 groups	2914	2916	2901
C=O stretching	1643	1644	1638
CH_2 bending	1431	1429	1430
C−H asymmetric stretching	1372	1372	1372
C−O−C stretching	1164	1162	10163
C−H	897	895	
C=O (lignin/hemicellulose)	1730	Not Observed	Not Observed
Sulphate group	Not Observed	Not observed	1203

4.6 Evaluation of glucose produced from cellulose

4.6.1 Carbohydrate analysis of cellulose hydrolysis

The major classes of carbohydrates include sugars (glucose, fructose, sucrose, lactose, and maltose), sugar polyols (sorbitol and mannitol), oligosaccharides, and polysaccharides (starch and non-starch polysaccharides). The phenol–sulfuric acid method is deemed the most dependable one among various colorimetric methods for carbohydrate analysis and it is useful for measuring neutral sugars in oligosaccharides, glycoproteins, proteoglycans, and glycolipids. This method has been used extensively due

to its simplicity and sensitivity (Masuko *et al.*, 2005; Herrero *et al.*, 2011; Popping and Diaz-Amigo, 2014). The calculation of carbohydrate content in CLLS, MLLS, and NLLS was based on the linear equation from the regression data: y = 0.7757x + 0.0138 as shown in Figure 4. 17.

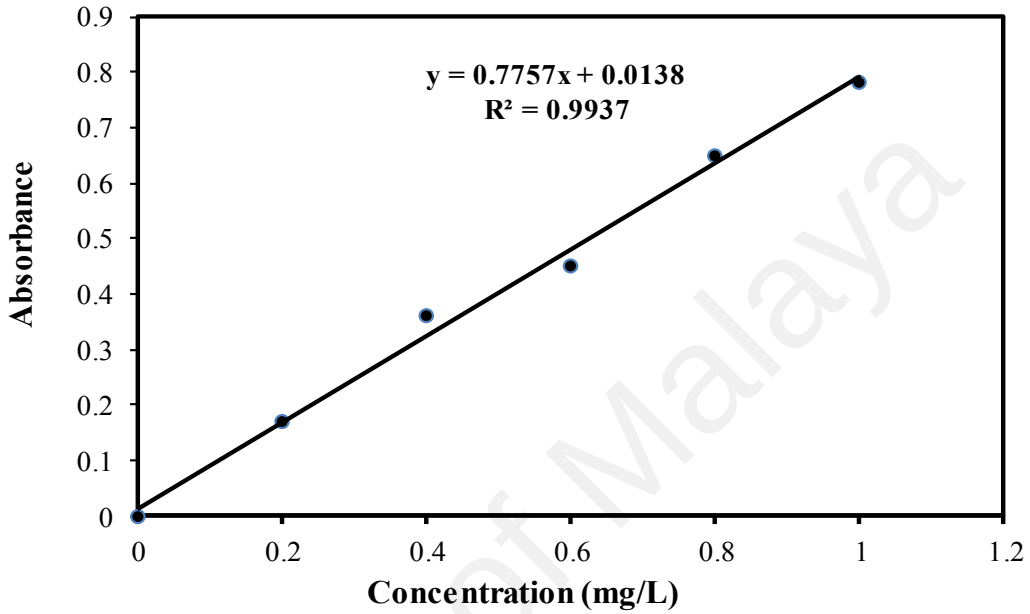

Figure 4.17: The calibration curve of standard glucose.

Table 4.4 summarizes the calculated results of the total carbohydrate content. The high carbohydrate content obtained from this sample indicated the possibility that the amount of sugar (glucose) in these seeds would be high.

Table 4.4: Results of carbohydrate content analysis.

Samples	Weight of sugar, g	Total carbohydrate content, (wt%)
CLLS	6.12±0.417	78.72±0.676
MLSS	5.91±0.262	88.52±0.8.97
NLLS	5.97±0.226	80.89±0.7.45

4.6.2 Sugar analysis

The sugar content of cellulose hydrolysate was also determined by reading sugar aqueous solution using a refractometer (Abbe Refractometers NAR 2T L, Germany). Results were expressed as degrees Brix (°Brix). Even though in principle, the unit °Brix for example, 1 °Brix by means is equivalent to 1 g of sugars (sucrose, glucose, and fructose, sorbitol). However, the above assumption does not hold true in samples as sugars are not the only components present in the solution (Magwaza & Opara, 2015). The sugar aqueous solution was prepared by homogenizing different ranges of mass sugar hydrolyzate in 100 mL distilled water by stirring on a magnet for 2 min. Figure 4.18 shows the regression between mass of cellulose hydrolyzate and °Brix; as expected, it gave a linear line. During ethanol fermentations, the consumption of sugar (Brix value decreases) with time was accompanied with an increase in the ethanol content (Hajar *et al*., 2012).

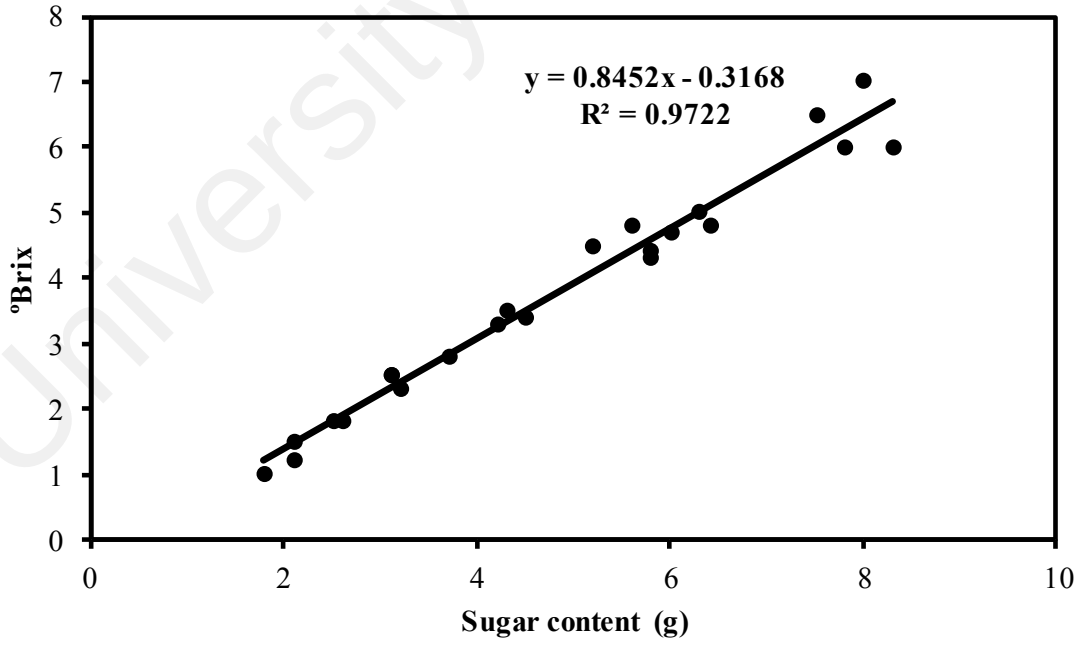

Figure 4.18: Relationship between sugar content and °Brix.

4.6.3 Comparison of glucose production from LLS waste

Acid hydrolysis is the most favorable way to synthesize sugars from lignocellulosic biomass which consists of polysaccharides, cellulose, and hemicellulose (Sun *et al*., 2015). This study focused on the production glucose from microcrystalline cellulose (MCC) obtained from two types of waste *Leucaena leucocephala* seeds. The waste seeds of *Leucaena leucocephala* (LLS) used in this study were unused residues obtained after oil (MCC-OELLS) and polysaccharides extraction (MCC-PELLS). The microcrystalline cellulose was isolated from LLS by acid treatment. MCC produced was then further converted to glucose by using sulphuric acid hydrolysis. The sugar composition was analyzed by using the phenol-sulfuric acid method and pre-column derivatization HPLC technique.

Cellulose is made up of hexosans; therefore, it is apparent that a high yield of glucose could be derived from acid hydrolysis. Figure 4.19 shows the retention time (min) of glucose by HPLC for MCC-PELLS and MCC-OELLS, where it can be confirmed that glucose was largely present in the hydrolyzed product (sugar).

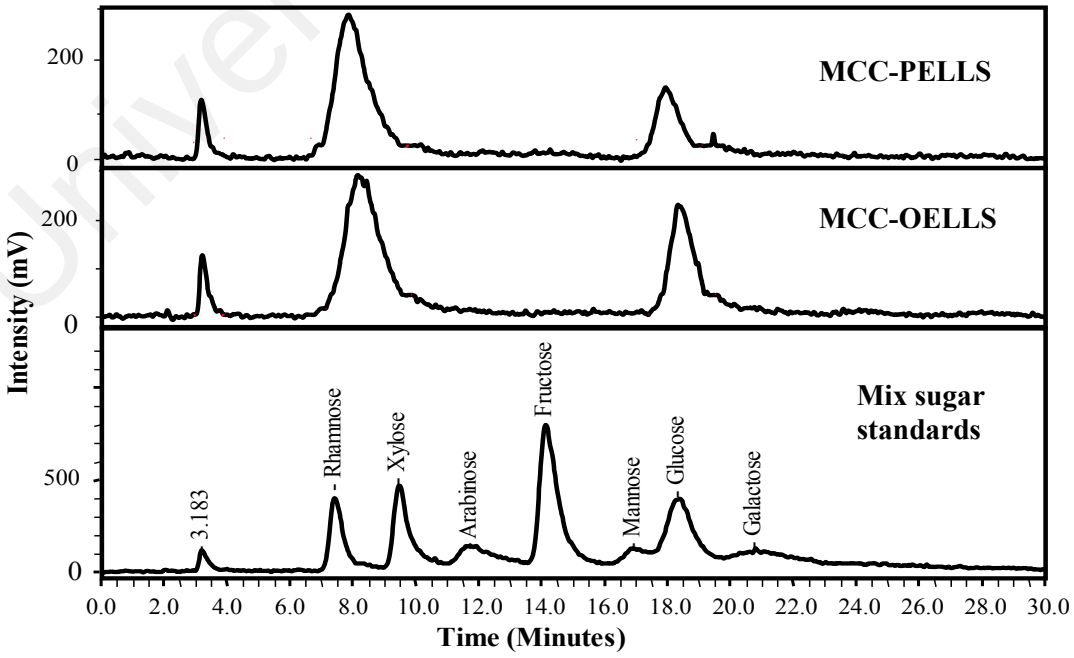

Figure 4.19: HPLC chromatogram of MCC-PELLS and MCC-OELLS hydrolysates in comparison with mix sugar standards.

Based on the significant contents of glucose that can be obtained through acid hydrolysis of cellulose, this work evaluates the effect of the concentration of acid and reaction time on glucose production as a pre-processing stage before transformation to ethanol LLS. The effect of acid sulphuric concentration and reaction time on cellulose hydrolysis for both *Leucaena leucocephala* seed wastes were studied at constant temperature of 121 °C. From the previous findings, many factors such as hydrolysis time, temperature, pressure, and also solvent to solid ratio among others may significantly influence the cellulose conversion to glucose of diverse lignocellulosic sources. The variable that has a significant and positive effect on the acid hydrolysis of the lignocellulosis sources is the acid concentration (Reales-Alfaro *et al*., 2013).

In Figure 4.20, treatment using acid concentration of 5% v/v was found to show a higher percentage of glucose at 71% for MCC-PELLS and 70% for MCC-OELLS hydrolysate. The color of hydrolysate products from sulphuric acid hydrolysis varies from light to dark yellow as the acid concentration increases, suggesting the presence of by-products. It was found that the percentage of glucose in the total sugar yield varied largely on the acid concentration. Hutomo *et al*. (2015) compared the cellulose hydrolysis to glucose using two different acids. Based on their study, sulphuric acid gave higher glucose yield in comparison to hydrochloric acid. In another study, Wijaya *et al*. (2014) evaluated the effect of crystallinity on cellulose degradation of different categories of biomass (hardwood, softwood, and non-woody biomass). They reported that the lowest crystallinity gave the highest glucose yield.

In total, 58% of MCC was found to be converted to glucose. Das *et al*. (2016) reported that the highest yield of glucose (60%) from cellulose rice husk was obtained in the presence of H_2SO_4 (5% v/v), at 140 °C for 60 min. Sasaki *et al*. (2012) reported that the highest yield of glucose (63.1%) from microcrystalline cellulose powder was obtained at a steam pressure of 62 atm for the steaming time of 1 min. However, as the acid

concentration increased, further enhancement of glucose formation could not be observed. This was probably due to the inevitable side reaction in glucose degradation. These data were consistent with the results by Ni *et al*. (2013) and Sun *et al.* (2015). This may be explained by the greater presence of acid, where some portions of sugars are further transformed into furans (furfural and HMF) and other by-products, which leads to the loss of sugars. In the fermentation process, the HMF is an undesired component and will affect the yield of biofuel. HMF inhibits yeast and other microorganisms used during the fermentation stage. However, HMF is also a beneficial renewable feedstock that can be converted into 2,5-dimethylfuran (Li *et al*., 2009).

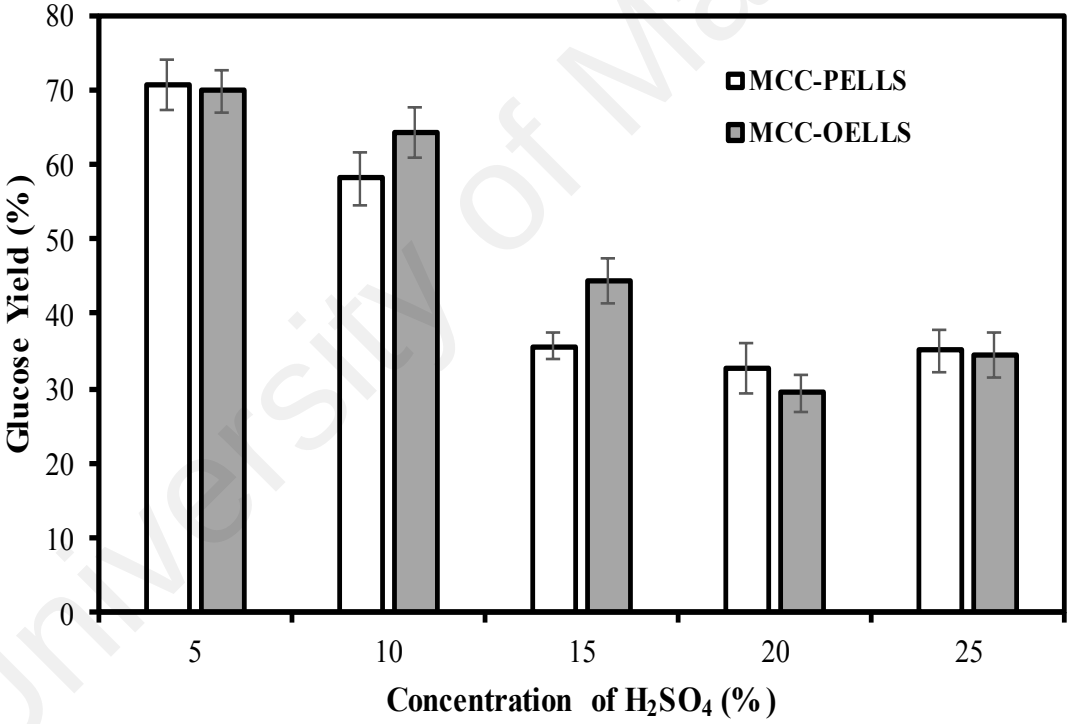

Figure 4.20: Effect of different concentration of H_2SO_4 to the yield of glucose at 60 min.

Residence time and temperature were significantly influenced by the hydrolysis of cellulose to sugars (Dussán *et al.*, 2014). This is due to the rigid crystalline structure of cellulose and making it difficult to be destroyed. Therefore, the effect of reaction time on glucose yield was investigated by varying the hydrolysis time from 30 min to 120 min at a constant sulphuric acid concentration (5%). Figure 4.21 show the reaction time of 120

min for selected acid concentrations giving significant effects to the yield of glucose. It could be suggested that the heating or reaction time showed significant influence on the hydrolysis of cellulose. This trend agrees with the results of Morales-delaRosa *et al*. (2012) in the hydrolysis of cellulose using ionic liquid. However, Lanzafame *et al*. (2012) which utilized acid catalysts in their study showed an increment in hydrolysis productivity, although with low selectivity to glucose due to the secondary reactions of glucose conversion.

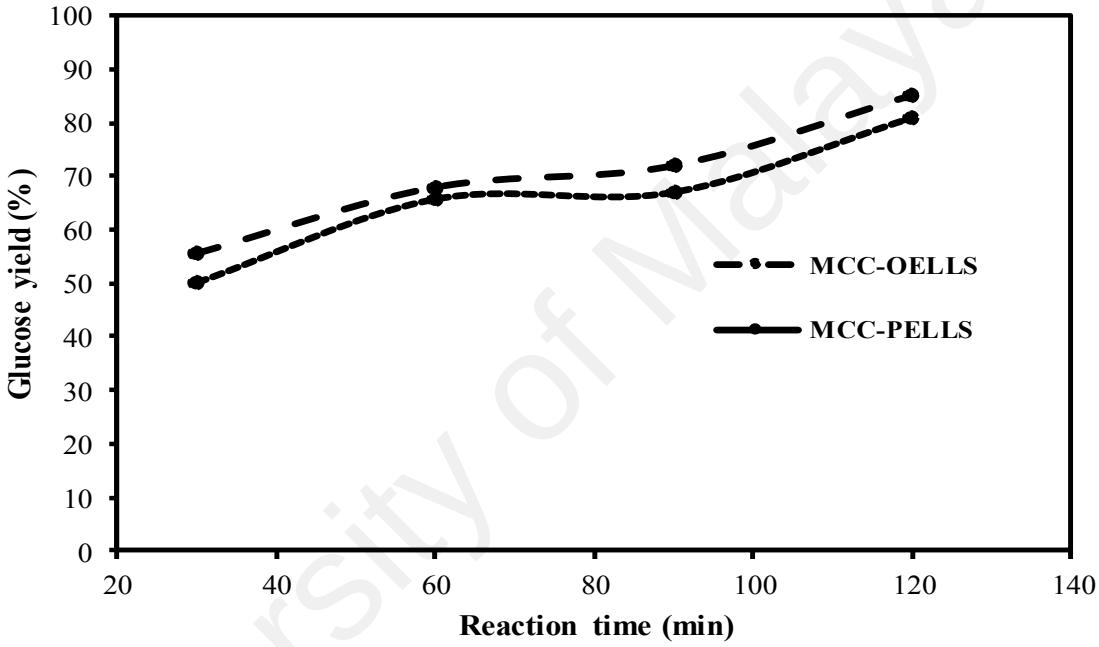

Figure 4.21: Effect of reaction time to the yield of glucose.

For both conditions, MCC-OELLS gave a yield of glucose (around 84%) and it is not largely different from the yield of MCC-PELLS (82%). Given that, cellulose conversion increased for both samples at around 71% to 75%. This might be explained by the fact that the crystallinity index of both samples was almost similar. Besides the crystalline region, cellulose also contains bundles of amorphous regions, which influences sugar yield. This is supported by Zhao *et al*. (2005) in their study which showed easier hydrolysis of non-crystalline (amorphous) than the crystalline fraction of cellulose. Ni *et al*. (2013) also reported that lower sugar yield contributed to higher crystallinity of cellulose. Phaiboonsilpa and Saka (2011) also reported that Japanese cedar (*Cryptomeria*

japonica) was liquefied by semi-flow hot-compressed water at 230°C/10 MPa for 15 min and 280°C/10 MPa for 30 min in the first and second stages where 87.76% of the sample was converted to various compounds in the water-soluble portion although the rest remained in the water-insoluble residue.

Cellulose was successfully extracted from two types of waste *Leucaena leucocephala* seeds. Further, extracted cellulose can be used as a source for various applications. Cellulose can be produced from different kinds of raw material. The most important factor to be considered is the availability of raw materials for the targeted production. The results from this study demonstrated that acid concentration has a profound influence on glucose production. The main sugar product from hydrolyzates was glucose, indicating that pre-treatment is not required for the production of glucose from waste seed evaluation. 5% acid concentration (H_2SO_4) with a heating rate of 2 hr at 121°C gave the favorable reaction conditions for the conversion of cellulose to glucose from *Leucaena leucocephala* waste seeds. This study suggested that the use of waste *Leucaena leucocephala* seeds may be a feasible option as a feed material for the production of cellulose and sugars for bioethanol and other value-added chemicals due its low cost and high sugar yields.

4.7 Conversion of glucose from LLS to bioethanol

4.7.1 Optimization of bioethanol

Known as a renewable and sustainable liquid fuel, bioethanol is considered as a good alternative to replace petroleum oil (Mussatto *et al*., 2010). In 2012–2015, the production and consumption of bioethanol in the world was expected to increase up to 3–7% due to limited oil reserves, the concern towards climate change from greenhouse gas emissions, and the need to promote domestic rural economies that will increase the agricultural income (Balat & Balat, 2009; Aditiya *et al.*, 2016). However, multiple uncertainties may influence the future of biofuel market, e.g. the evolution of environment in terms of policies and economic as well as inadequate raw material resulting from the competition of food against fuel from agricultural raw materials and crops (Brethauer & Wyman, 2010; López-Bellido *et al.*, 2014). Bioethanol can be produced from direct fermentation of simple sugars or polysaccharides like starch or cellulose that can be converted into sugars. However, obtaining fermentable sugar from cellulose is more difficult than sugar, grain, and starch based feed stocks (Sharma *et al.*, 2007; Mussatto *et al*., 2010; Lin *et al*., 2012; Xiros *et al*., 2013). In addition, sugar hydrolysates contain a broader range of inhibitory compounds, whose composition and concentration depend on the type of lignocellulosic materials, the pretreatment, and hydrolysis processes (Reales-Alfaro *et al*., 2013; Hoşgün *et al*., 2017).

Critical parameters in the fermentation process are fermentation time, pH, enzyme and yeast concentration, and substrate loading (Mussatto *et al*., 2010). In this study, the optimization of fermentation process of bioethanol was carried out using the glucose obtained from MLLS by means of response surface methodology. Ethanol production from MLLS is a relatively new topic and limited research has been conducted on the utilization of LLS for biofuel production. In this present study, response surface methodology was used to determine the optimum condition for the factors affecting

bioethanol production. The effect of the three (3) experimental factors, test variables or independent variables of X_1: pH, X_2: volume of inoculum and X_3: fermentation time at five levels on the dependent variable or response in volume ethanol and concentration was analysed. The experimental design was generated using MINITAB software version 17. In relation to this, the coded values of independent variables along with their minimum and maximum values are shown in Table 4.5.

Table 4.5: Coded and uncoded factors for the design experiment.

Variables	**-1.682 (-α)**	**Low (-1)**	**0**	**High (+1)**	**1.682 (+α)**
X_1	4	4.5	5.0	5.5	16
X_2	8	10	12	14	6
X_3	48	78	108	138	158

Where: X_1= pH of solution, X_2= volume of inoculum (ml), X_3= fermentation time (hr).

Based on Table 4.5, twenty experimental runs were performed according to Table 4.6. Studies done by Lin *et al*. (2012) on the effect of pH on glucose fermentation revealed that the optimum pH range of 4.0-5.0 may be observed as the operational limit for ethanol production process. In general, the maximum fermentation time in batch process for a complete fermentation of glucose for ethanol production by yeast is 72 hr (Phisalaphong *et al.*, 2006). Nevertheless, it depends on the influence of temperature. Studies done by Lin *et al*. (2012) showed that ethanol concentration increased steadily at 20 °C and did not decline within 168 hr. The ideal temperature range for fermentation is 20 - 35°C while at higher temperatures, almost all fermentation would be problematic (Lin *et al.*, 2012).

Table 4.6: Experimental Design Recommended by MINITAB Software Version 17.

Run no.	X_1	X_2	X_3
1	4.50	10.00	78.00
2	5.50	10.00	78.00
3	4.50	14.00	78.00
4	5.50	14.00	78.00
5	4.50	10.00	138.00
6	5.50	10.00	138.00
7	4.50	14.00	138.00
8	5.50	14.00	138.00
9	4.16	12.00	108.00
10	5.84	12.00	108.00
11	5.00	8.63	108.00
12	5.00	15.36	108.00
13	5.00	12.00	57.55
14	5.00	12.00	158.45
15	5.00	12.00	108.00
16	5.00	12.00	108.00
17	5.00	12.00	108.00
18	5.00	12.00	108.00
19	5.00	12.00	108.00
20	5.00	12.00	108.00

4.7.1.1 Effect of volume ethanol (Y_1)

As shown in Table 4.7, the highest actual and predicted responses were 11.00 ml and 9.91 ml respectively under the predetermined factors, whereby pH of solution at 5 was used and inoculum volume of 12 ml as well as fermentation time of 108 hours were decided. The lowest actual and predicted responses were 2.40 ml and 2.37 ml respectively using pH of solution at 5, volume of inoculum at 12 ml, and settling on fermentation time of 57.55 hr.

Table 4.7: Factors and comparison between actual (Y) and predicted (FITS) responses.

No of Run	Factors			Response (Volume of ethanol)	
	X_1	X_2	X_3	Y_1	FITS
1	4.50	10.00	78.00	5.00	4.98
2	5.50	10.00	78.00	4.86	4.96
3	4.50	14.00	78.00	4.80	5.08
4	5.50	14.00	78.00	4.80	4.58
5	4.50	10.00	138.00	8.20	8.55
6	5.50	10.00	138.00	6.30	6.15
7	4.50	14.00	138.00	8.00	8.02
8	5.50	14.00	138.00	5.00	5.14
9	4.16	12.00	108.00	8.40	8.08
10	5.84	12.00	108.00	5.50	5.63
11	5.00	8.63	108.00	8.00	7.89
12	5.00	15.36	108.00	7.20	7.12
13	5.00	12.00	57.55	2.40	2.37
14	5.00	12.00	158.45	6.00	5.85
15	5.00	12.00	108.00	11.00	9.91
16	5.00	12.00	108.00	9.70	9.91
17	5.00	12.00	108.00	9.50	9.91
18	5.00	12.00	108.00	9.60	9.91
19	5.00	12.00	108.00	10.6	9.91
20	5.00	12.00	108.00	11.00	9.91

Where: X_1 = pH of solution, X_2 = volume of inoculum (ml), X_3 = fermentation time (hr).

4.7.1.2 Effect of concentration ethanol (Y_2)

The highest concentration of ethanol obtained from the experiment was at run 16, where the pH was set at 5, the volume of inoculum was 12 ml, and the fermentation time was 108 hr, by which 24.23% of ethanol content was produced as shown in Table 4.8.

Table 4.8: Factors and comparison between actual (Y) and predicted (FITS) responses.

No of Run	Factors			Response (Volume of ethanol)	
	X_1	X_2	X_3	Y_2	FITS
1	4.50	10.00	78.00	14.66	14.85
2	5.50	10.00	78.00	13.01	13.56
3	4.50	14.00	78.00	13.54	13.58
4	5.50	14.00	78.00	13.92	13.79
5	4.50	10.00	138.00	18.30	18.14
6	5.50	10.00	138.00	14.66	14.33
7	4.50	14.00	138.00	18.60	17.77
8	5.50	14.00	138.00	15.94	15.47
9	4.16	12.00	108.00	14.08	14.40
10	5.84	12.00	108.00	11.29	11.38
11	5.00	8.63	108.00	16.73	16.44
12	5.00	15.36	108.00	15.63	16.32
13	5.00	12.00	57.55	15.94	15.42
14	5.00	12.00	158.45	18.68	19.60
15	5.00	12.00	108.00	20.33	22.37
16	5.00	12.00	108.00	24.23	22.37
17	5.00	12.00	108.00	21.74	22.37
18	5.00	12.00	108.00	23.13	22.37
19	5.00	12.00	108.00	24.13	22.37
20	5.00	12.00	108.00	20.60	22.37

Where: X_1 = pH of solution, X_2 = volume of inoculum (ml), X_3 = fermentation time (hr).

The lowest percentage of ethanol content from experiments can be seen at run 10, where the pH of solution was 5.84, volume of inoculum was 12 ml, and the fermentation time was the same (108 hr), and they produced the concentration of 11.29% ethanol. From the prediction of RSM, the highest predicted response was 22.37%, whereas the lowest response was also seen at run 10 which was the same as the experimental run, where the response was 11.38%.

4.7.2 Fitting of second order polynomial equations and statistical analysis

The data analyzed by regression analysis were obtained by fitting various models to evaluate the effect of each independent factor in response with experimental data (Table 4.9 and Table 4.10) using Minitab software. Based on those tables, a second-order polynomial model equation for the optimization of volume and concentration of ethanol in MLLS is illustrated in Equation 1 and Equation 2 respectively. The second order polynomial model was predicted with RSM indicating linear, interaction, and quadratic effects of variables on the system response as either positive or negative. The final equations obtained in terms of coded factors were given below.

Volume ethanol (Y_1);

$$Y_1 = -200.1 + 52.33\ X_1 + 6.59\ X_2 + 0.7854\ X_3 - 4.806\ X_1^2 - 0.2429\ X_2^2 - 0.002415\ X_3^3 - 0.120\ X_1X_2 - 0.0397\ X_1X_3 - 0.00258\ X_2X_3 \quad (4.1)$$

Concentration ethanol (Y_2);

$$Y_2 = -1145 + 367.6\ X_1 + 31.77\ X_2 + 1.890\ X_3 - 37.89\ X_1^2 - 1.630\ X_2^2 - 0.005843\ X_3^3 + 1.429\ X_1X_2 - 0.1051\ X_1X_3 + 0.0014\ X_2X_3 \quad (4.2)$$

Where: X_1= pH of solution, X_2 = volume of inoculum (ml), X_3= fermentation time (hr); linear test variables = X_1, X_2, X_3; square test variables = X_1^2, X_2^2, X_3^2; quadratic test variables = X_1X_3, X_1X_3, X_2X_3.

Table 4.9: Estimated regression coefficient of second-order polynomial model for optimization of volume ethanol in LLS.

Term	Coefficient	SE Coefficient	T	P
Constant	9.905	0.233	42.49	0.000
X_1	-1.221	0.260	-4.70	0.001*
X_2	-0.382	0.260	-1.47	0.172
X_3	1.736	0.260	6.67	0.000*
X_1^2	-3.045	0.426	-7.15	0.000*
X_2^2	-2.395	0.426	-5.62	0.000*
X_3^2	-5.795	0.426	-13.61	0.000*
X_1X_2	-0.339	0.572	-0.59	0.566
X_1X_3	-1.683	0.572	-2.94	0.015*
X_2X_3	-0.438	0.572	-0.77	0.461
$R^2 = 96.89\%$ $R^2(adj) = 94.10\%$				

Note: * = Significant

Table 4.10: Estimated regression coefficient of second-order polynomial model for optimization of concentration ethanol in LLS.

Term	Coefficient	SE Coefficient	T	P
Constant	22.365	0.553	40.44	0.000
X_1	-1.510	0.617	-2.45	0.034*
X_2	-0.059	0.617	-0.10	0.92
X_3	2.091	0.617	3.39	0.007*
X_1^2	-9.48	1.01	-9.38	0.000*
X_2^2	-5.98	1.01	-5.92	0.000*
X_3^2	-4.85	1.01	-4.80	0.001*
X_1X_2	1.06	1.36	0.78	0.451
X_1X_3	-1.78	1.36	-1.31	0.219
X_2X_3	0.63	1.36	0.47	0.651
$R^2 = 93.55\%$ $R^2(adj) = 87.75\%$				

Note: * = Significant

From Table 4.9 and Table 4.10, it was found that linear factors X_1, and X_3 showed positive coefficients. These positive values of coefficient for the particle terms of all three experimental factors indicated that the volume and concentration of ethanol will be increased due to these particle terms. Further, quadratic or square factors for all three (3) factors of X_1X_1, X_2X_2 and X_3X_3 for both dependent variables (volume and concentration of ethanol) showed negative coefficients. All three interactions or cross-product factors such as X_1X_2, X_1X_3, and X_2X_3 for dependent variable of volume of ethanol showed negative coefficients. Negative coefficients indicated that the volume of ethanol will be decreased due to these particle terms. While for ethanol concentration, two terms gave positive values of coefficient for the interaction of (X_1X_2) and (X_1X_3). Positive coefficients indicated that concentration ethanol will be increased due to these particle terms.

The t-test is used to evaluate the significance of regression equation with the estimated coefficient and it is obtained by dividing each coefficient with their standard error (SE) (Mourabet *et al*., 2015). Meanwhile, the *p*-values are used as a tool to check the significance of each coefficient, which in turn might indicate the pattern of the interactions between the variables (Mourabet *et al*., 2015). The larger the t value and the smaller the *p* value, the more significant is the corresponding coefficient (Sudamalla *et al*., 2012). In generally, *P* values lower than 0.001 indicate that the model is considered to be statistically significant at the 99% confidence level.

From Table 4.9, the most significant effect ($P = 0.000$) on ethanol volume was the quadratic term for all three factors (X_1^2, X_2^2, X_3^2), followed by linear term of pH, X_1 (P=0.001) and interaction term of pH and fermentation time, X_1X_3 ($p = 0.015$). The main effects of volume of inoculum (X_2) and fermentation time (X_3) and the effect of their interaction between volume of inoculum with fermentation time and pH (X_1X_2, X_2X_3)

were insignificant (P>0.05). In addition, from Table 4.10, the squared effect of all the parameters was found to be highly significant (p = 0.000) on ethanol concentration. The main effects of pH (X_1) and fermentation time (X_3) were also found to be significant. However, the coefficient of the interaction terms of all parameters were insignificant (P>0.05). Although the values were insignificant, they were maintained in the model to minimize error determination (Jargalsaikhan & Saraçoğlu, 2009).

Correlation coefficient, R^2 value is significant for the validation of the developed model; the aptness of the model is indicated by the value of R-square >0.75 (Dash *et al.*, 2017). In a statistical study, the closer the R^2 value to 1, the better the model will be, as this will give a predicted value that is closer to the actual values. The R^2 values for Equation 4.1 and Equation 4.2 were 97.18 and 96.66%, respectively. The R^2 values for both dependent (Y_1 and Y_2) were considered relatively high and this indicated that 97.18% and 96.66% of the variability in the response could be explained by the model. Thus, the total variation on response cannot be suitably explained by the model with only 2.2% and 3.34% respectively. These variations could be due to other factors which are not included in the model. In addition, adjusted R^2 functions as a way to measure the quality of the model that predicts a response value. While good agreement model results in the value of adjusted R^2 and predicted R^2 within 5% of each other approximately, the vice versa results indicate that a problem might have occurred to either the data or the model (Mourabet *et al.*, 2015). The adjusted R^2 is a corrected value for R^2 after unnecessary model terms are eliminated. If there are many non-significant terms included in the model, the adjusted R^2 would be smaller than R^2. In this study, the R^2 values for both Y_1 and Y_2 were high and very close to the adjusted R^2 with 94.89% and 87.75% respectively. These high R^2 values indicated that the predicted responses were close to the experimental values and the models were suitable to correlate with the experiment data.

Nevertheless, the optimization of a fitted response surface might give poor or misleading results (Prakash Maran & Manikandan, 2012). Therefore, it is very important to check if the model exhibited a good fit or not. The adequacy of each term in the second-order polynomial equation was validated by the statistical tests called Analysis-of-variance (ANOVA) and the results were given in Tables 4.11 and 4.12 for the volume and concentration of ethanol respectively.

The model parameters usually indicated in ANOVA are the degrees of freedom (DF), sum of squares (SS) and mean squares (MS), F-value, and *P*-value. The MS value of a model term in an ANOVA table is obtained by dividing SS over DF and its F value is obtained by dividing MS due to the model term by MS due to error. The F-value predicts the quality of the entire model considering all design variables at one stage, while the *P*-value is the probability of the independent design variable having very little or insignificant effect on the dependent variable (response) (Datta & Kumar, 2012). Normally, a larger F- and lower *P*-value of a model term in ANOVA indicates more significant corresponding coefficient term (Sudamalla *et al*., 2012). However, the *p*-value should be lower than 0.05 for the model to be statistically significant (Patel *et al*., 2011). In this study, the ANOVA of the polynomial model demonstrated that it was highly significant as evidenced from the calculated F-value (F-model = 34.65 for Y_1 and F-model 16.12 for Y_2) and probability value ($p = 0.000$) for both Y_1 and Y_2 as shown in Table 4.12 and Table 4.13. It was also evident from ANOVA from both tables that the linear ($p < 0.001$) and quadratic effect ($p = 0.000$) of the model have greater influence on ethanol production (Y_1 and Y_2) and no significant influence ($p > 0.05$) was observed due to the interaction effect of the variables. However, for both dependent variables (Y_1 and Y_2), the volume (X_2) was not significant whereas only the effect of interaction terms X_1X_2 on Y_1 was significant to the responses.

Table 4.11: ANOVA for optimization of volume of ethanol in LLS.

Source	DF	Adj SS	Adj MS	F	P	Remarks
Model	9	101.85	11.32	34.64	0.00	Significant*
Linear	3	22.45	7.48	22.91	0.00	Significant*
X_1	1	7.20	7.20	22.05	0.00	
X_2	1	0.71	0.71	2.16	0.17	
X_3	1	14.55	14.55	44.53	0.00	
Square	3	76.26	25.42	77.82	0.00	Significant*
X_1^2	1	16.70	16.70	51.12	0.00	
X_2^2	1	10.33	10.33	31.63	0.00	
X_3^2	1	60.49	60.49	185.19	0.00	
2-way interaction	3	3.14	1.047	3.20	0.07	Not significant
X_1X_2	1	0.12	0.12	0.35	0.57	
X_1X_3	1	2.83	2.83	8.67	0.02	
X_2X_3	1	0.19	0.19	0.59	0.46	
Error	10	3.27	0.33			
Lack of fit	5	0.47	0.09	0.17	0.96	Not significant
Pure Error	5	2.80	0.56			
Total	19	105.11				

The lack of fit test was used to measure the variation of data. Lack of fit test usually compares the error to the pure error from the replicated design points, which in this study, was from run 15 to 20 in the experimental design (Mohamad *et al*., 2017; Mourabet *et al*., 2015). In reference to Table 4.11 and Table 4.12, the results showed that the respective *p*-values of lack of fit test for Y_1 and Y_2 were 0.964 and 0.944 ($p>0.05$), hence denoting that the lack of fit test was not relatively significant to the pure error. This demonstrates that the model was good and fitted well with the experimental data and there is significant effect on linear (X_1, X_3) and quadratic factors (X_1, X_2, X_3) with the responses (Y_1 and Y_2).

Table 4.12: ANOVA for optimization of concentration of ethanol in LLS.

Source	DF	Adj SS	Adj MS	F	P	Remarks
Model	9	266.72	29.64	16.12	0.00	Significant*
Linear	3	32.13	10.71	5.83	0.01	Significant**
X_1	1	11.01	11.01	5.99	0.03	Significant**
X_2	1	0.02	0.02	0.01	0.93	Not significant
X_3	1	21.11	21.12	11.48	0.01	Significant**
Square	3	229.89	76.63	41.68	0.00	Significant*
X_1^2	1	161.77	161.77	88.00	0.00	Significant*
X_2^2	1	64.45	64.45	35.06	0.00	Significant*
X_3^2	1	42.40	42.40	23.06	0.00	Significant**
2-way interaction	3	4.70	1.57	0.85	0.50	Not significant
X_1X_2	1	1.13	1.13	0.62	0.45	Not significant
X_1X_3	1	3.16	3.16	1.72	0.22	Not significant
X_2X_3	1	0.40	0.40	0.22	0.65	Not significant
Error	10	18.38	1.84			
Lack of fit	5	3.20	0.64	0.21	0.94	Not significant
Pure Error	5	15.20	3.04			
Total	19	285.10				

Where; DF = degree of freedom, Adj SS = adjusted sum of square, Adj MS = adjusted mean square, F = fischer, P = probability (* = significant at $P < 0.05$, ** = significant at $P < 0.01$).

4.7.3 Surface plot and contour plot

The response optimizer was obtained and the results at the optimum condition for the target as well as maximum and minimum goals for both dependent variables (Y_1 and Y_2) are shown in Figures 4.22, 4.23, and 4.24 respectively. Meanwhile, the feasibility of the experiments for target, maximum, and minimum goals was determined from the overlaid contour plot and the results are shown in Figures 4.25, 4.26, and 4.27 respectively. The results of the optimum conditions for the different goals of actual and predicted responses and the feasibility of experiments obtained from the response optimizer are shown in Table 4.14.

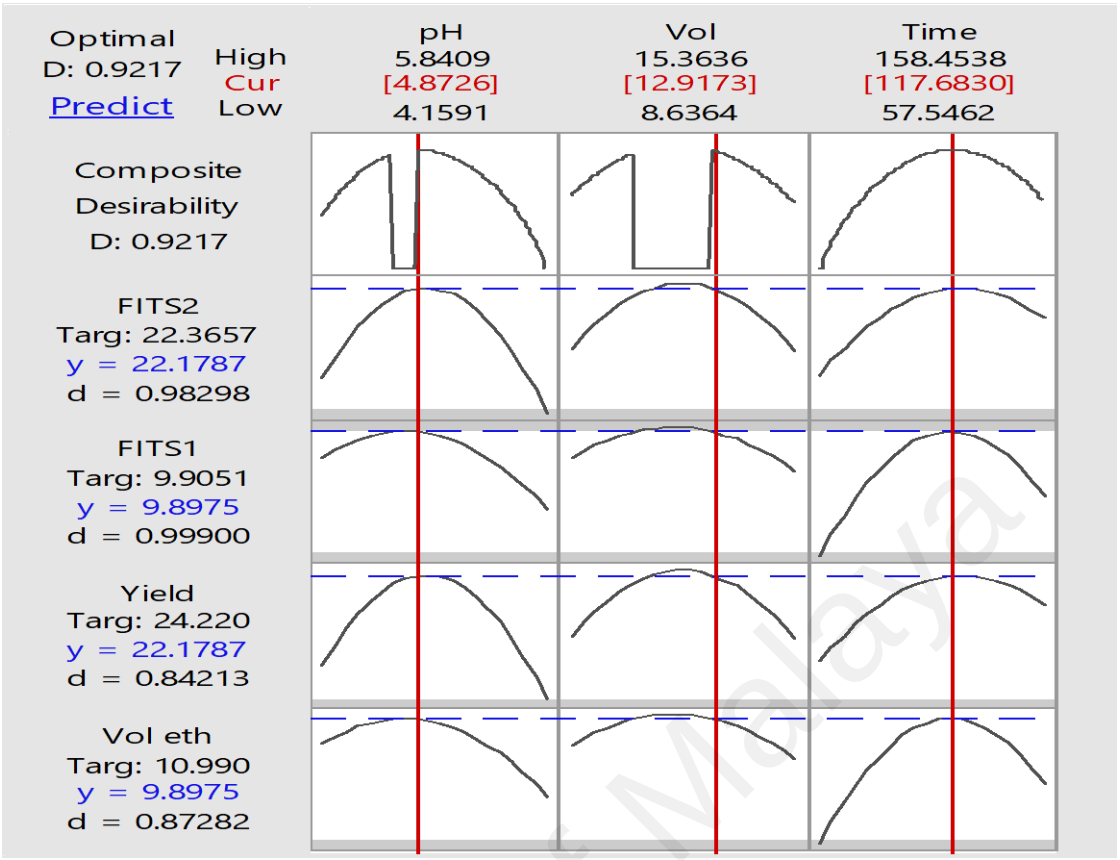

Figure 4.22: The response optimizer at the optimum condition for the target goal.

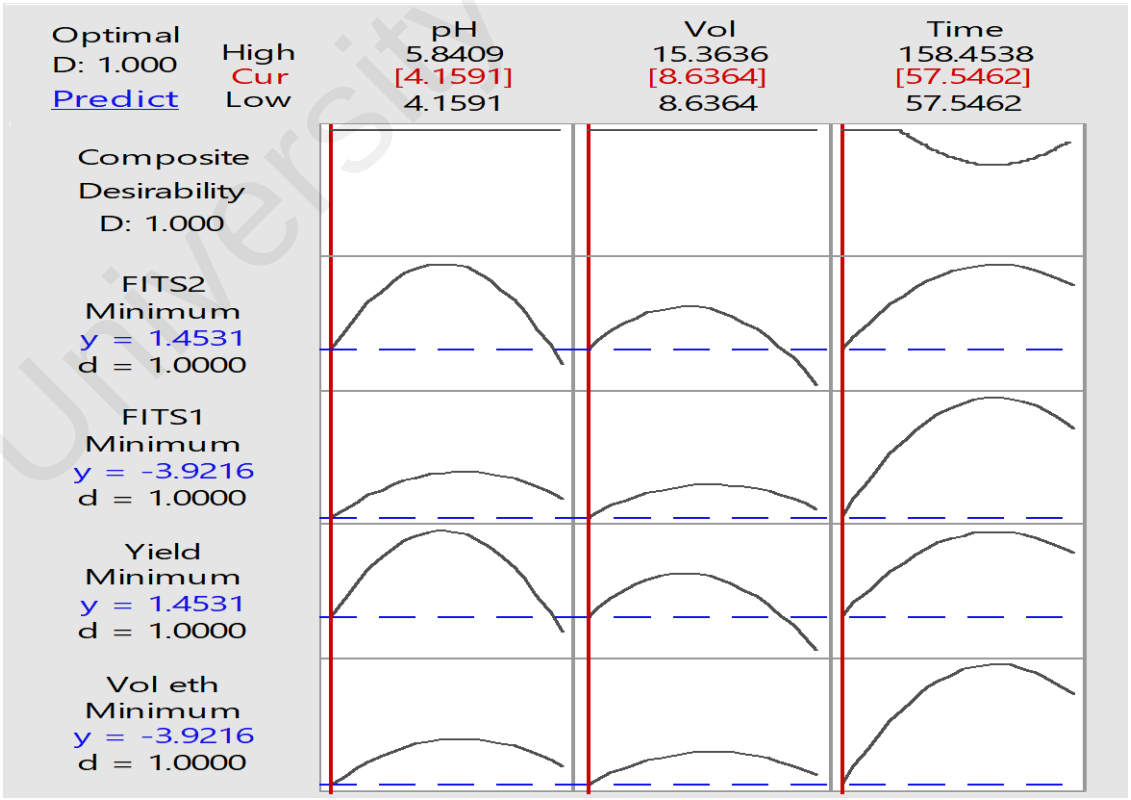

Figure 4.23: The response optimizer at the optimum condition for the minimum goal.

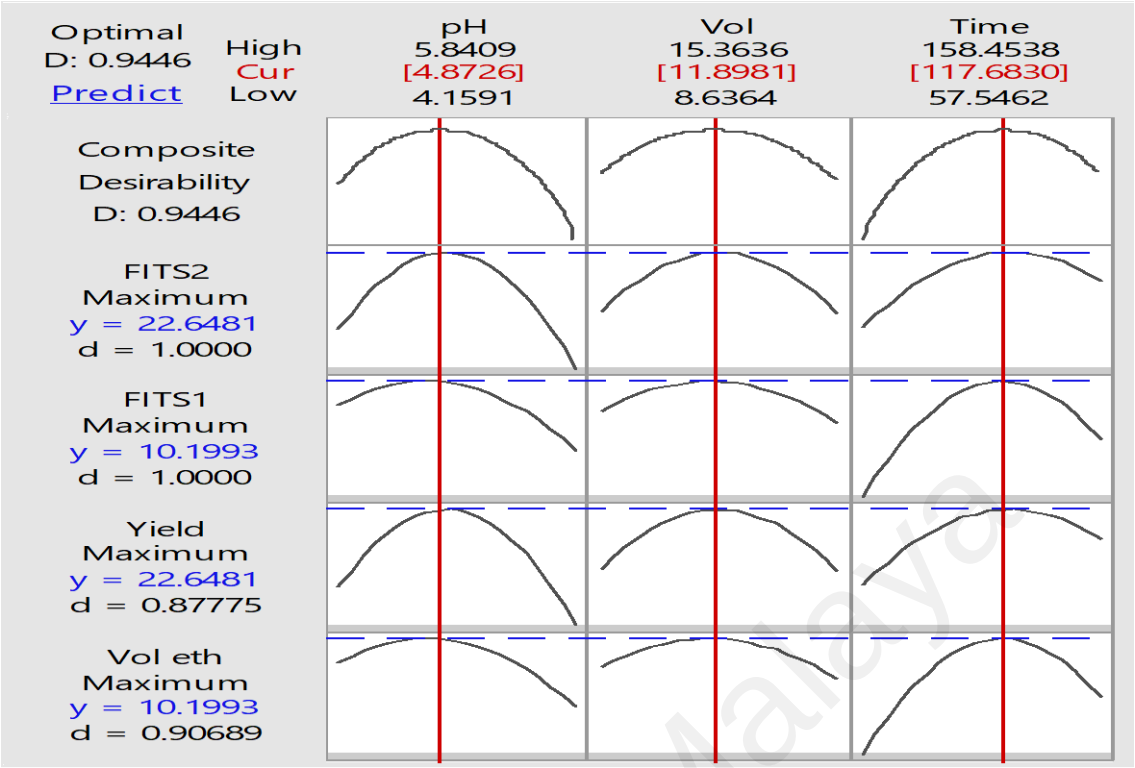

Figure 4.24: The response optimizer at the optimum condition for the maximum goal.

Based on Table 4.13, it was found that the optimum conditions for the target goal with pH of solution at 4.8726, volume of inoculum of 12.92 ml, and fermentation time of 117.68 hr were feasible to be carried out. Meanwhile, the minimum goal with pH of solution at 4.15, volume of inoculum of 15.36 ml, and fermentation time of 57.55 hr as well as the optimum conditions for the maximum goal with pH of solution at 4.87, volume of inoculum of 11.90 ml, and fermentation time of 117.68 hr were not feasible to be carried out.

This is in accordance with the optimum conditions for the target being located in the white area or in the feasible region based on the overlaid contour plots obtained as shown in Figure 4.25. Meanwhile, the optimum conditions for the maximum goal and minimum goal, as shown in Figures 4.26 and 4.27, were located in the grey area or non-feasible region. Therefore, the optimum conditions for the target goal were chosen as summarized in Table 4.14.

Table 4.13: Comparison values of target and predicted responses for different optimum conditions and experiment feasibilities.

Goal		Lower	Target	Upper	Optimum conditions			Predicted Response FITS Y_1= volume; Y_2 = concentration	F/NF
					X_1	X_2	X_3		
Target	Volume of ethanol	2.40	10.99	11.00	4.8726	**12.9173**	117.6830	$Y_1 = 9.8975$	F
	FITS 1	2.37478	9.90511	9.90512					
	Concentration of ethanol	11.29	24.22	24.23				$Y_2 = 22.1787$	
	FITS 2	11.3787	22.36.57	22.3658					
Maximum	Volume of ethanol	2.40	11.00	11.00	4.8726	11.8981	117.6830	$Y_2 = 10.1993$	NF
	FITS 1	2.3873	9.90512	9.90512					
	Concentration of ethanol	28.00	24.23	24.23				$Y_2 = 22.6481$	
	FITS 2	27.7155	2.40	22.3658					
Minimum	Volume of ethanol	2.40	2.3873	11.00	4.1591	8.6364	57.5462	$Y_2 = -3.9216$	NF
	FITS 1	2.3873	28.00	9.90512					
	Concentration of ethanol	28.00	27.7155	24.23				$Y_2 = 1.4531$	
	FITS 2	27.7155	2.40	22.3658					

Where: F = Feasible; NF = Not feasible

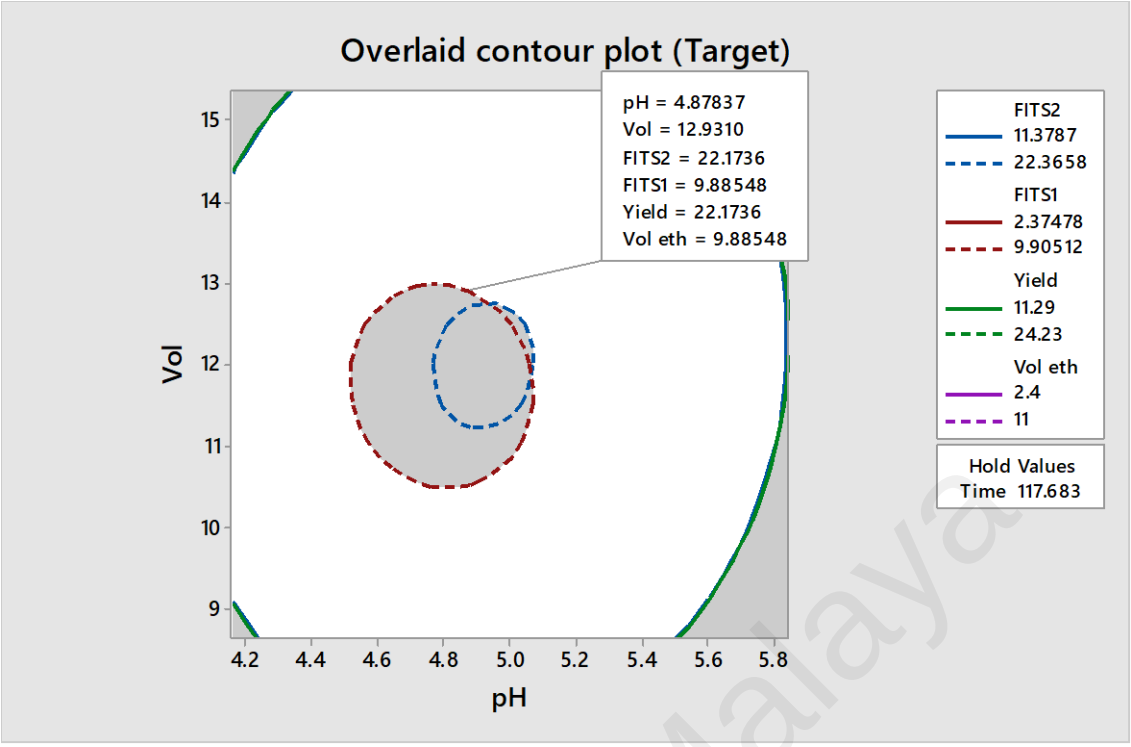

Figure 4.25: Overlaid contour plot at optimum target goal: pH of 4.88, volume inoculum of 12.92 ml and fermentation time of 117.68 hr.

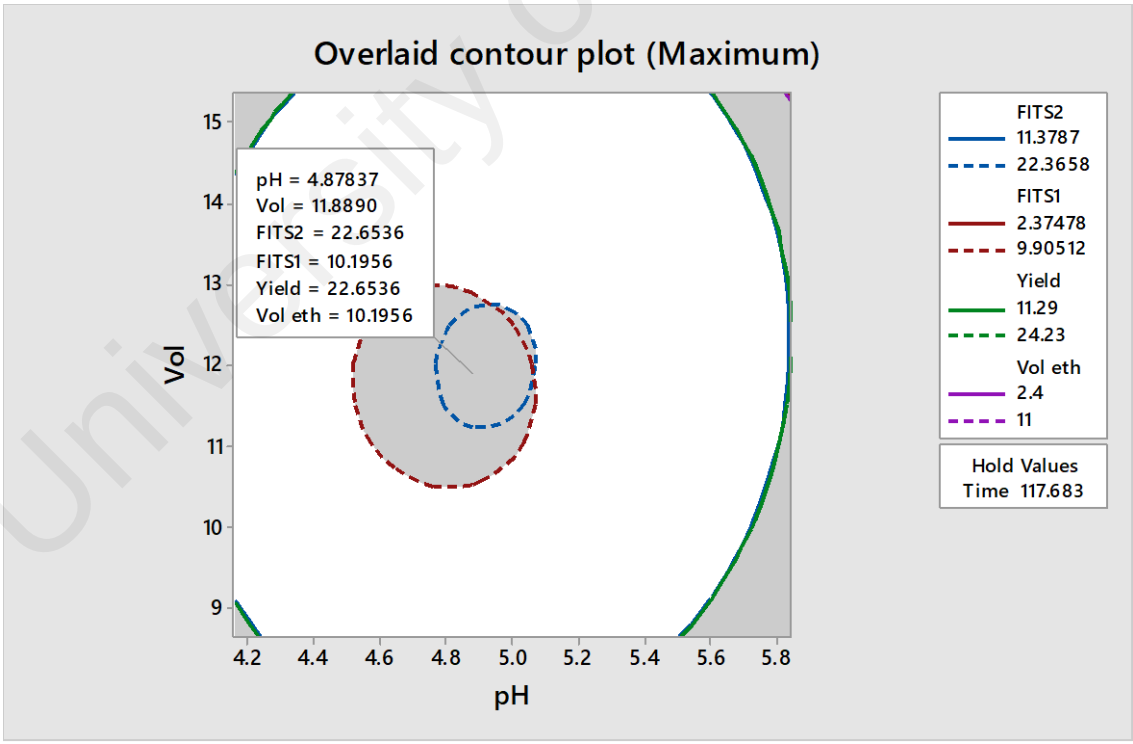

Figure 4.26: Overlaid contour plot at optimum maximum goal: pH of 4.87, volume inoculum of 11.88 ml and fermentation time of 117.68 hr.

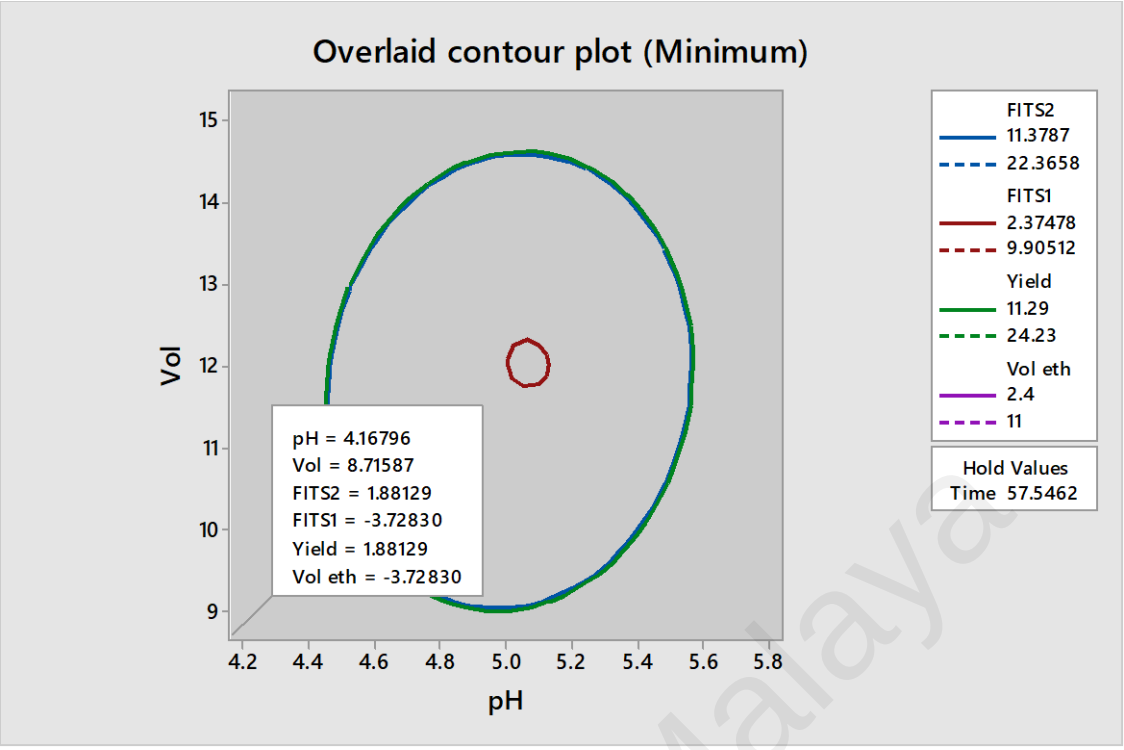

Figure 4.27: Overlaid contour plot at optimum minimum goal: pH of 4.17, volume inoculum of 8.72 ml and fermentation time of 57.50 hr.

Table 4.14: Optimum value for ethanol production from LLS.

Parameter	**Optimum value for ethanol production**
pH	4.87
Volume inoculum (ml)	12.92
Fermentation (hr)	117.68

Three-dimensional response surface and contour plots can give a clearer geometrical representation of the interaction between the variables and response within the experimental range studied by considering the possible combinations. They showed the relative effects of any two variables when the remaining variable was kept constant (Jung *et al*., 2013; Prakash Maran & Manikandan, 2012). The plot illustrates the main and the interactive effects of the independent variables on the dependent ones as can be seen in Figure 4.28 and Figure 4.29. Response surfaces plots of glucose conversion from LLS was obtained using predicted values from the fitted model by keeping one of the

independent variables fixed at the optimum value while modifying the other two variables. Figure 4.30 demonstrates the interaction effect on the process variables (pH,

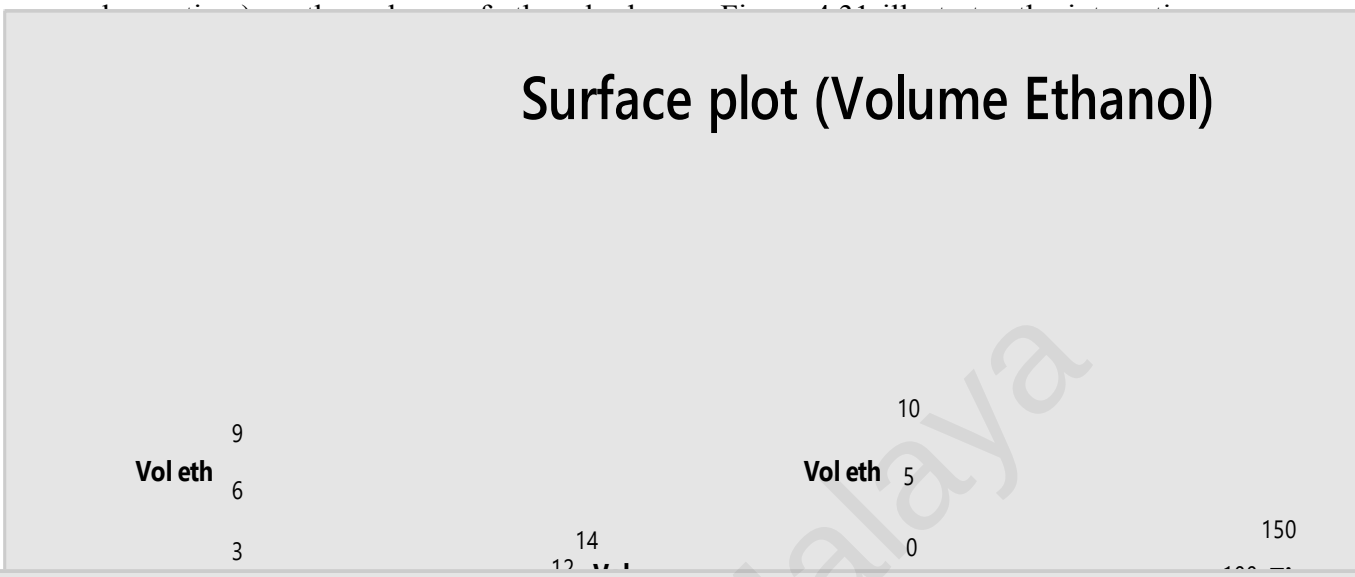

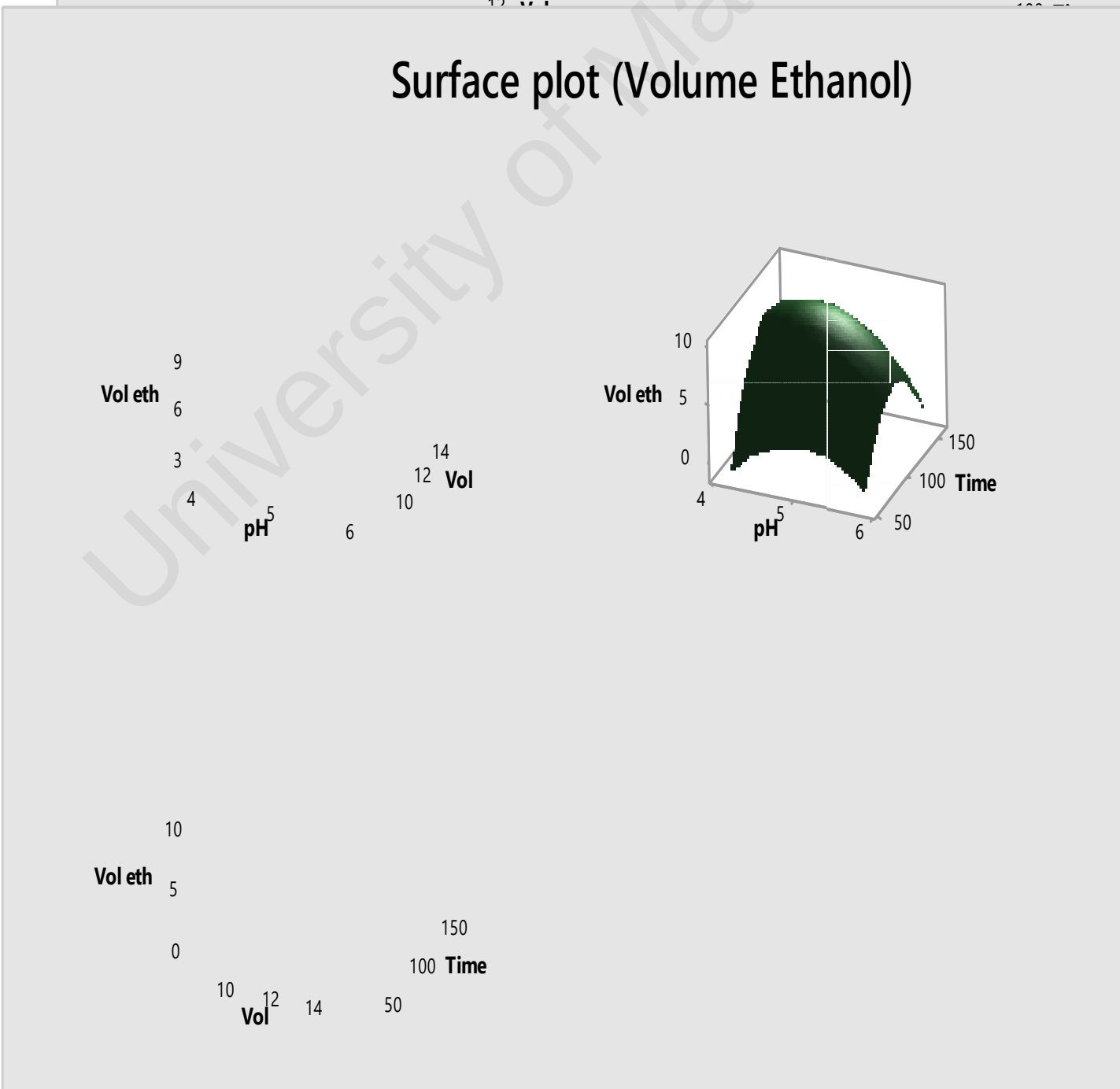

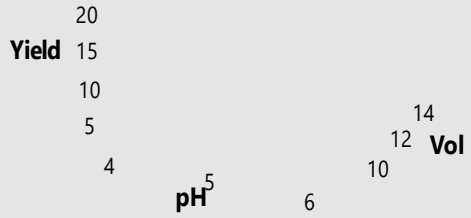

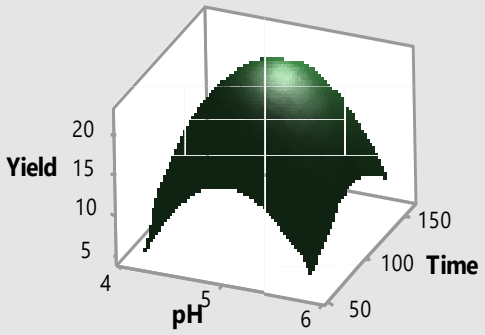

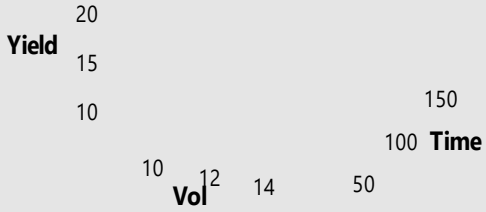

When the level of fermentation period was increased, a linear increase in ethanol production was recorded up to 120 hours. Additionally, as the fermentation time was prolonged, the ethanol concentration decreased due to either insufficient glucose left in the fermentation flask or very slight increase in the acidity of the medium could have caused this change (Uncu & Cekmecelioglu, 2011). This result corroborated a study by Canilha *et al*. (2010), which produced ethanol from non-detoxified sugarcane bagasse hydrolysate in 120 hr. Meanwhile, the fermentation of the detoxification sugarcane bagasse hydrolysate by pH alteration that was combined with active charcoal treatment and adsorption into ion-exchange resins had provided less fermentation time of 48 hours (Canilha *et al*., 2010). Thus, these results confirmed the idea that sufficient time is necessary for the complete consumption of sugar found in the lignocellulosic hydrolysate, whereas the fermentation time decreases considerably when using the detoxified hydrolysates instead of the non-detoxified hydrolysate.

The response between fermentation time and inoculum volume indicated that inoculum volume at 12.92 ml was optimum with 117.68 hr' fermentation time for bioethanol production. It can be seen from both figures (Figure 4.28 and Figure 4.29) that up to the mid-values of inoculum volume and fermentation time, ethanol concentrations increased but then showed a slight decrease at higher values of inoculum and fermentation time. Uncu and Cekmecelioglu (2011) stated that the high amount of inoculum can adversely affect the ethanol production due to the fact that high increase in inoculum size decreases the viability of yeast population and causes inadequate development of biomass and ethanol production. The response surface plots can be categorized into two shape terms known as elliptical or circular, which determine whether the interactions between the variables are significant or not (Panwal *et al*., 2011). A circular contour plot indicates that the interactions between the related variables are negligible while an elliptical contour plot indicates that the interactions between the related variables are significant (Mannan *et al*., 2007).

The circular shape of the contour plots between pH and inoculum volume (Figure 4.30a) as well as the fermentation time and pH (Figure 4.31c) indicated that there was no significant interaction effect between these variable sets on both responses whereas the elliptical shape of the contour plots between pH and fermentation time (Figure 4.30b and 4.31b), fermentation time and volume (Figure 4.30c), and inoculum volume and pH indicated that there was a significant interaction effect between these variable sets on the production of bioethanol.

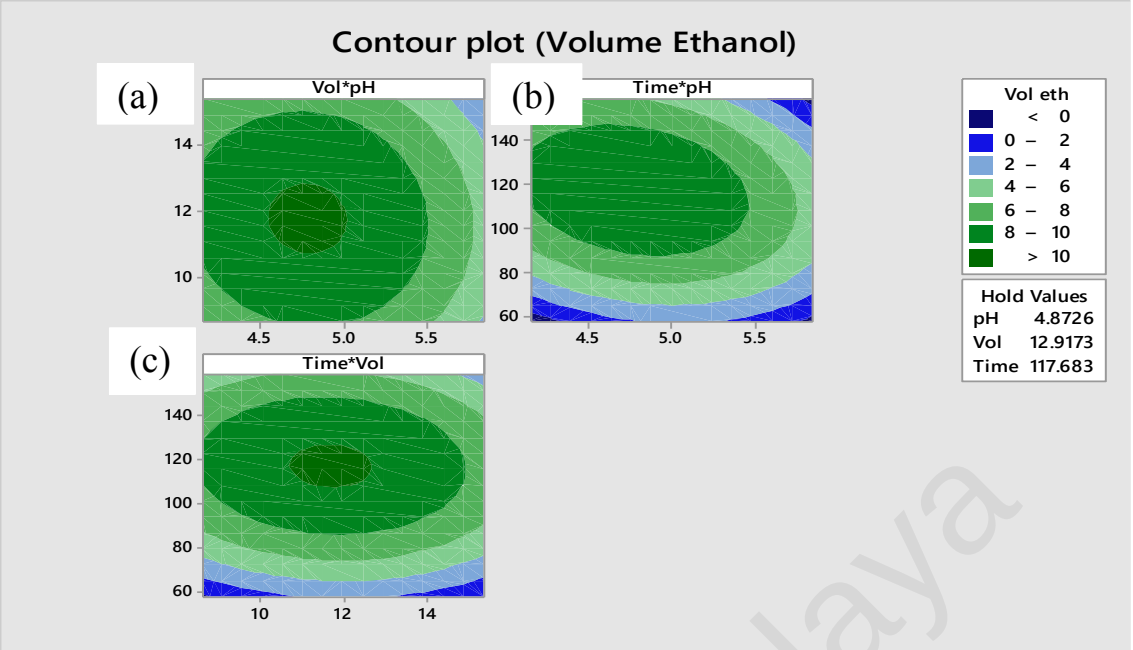

Figure 4.30: Contour plot of optimization of volume ethanol in LLS at the feasible optimum condition; pH of 4.87, volume inoculum of 12.92 ml and fermentation time of 117.68 hr.

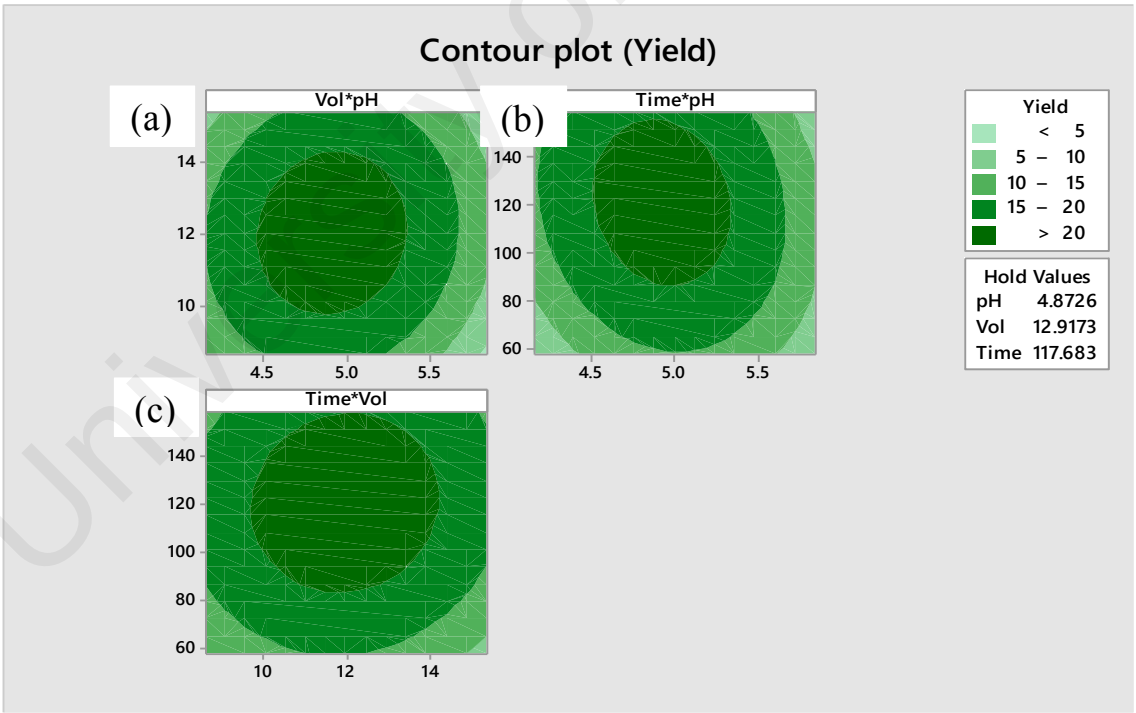

Figure 4.31: Contour plot of optimization of concentration ethanol in LLS at the feasible optimum condition; pH of 4.87, volume inoculum of 12.92 ml and fermentation time of 117.68 hr.

Validation for the optimum conditions of bioethanol production from glucose hydrolyzate MLLS was performed and the results are as shown in Table 4.16. The suitability of the model equation for predicting the optimum response value was evaluated for the optimum conditions of bioethanol production under conditions involving pH of 4.87, inoculum volume of 12.91, and fermentation time of 117.68 hr. Optimization using actual experimental values was tested using the t-test (SPSS). There was no significant difference ($p > 0.05$) between the predicted and verified values, thus indicating that the model was significant and can be used to predict the optimization of bioethanol in MLLS glucose hydrolysate.

Table 4.15: Comparison of the verified and predicted values of production ethanol at feasible optimum conditions.

Optimum condition			**Reponses**			
X_1	X_2	X_3	Volume ethanol (ml)		Concentration ethanol (% v/v)	
			V	P	V	P
4.87	12.92	117.6830	8.48 [a]	9.89[a]	21. 34[a]	22.18 [a]

Where: X_1= pH of solution, X_2= inoculumn volume (ml), X_3= fermentation time (hr), V= verification value, P= predicted value.

Value are expressed as mean (n=3). Mean within a column with different letters are significantly different ($p<0.05$, t test).

CHAPTER 5: CONCLUSION AND FUTURE WORK RECOMMENDATION

5.1 Conclusion

Leucaena leucocephala seeds were chosen as the raw material for this investigation because of their abundance and suitability. In this study, the experimental results showed that the boiling water under reflux can be considered as one of the cost effective and environmentally friendly methods to disrupt and remove some non-cellulosic compounds. Cellulose can be produced from different kinds of raw material. The most important factor to be considered is the availability of raw materials for the targeted production. Cellulose was successfully extracted from *Leucaena leucocephala* seeds and has better or similar properties to those of agricultural wastes reported in literature. The successful isolation of cellulose from LLS has given an opportunity for effective utilization of a natural product that would otherwise go as waste. Two types of cellulose isolation process namely acid and alkaline are conducted to investigate the effect these treatments on the yield and chemical properties of obtained cellulose. Purification of cellulose was performed using mixture of 80% acetic acid and 65% nitric acid. It was observed that this method produced high purity of cellulose and reduced the loss of cellulose as compared to alkaline method.

Further, cellulose was successfully extracted from waste *Leucaena leucocephala* seeds and disintegrated to microcrystalline and nanocellulose. The characteristics of cellulose, microcrystalline cellulose, and cellulose nanocrystal purified from *Leucaena leucochephala* were investigated by means of different techniques. Cellulose prepared from seed of *Leucaena leucochephala* has properties similar to others agricultural residue. FESEM micrographs showed that MLLS of CLLS comprised individual and few bundle forms. Meanwhile, the morphology of nanofibrils obtained displays a rod-like shape. An entangled network of cellulose fibres with a diameter in the range of 2-

11 nm was seen in the TEM images. The nanofibres also exhibited enhanced thermal properties. FTIR analyses demonstrated that most hemicellulose and lignin of the raw fibers were removed during the extraction process. Also, the results revealed that the removal of non-cellulosic components from the raw fibre was responsible for the increase in the cellulose content. Thermal gravimetric analysis and X-ray diffraction results were in agreement with the reported literatures. X-ray diffraction and thermal degradation analysis of various samples revealed that acid hydrolysis process potentially influenced the quality of the cellulose. The microcrystalline cellulose (MLLS) sample prepared exhibits improved thermal stability and crystallinity properties. The microcellulose and nanocellulose obtained are considered to be potential candidates for many industrial applications.

Further, the extracted cellulose can be used as a source for various applications. This study presented the hydrolysis of cellulose from LLS to glucose. The results from this study demonstrated that acid concentration has a profound influence on glucose production. 5% acid concentration (H_2SO_4) with a heating rate of 2 hours at 121 °C gave favorable reaction conditions for the conversion of cellulose to glucose from *Leucaena leucocephala* seeds. The glucose hydrolyzate obtained was used as a source for bioethanol production. Response surface model was developed to predict the ethanol production using various combinations of pH, inoculum volume, and fermentation time. According to the developed model, the maximum ethanol production from glucose hydrolyzate LLS in fermentation was obtained at incubation period of 117.68 hr, pH of 4.87, and inoculum volume of 12.92 ml by *S. cerevisiae*. This study suggested that the use of *Leucaena leucocephala* waste seeds may be a feasible option as a feed material for the production of glucose for bioethanol and other value-added chemicals due its low cost and high sugar yields.

5.2 Future work recommendation

A few suggestions for further studies are proposed below:

1. MCC and NCC particle populations consist of a mixture of single particle and agglomerates. These proportions will contribute to the different properties of these materials such as wettability, stability, and cohesiveness or dispersability. It is recommended that further research pertaining to these issues be sought by manipulating the parameter and processes involved in their production.
2. During acid hydrolysis of cellulose to glucose the inhibitory compounds like acetic acid, hydroxymethylfurfural, and lignin derivatives are also liberated in the hydrolysate. Such compounds act as inhibitors of the microbial metabolism, hindering the bioconversion of sugars into desired products. For this reason, the cellulose hydrolysate should be detoxified by different methods like pH adjustment, active charcoal adsorption, and ion-exchange resins adsorption. Also, the degree of inhibition to the ethanol yield need to be studied, by adding the glucose hydrolysate with different types of inhibitor.
3. Besides the scientific evidenced resulted from this study, future studies by other researcher on *Leucaena leucocephala* seeds are also important for promoting the use of these seeds as a valuable material, such as in biocomposite, food, packaging and pharmaceutical.
4. Isolation of the cellulose from stem of *Leucaena leucocephala* to investigate its possibility in producing similar results as reported in the seeds.

REFERENCES

Abdul Khalil, H. P. S., Davoudpour, Y., Islam, M. N., Mustapha, A., Sudesh, K., Dungani, R., & Jawaid, M. (2014). Production and modification of nanofibrillated cellulose using various mechanical processes: A review. *Carbohydrate Polymers*, *99*, 649-665.

Abraham, E., Deepa, B., Pothan, L. A., Jacob, M., Thomas, S., Cvelbar, U., & Anandjiwala, R. (2011). Extraction of nanocellulose fibrils from lignocellulosic fibres: A novel approach. *Carbohydrate Polymers*, *86*(4), 1468-1475.

Abu Zarin, M., Wan, H. Y., Isha, A., & Armania, N. (2016). Antioxidant, antimicrobial and cytotoxic potential of condensed tannins from *Leucaena leucocephala* hybrid-Rendang. *Food Science and Human Wellness*, *5*(2), 65-75.

Aderibigbe, S. A., Adetunji, O. A., & Odeniyi, M. A. (2011). Antimicrobial and pharmaceutical properties of the seed oil of *Leucaena leucocephala* (Lam.) De Wit (Leguminosae). *African Journal of Biomedical Research*, *14*(1), 63-68.

Aditiya, H. B., Mahlia, T. M. I., Chong, W. T., Nur, H., & Sebayang, A. H. (2016). Second generation bioethanol production : A critical review. *Renewable and Sustainable Energy Reviews*, *66*, 631-653.

Ahmed, M. E., & Abdelati, K. A. (2009). Chemical composition and amino acids profile of *Leucaena leucocephala* seeds. *International Journal of Poultry Science*, *8*(10), 966-970.

Al-Judaibi, A. A. (2011). Effect of some fermentation parameters on ethanol production from beet molasses by *Saccharomyces cerevisiae* CAIM13. *American Journal of Agricultural and Biological Science*, *6*(2), 301-306.

Al-Mefarrej, H. A., Abdel-Aal, M. A., Nasser, R. A., & Shetta, N. D. (2011). Impact of initial tree spacing and stem height levels on chemical composition of *Leucaeana leucocephala* trees grown in Riyadh region. *World Applied Sciences*, *12*(7), 912-918.

Alliet, D. (1967). Analysis of the negative peaks in gel permeation chromatography. *Journal of Polymer Science Part A: Polymer Chemistry*, *5*(7), 1783-1787.

Almagro, A., Prista, C., Castro, S., Quintas, C., Madeira-Lopes, A., Ramos, J., & Loureiro-Dias, M. C. (2000). Effects of salts on *Debaryomyces hansenii* and *Saccharomyces cerevisiae* under stress conditions. *International Journal of Food Microbiology*, *56*(2-3), 191-197.

Álvarez, A., Cachero, S., González-Sánchez, C., Montejo-Bernardo, J., Pizarro, C., & Bueno, J. L. (2018). Novel method for holocellulose analysis of non-woody biomass wastes. *Carbohydrate Polymers*, *189*, 250-256.

Aminah, A., & Wong, C. C. (2004). Dry matter productivity and nutritive quality of *leucaena* hybrid lines for high protein feed production. *Journal of Tropical Agriculture and Food Science*, *32*(2), 251.

Amiri, H., & Karimi, K. (2013). Efficient dilute-acid hydrolysis of cellulose using solvent pretreatment. *Industrial and Engineering Chemistry Research*, *52*(33), 11494-11501.

Antal, M. J., Allen, S. G., Dai, X., Shimizu, B., Tam, M. S., & Grønli, M. (2000). Attainment of the theoretical yield of carbon from biomass. *Industrial and Engineering Chemistry Research*, *39*(11), 4024-4031.

Atabani, A. E., Silitonga, A. S., Ong, H. C., Mahlia, T. M. I., Masjuki, H. H., Badruddin, I. A., & Fayaz, H. (2013). Non-edible vegetable oils: a critical evaluation of oil extraction, fatty acid compositions, biodiesel production, characteristics, engine performance and emissions production. *Renewable and Sustainable Energy Reviews*, *18*, 211-245.

Balat, M. (2011). Production of bioethanol from lignocellulosic materials via the biochemical pathway : A review. *Energy Conversion and Management*, *52*(2), 858-875.

Balat, M., & Balat, H. (2009). Recent trends in global production and utilization of bio-ethanol fuel. *Applied Energy*, *86*(11), 2273-2282.

Bano, S., & Negi, Y. S. (2017). Studies on cellulose nanocrystals isolated from groundnut shells. *Carbohydrate Polymers*, *157*, 1041-1049.

Battista, O. A. (1950). Hydrolysis and crystallization of cellulose. *Industrial & Engineering Chemistry*, *42*(3), 502-507.

Benjakul, S., Kittiphattanabawon, P., Sumpavapol, P., & Maqsood, S. (2012). Antioxidant activities of lead (*Leucaena leucocephala*) seed as affected by extraction solvent, prior dechlorophyllisation and drying methods. *Journal of Food Science and Technology*, *51*(11), 3026-3037.

Bhatnagar, A., & Sain, M. (2005). Processing of cellulose nanofiber-reinforced composites. *Journal of Reinforced Plastics and Composites*, *24*(12), 1259-1268.

Bhattacharya, D., Germinario, L. T., & Winter, W. T. (2008). Isolation, preparation and characterization of cellulose microfibers obtained from bagasse. *Carbohydrate Polymers*, *73*(3), 371-377.

Bian, J., Peng, F., Peng, X. P., Peng, P., Xu, F., & Sun, R. C. (2012). Acetic acid enhanced purification of crude cellulose from sugarcane bagasse: Structural and morphological characterization. *BioResources*, *7*(4), 4626-4639.

Binod, P., Sindhu, R., Singhania, R. R., Vikram, S., Devi, L., Nagalakshmi, S., … Pandey, A. (2010). Bioethanol production from rice straw : An overview. *Bioresource Technology*, *101*(13), 4767-4774.

Bondeson, D., Mathew, A., & Oksman, K. (2006). Optimization of the isolation of nanocrystals from microcrystalline cellulose by acid hydrolysis. *Cellulose*, *13*(2), 171-180.

Boonterm, M., Sunyadeth, S., Dedpakdee, S., Athichalinthorn, P., Patcharaphun, S., Mungkung, R., & Techapiesancharoenkij, R. (2016). Characterization and comparison of cellulose fiber extraction from rice straw by chemical treatment and thermal steam explosion. *Journal of Cleaner Production*, *134*, 592-599.

Brethauer, S., & Wyman, C. E. (2010). Review : Continuous hydrolysis and fermentation for cellulosic ethanol production. *Bioresource Technology*, *101*(13), 4862-4874.

Brinchi, L., Cotana, F., Fortunati, E., & Kenny, J. M. (2013). Production of nanocrystalline cellulose from lignocellulosic biomass: Technology and applications. *Carbohydrate Polymers*, *94*(1), 154-169.

Canilha, L., Carvalho, W., De Almeida Felipe, M. D. G., De Almeida E Silva, J. B., & Giulietti, M. (2010). Ethanol production from sugarcane bagasse hydrolysate using *Pichia stipitis*. *Applied Biochemistry and Biotechnology*, *161*(1-8), 84-92.

Cardenas-toro, F. P., Alcazar-alay, S. C., Forster-carneiro, T., & Meireles, M. A. A. (2014). Obtaining oligo and monosaccharides from agroindustrial and agricultural residues using hydrothermal treatments. *Food and Public Health*, *4*(3), 123-139.

Casey, E., Mosier, N. S., Adamec, J., Stockdale, Z., Ho, N., & Sedlak, M. (2013). Effect of salts on the co-fermentation of glucose and xylose by a genetically engineered strain of *Saccharomyces cerevisiae*. *Biotechnology for Biofuels*, *6*(1), 1-10.

Castro, C., Zuluaga, R., Putaux, J. L., Caro, G., Mondragon, I., & Gañán, P. (2011). Structural characterization of bacterial cellulose produced by *Gluconacetobacter swingsii sp.* from Colombian agroindustrial wastes. *Carbohydrate Polymers*, *84*(1), 96-102.

Chen, W., Li, Q., Wang, Y., Yi, X., Zeng, J., Yu, H., Liu, Y & Li, J. (2014). Comparative study of aerogels obtained from differently prepared nanocellulose fibers. *ChemSusChem*, *7*(1), 154-161.

Cheng, Q., Wang, S., Rials, T. G., & Lee, S. H. (2007). Physical and mechanical properties of polyvinyl alcohol and polypropylene composite materials reinforced with fibril aggregates isolated from regenerated cellulose fibers. *Cellulose*, *14*(6), 593-602.

Chandraju, S., Kumar, C. C., & Venkatesh, R. (2014). Estimation of reducing sugar by acid hydrolysis of black grape (*Vitis vinifera L.*) peels by standard methods. *Journal of Chemical and Pharmaceutical Research*, *6*(5), 862-866.

Chandrasekhara Rao, T., Lakshminarayana, G., Prasad, N. B. L., Jagan Mohan Rao, S., Azeemoddin, G., Atchyuta Ramayya, D., & Thirumala Rao, S. D. (1984). Characteristics and compositions of *Carissa spinarum*, *Leucaena leucocephala* and *Physalis* minima seeds and oils. *Journal of the American Oil Chemists' Society*, *61*(9), 1472-1473.

Cherian, B. M., Leão, A. L., de Souza, S. F., Costa, L. M. M., de Olyveira, G. M., Kottaisamy, … Thomas, S. (2011). Cellulose nanocomposites with nanofibres isolated from pineapple leaf fibers for medical applications. *Carbohydrate Polymers*, *86*(4), 1790-1798.

Chinwan, D., & Pant, S. (2013). Bioethanol, butanol & biodiesel from crop residue. *International Journal of Engineering & Science Research*, *4*(11),812-819.

Chirayil, C. J., Joy, J., Mathew, L., Mozetic, M., Koetz, J., & Thomas, S. (2014). Isolation and characterization of cellulose nanofibrils from *Helicteres isora* plant. *Industrial Crops and Products*, *59*, 27-34.

Chirayil, C. J., Mathew, L., & Thomas, S. (2014). Review of recent research in nano cellulose preparation from different lignocellulosic fibers. *Reviews on Advanced Materials Science*, *37*(1-2), 20-28.

Chotchutima, S., Kangvansaichol, K., Tudsri, S., & Sripichitt, P. (2013). Effect of spacing on growth, biomass yield and quality of *Leucaena* (*Leucaena leucocephala* (Lam.) de Wit.) for renewable energy in Thailand. *Journal of Sustainable Bioenergy Systems*, *3*(1), 48.

Chowtivannakul, P., Srichaikul, B., & Talubmook, C. (2016). Antidiabetic and antioxidant activities of seed extract from *Leucaena leucocephala* (Lam.) de Wit. *Agriculture and Natural Resources*, *50*(5), 357-361.

Chuayjuljit, S., Su-uthai, S., & Charuchinda, S. (2010). Poly (vinyl chloride) film filled with microcrystalline cellulose prepared from cotton fabric waste: Properties and biodegradability study. *Waste Management & Research*, *28*(2), 109-117.

Colom, X., & Carrillo, F. (2005). Comparative study of wood samples of the northern area of Catalonia by FTIR. *Journal of Wood Chemistry and Technology*, *25*(1-2), 1-11.

Da Silva, A. S. A., Inoue, H., Endo, T., Yano, S., & Bon, E. P. S. (2010). Milling pretreatment of sugarcane bagasse and straw for enzymatic hydrolysis and ethanol fermentation. *Bioresource Technology*, *101*(19), 7402-7409.

Dahnum, D., Tasum, S. O., Triwahyuni, E., Nurdin, M., & Abimanyu, H. (2015). Comparison of SHF and SSF processes using enzyme and dry yeast for optimization of bioethanol production from empty fruit bunch. *Energy Procedia*, *68*, 107-116.

Das, A. M., Hazarika, M. P., Goswami, M., Yadav, A., & Khound, P. (2016). Extraction of cellulose from agricultural waste using Montmorillonite K-10/LiOH and its conversion to renewable energy: Biofuel by using *Myrothecium gramineum*. *Carbohydrate Polymers*, *141*, 20-27.

Dash, P. K., Mohaptra, S., Swain, M. R., & Thatoi, H. (2017). Optimization of bioethanol production from saccharified sweet potato root flour by co-fermentation of *Saccharomyces cerevisiae* and *Pichia sp.* using OVAT and response surface methodologies. *Acta Biologica Szegediensis*, *61*(1), 13-23.

Datta, D., & Kumar, S. (2012). Modeling and optimization of recovery process of glycolic acid using reactive extraction. *Journal of Chemical Engineering and Applications*, *3*(2), 141-146.

De Lima, C. J. B., Coelho, L. F., Contiero, J., Lima, C. J. B. De, Coelho, L. F., & Contiero, J. (2010). The use of response surface methodology in optimization of lactic acid production: Focus on medium supplementation, temperature and pH control. *Food Technology and Biotechnology*, *48*(2), 175-181.

Deepa, B., Abraham, E., Cordeiro, N., Mozetic, M., Mathew, A. P., Oksman, K., … Pothan, L. A. (2015). Utilization of various lignocellulosic biomass for the production of nanocellulose: A comparative study. *Cellulose*, *22*(2), 1075-1090.

Demirbas, M. F., Balat, M., & Balat, H. (2009). Potential contribution of biomass to the sustainable energy development. *Energy Conversion and Management*, *50*(7), 1746-1760.

Deodhar, U. P., Paradkar, A. R., & Purohit, A. P. (1998). Preliminary evaluation of *Leucaena leucocephala* seed gum as a tablet binder. *Drug Development and Industrial Pharmacy*, *24*(6), 577-582.

Díaz, M. J., García, M. M., Eugenio, M. E., Tapias, R., Fernández, M., & López, F. (2007). Variations in fiber length and some pulp chemical properties of *Leucaena* varieties. *Industrial Crops and Products*, *26*, 142-150.

Ditzel, F. I., Prestes, E., Carvalho, B. M., Demiate, I. M., & Pinheiro, L. A. (2017). Nanocrystalline cellulose extracted from pine wood and corncob. *Carbohydrate Polymers*, *157*, 1577-1585.

Driscoll, M., Stipanovic, A., Winter, W., Cheng, K., Manning, M., Spiese, J., ... & Cleland, M. R. (2009). Electron beam irradiation of cellulose. *Radiation Physics and Chemistry*, *78*(7-8), 539-542.

Dubois, M., Gilles, K. A., Hamilton, J. K., Rebers, P. T., & Smith, F. (1956). Colorimetric method for determination of sugars and related substances. *Analytical chemistry*, *28*(3), 350-356.

Duff, S. J. B., & Murray, W. D. (1996). Bioconversion of forest products industry waste cellulosics to fuel ethanol: A review. *Bioresource Technology*, *55*, 1-33.

Duque, A., Manzanares, P., & Ballesteros, M. (2017). Extrusion as a pretreatment for lignocellulosic biomass: Fundamentals and applications. *Renewable Energy*, *114*, 1427-1441.

Dussan, K. J., Silva, D. D., Moraes, E. J., Arruda, P. V., & Felipe, M. G. (2014). Dilute-acid hydrolysis of cellulose to glucose from sugarcane bagasse. *Chemical Engineering Transaction*, *38*, 433-438.

El-Sakhawy, M., & Hassan, M. L. (2007). Physical and mechanical properties of microcrystalline cellulose prepared from agricultural residues. *Carbohydrate Polymers*, *67*(1), 1-10.

Elanthikkal, S., Gopalakrishnapanicker, U., Varghese, S., & Guthrie, J. T. (2010). Cellulose microfibres produced from banana plant wastes: Isolation and characterization. *Carbohydrate Polymers*, *80*(3), 852-859.

Esfahanian, M., Nikzad, M., Najafpour, G., & Ghoreyshi, A. (2013). Modeling and optimization of ethanol fermentation using *Saccharomyces cerevisiae*: Response surface methodology and artificial neural network. *Chemical Industry and Chemical Engineering Quarterly*, *19*(2), 241-252.

Fahma, F., Iwamoto, S., Hori, N., Iwata, T., & Takemura, A. (2010). Isolation, preparation, and characterization of nanofibers from oil palm empty-fruit-bunch (OPEFB). *Cellulose*, *17*(5), 977-985.

Feria, M. J., García, J. C., Díaz, M. J., Fernández, M., & López, F. (2012). Biorefinery process for production of paper and oligomers from *Leucaena leucocephala* K360 with or without prior autohydrolysis. *Bioresource Technology*, *126*, 64-70.

Feria, M. J., López, F., García, J. C., Pérez, A., Zamudio, M. A., & Alfaro, A. (2011). Valorization of *Leucaena leucocephala* for energy and chemicals from autohydrolysis. *Biomass and Bioenergy*, *35*(5), 2224-2233.

Ferreira, F. V., Mariano, M., Rabelo, S. C., Gouveia, R. F., & Lona, L. M. F. (2018). Isolation and surface modification of cellulose nanocrystals from sugarcane bagasse waste: From a micro to a nano-scale. *Applied Surface Science*, *436*, 1113-1122.

Ferro, M. D., Fernandes, M. C., Paulino, A. F. C., Prozil, S. O., Gravitis, J., Evtuguin, D. V, & Xavier, A. M. R. B. (2015). Bioethanol production from steam explosion pretreated and alkali extracted *Cistus ladanifer* (rockrose). *Biochemical Engineering Journal*, *104*, 98-105.

Frone, A. N., Chiulan, I., Panaitescu, D. M., Nicolae, C. A., Ghiurea, M., & Galan, A. M. (2017). Isolation of cellulose nanocrystals from plum seed shells, structural and morphological characterization. *Materials Letters*, *194*, 160-163.

Frone, A. N., Panaitescu, D. M., & Donescu, D. (2011). Some aspects concerning the isolation of cellulose micro and nano-fibers. *UPB Scientific Bulletin, Series B: Chemistry and Materials Science*, *73*(2), 133-152.

Frone, A. N., Panaitescu, D. M., Spataru, D. D., Radovici, C., Trusca, R., & Somoghi, R. (2011). Preparation and characterization of PVA composites with cellulose nanofibers obtained by ultrasonication. *BioResources*, *6*(1), 487-512.

Gamble, J. F., Chiu, W. S., & Tobyn, M. (2011). Investigation into the impact of sub-populations of agglomerates on the particle size distribution and flow properties of conventional microcrystalline cellulose grades. *Pharmaceutical Development and Technology*, *16*(5), 542-548.

Gámez, S., González-Cabriales, J. J., Ramírez, J. A., Garrote, G., & Vázquez, M. (2006). Study of the hydrolysis of sugar cane bagasse using phosphoric acid. *Journal of Food Engineering*, *74*(1), 78-88.

García, A., Gandini, A., Labidi, J., Belgacem, N., & Bras, J. (2016). Industrial and crop wastes: A new source for nanocellulose biorefinery. *Industrial Crops and Products*, *93*, 26-38.

Garnayak, D. K., Pradhan, R. C., Naik, S. N., & Bhatnagar, N. (2008). Moisture-dependent physical properties of jatropha seed (*Jatropha curcas L.*). *Industrial Crops and Products*, *27*(1), 123-129.

Gericke, M., Fardim, P., & Heinze, T. (2012). Ionic liquids - promising but challenging solvents for homogeneous derivatization of cellulose. *Molecules*, *17*(6), 7458-7502.

Ghani, W. W. A. K., Abdullah, M. F., Loung, C., Ho, C., & Matori, K. (2008). Characterization of vitrified Malaysian agrowaste ashes as potential recycling material. *International Journal of Engineering and Technology*, *5*(2), 111-117.

Ghosh, S., Chakraborty, R., Chatterjee, G., & Raychaudhuri, U. (2012). Study on fermentation conditions of palm juice vinegar by response surface methodology and development of a kinetic model. *Brazilian Journal of Chemical Engineering*, *29*(3), 461-472.

Goldberg, R. N., Schliesser, J., Mittal, A., Decker, S. R., Santos, A. F. L. O. M., Freitas, V. L. S., … Johnson, D. K. (2015). A thermodynamic investigation of the cellulose allomorphs: Cellulose(am), cellulose Iβ(cr), cellulose II(cr), and cellulose III(cr). *Journal of Chemical Thermodynamics*, *81*, 184-226.

Gomes, N., Teixeira, J. A., & Belo, I. (2011). Empirical modelling as an experimental approach to optimize lactone production. *Catalysis Science & Technology*, *1*(1), 86.

Gómez H., C., Serpa, A., Velásquez-Cock, J., Gañán, P., Castro, C., Vélez, L., & Zuluaga, R. (2016). Vegetable nanocellulose in food science: A review. *Food Hydrocolloids*, *57*, 178-186.

González-Hernández, J. C., Farías Rosales, L., Zamudio Jaramillo, M. Á., Álvarez-Navarrete, M., Vera Villa, J. C., Martínez Corona, R., … Peña, A. (2012). Chemical hydrolysis of the polysaccharides of the tamarind seed. *Journal of the Mexican Chemical Society*, *56*(4), 395-401.

Gupta, A., & Verma, J. P. (2015). Sustainable bio-ethanol production from agro-residues: A review. *Renewable and Sustainable Energy Reviews*, *41*, 550-567.

Gupta, R., Sharma, K. K., & Kuhad, R. C. (2009). Separate hydrolysis and fermentation (SHF) of *Prosopis juliflora*, a woody substrate, for the production of cellulosic ethanol by *Saccharomyces cerevisiae* and *Pichia stipitis*-NCIM 3498. *Bioresource Technology*, *100*(3), 1214-1220.

Haafiz, M. K. M., Hassan, A., Zakaria, Z., & Inuwa, I. M. (2014). Isolation and characterization of cellulose nanowhiskers from oil palm biomass microcrystalline cellulose. *Carbohydrate Polymers*, *103*(1), 119-125.

Habeeb, S., Yazaji, S., & Al-Amir, L. (2016). Optimization of glucose isomerase production from *Streptomyces sp.* SH10 using the response surface methodology. *International Food Research Journal*, *23*(2), 756-761.

Haghighi Mood, S., Hossein Golfeshan, A., Tabatabaei, M., Salehi Jouzani, G., Najafi, G. H., Gholami, M., & Ardjmand, M. (2013). Lignocellulosic biomass to bioethanol, a comprehensive review with a focus on pretreatment. *Renewable and Sustainable Energy Reviews*, *27*, 77-93.

Hajar, N., Zainal, S., Atikah, O., & Elida, T. (2012). Optimization of ethanol fermentation from pineapple peel extract using response surface methodology (RSM). *International Journal of Biological, Biomolecular, Agricultural, Food and Biotechnological Engineering*, *6*(12), 1102-1108.

Hakimi, M. I., Goembira, F., & Ilham, Z. (2017). Engine-compatible biodiesel from *Leucaena leucocephala* seed oil. *Journal of the Society of Automotive Engineers Malaysia*, *1*(2), 86-93.

Han, G., Deng, J., Zhang, S., Bicho, P., & Wu, Q. (2010). Effect of steam explosion treatment on characteristics of wheat straw. *Industrial Crops and Products*, *31*(1), 28-33.

Han, M. D., Han, J. S., Hyun, S. H., & Shin, H. W. (2008). Solubilization of water-insoluble beta-glucan isolated from *Ganoderma lucidum*. *Journal of Environmental Biology*, *29*(2), 237.

Hassan, S. N. A. M., Ishak, M. A. M., Ismail, K., Ali, S. N., & Yusop, M. F. (2014). Comparison study of rubber seed shell and kernel (*Hevea brasiliensis*) as raw material for bio-oil production. *Energy Procedia*, *52*, 610-617.

Hegner, J., Pereira, K. C., DeBoef, B., & Lucht, B. L. (2010). Conversion of cellulose to glucose and levulinic acid via solid-supported acid catalysis. *Tetrahedron Letters*, *51*(17), 2356-2358.

Henrique, M. A., Silvério, H. A., Flauzino Neto, W. P., & Pasquini, D. (2013). Valorization of an agro-industrial waste, mango seed, by the extraction and characterization of its cellulose nanocrystals. *Journal of Environmental Management*, *121*, 202-209.

Herrero, M., Cifuentes, A., Ibáñez, E., & Castillo, M. D. El. (2011). Advanced analysis of carbohydrates in foods. *Methods of Analysis of Food Components and Additctives*, 135-164.

Hirai, A., Inui, O., Horii, F., & Tsuji, M. (2009). Phase separation behavior in aqueous suspensions of bacterial cellulose nanocrystals prepared by sulfuric acid treatment. *Langmuir*, *25*(1), 497-502.

Hoşgün, E. Z., Berikten, D., Kıvanç, M., & Bozan, B. (2017). Ethanol production from hazelnut shells through enzymatic saccharification and fermentation by low-temperature alkali pretreatment. *Fuel*, *196*, 280-287.

Hsu, W., Lee, Y., Peng, W., & Wu, K. C. (2011). Cellulosic conversion in ionic liquids (ILs): Effects of H_2O / cellulose molar ratios , temperatures , times , and different ILs on the production of monosaccharides and. *Catalysis Today*, *174*(1), 65-69.

Hu, Y., Catchmark, J. M., Zhu, Y., Abidi, N., Zhou, X., Wang, J., & Liang, N. (2014). Engineering of porous bacterial cellulose toward human fibroblasts ingrowth for tissue engineering. *Journal of Materials Research*, *29*(22), 2683-2693.

Hung, L. V., Wanapat, M., & Cherdthong, A. (2013). Effects of *Leucaena* leaf pellet on bacterial diversity and microbial protein synthesis in swamp buffalo fed on rice straw. *Livestock Science*, *151*(2-3), 188-197.

Hutomo, G. S., Rahim, A., & Kadir, S. (2015). The effect of sulfuric and hydrochloric acid on cellulose degradation from pod husk cacao. *International Journal on Current Microbiology and Applied Sciences*, *4*(10), 89-95.

Ilham, Z., Hamidon, H., Rosji, N. A., Ramli, N., & Osman, N. (2015). Extraction and quantification of toxic compound mimosine from *Leucaena leucocephala* leaves. *Procedia Chemistry*, *16*, 164-170.

Ilindra, A., & Dhake, J. D. (2008). Microcrystalline cellulose from bagasse and rice straw. *Indian Jurnal of Technology, 15*, 497-499.

Iryani, D. A., Kumagai, S., Nonaka, M., Nagashima, Y., Sasaki, K., & Hirajima, T. (2014). The hot compressed water treatment of solid waste material from the sugar industry for valuable chemical production. *International Journal of Green Energy*, *11*, 577-588.

Isikgor, F. H., & Becer, C. R. (2015). Lignocellulosic biomass: A sustainable platform for the production of bio-based chemicals and polymers. *Polymer Chemistry*, *6*(25), 4497-4559.

Islam, J. M. M., Hossan, M. A., Alom, F. R., Khan, M. I. H., & Khan, M. A. (2017). Extraction and characterization of crystalline cellulose from jute fiber and application as reinforcement in biocomposite: Effect of gamma radiation. *Journal of Composite Materials*, *51*(1), 31-38.

Istirokhatun, T., Rokhati, N., Rachmawaty, R., Meriyani, M., Priyanto, S., & Susanto, H. (2015). Cellulose isolation from tropical water hyacinth for membrane preparation. *Procedia Environmental Sciences*, *23*, 274-281.

Iwamoto, S., Kai, W., Isogai, A., & Iwata, T. (2009). Elastic modulus of single cellulose microfibrils from tunicate measured by atomic force microscopy. *Biomacromolecules*, *10*(9), 2571-2576.

Izmirlioglu, G., & Demirci, A. (2012). Ethanol production from waste potato mash by using *Saccharomyces cerevisiae*. *Applied Sciences*, *2*(4), 738-753.

Jackson de Moraes Rocha, G., Martin, C., Soares, I. B., Souto Maior, A. M., Baudel, H. M., & Moraes de Abreu, C. A. (2011). Dilute mixed-acid pretreatment of sugarcane bagasse for ethanol production. *Biomass and Bioenergy*, *35*(1), 663-670.

Jahan, M. S., Saeed, A., He, Z., & Ni, Y. (2011). Jute as raw material for the preparation of microcrystalline cellulose. *Cellulose*, *18*(2), 451-459.

Jargalsaikhan, O., & Saraçoğlu, N. (2009). Application of experimental design method for ethanol production by fermentation of sunflower seed hull hydrolysate using *pichia stipitis* NRRL-124. *Chemical Engineering Communications*, *196*(1-2), 93-103.

Jiang, F., & Hsieh, Y.-L. (2015). Cellulose nanocrystal isolation from tomato peels and assembled nanofibers. *Carbohydrate Polymers*, *122*, 60-68.

Jiang, M., Zhao, M., Zhou, Z., Huang, T., Chen, X., & Wang, Y. (2011). Isolation of cellulose with ionic liquid from steam exploded rice straw. *Industrial Crops and Products*, *33*(3), 734-738.

Jiménez, L., Pérez, A., de la Torre, M. J., Moral, A., & Serrano, L. (2007). Characterization of vine shoots, cotton stalks, *Leucaena leucocephala* and *Chamaecytisus proliferus*, and of their ethyleneglycol pulps. *Bioresource Technology*, *98*, 3487-3490.

Johar, N., Ahmad, I., & Dufresne, A. (2012). Extraction, preparation and characterization of cellulose fibres and nanocrystals from rice husk. *Industrial Crops and Products*, *37*(1), 93-99.

Jonoobi, M., Harun, J., Tahir, P. M., Shakeri, A., Saifulazry, S., & Makinejad, M. D. (2011). Physicochemical characterization of pulp and nanofibers from kenaf stem. *Materials Letters*, *65*(7), 1098-1100.

Jose, C., Joy, J., Mathew, L., Koetz, J., & Thomas, S. (2014). Nanofibril reinforced unsaturated polyester nanocomposites : Morphology, mechanical and barrier properties, viscoelastic behavior and polymer chain confinement. *Industrial Crops & Products*, *56*, 246-254.

Julie Chandra, C. S., George, N., & Narayanankutty, S. K. (2016). Isolation and characterization of cellulose nanofibrils from arecanut husk fibre. *Carbohydrate Polymers*, *142*, 158-166.

Jung, J. Y., Choi, M. S., & Yang, J. K. (2013). Optimization of concentrated acid hydrolysis of waste paper using response surface methodology. *Journal of the Korean Wood Science and Technology*, *41*(2), 87-99.

Kabyemela, B. M., Adschiri, T., Malaluan, R. M., & Arai, K. (1997). Kinetics of glucose epimerization and decomposition in subcritical and supercritical water. *Industrial and Engineering Chemistry Research*, *36*(5), 1552-1558.

Kalia, S., Dufresne, A., Cherian, B. M., Kaith, B. S., Av, L., Njuguna, J., & Nassiopoulos, E. (2011). Cellulose-based bio and nanocomposites : A Review. *International Journal of Polymer Science*, 1-35.

Kalita, R. D., Nath, Y., Ochubiojo, M. E., & Buragohain, A. K. (2013). Extraction and characterization of microcrystalline cellulose from fodder grass; *Setaria glauca* (L) *P. Beauv*, and its potential as a drug delivery vehicle for isoniazid, a first line antituberculosis drug. *Colloids and Surfaces B: Biointerfaces*, *108*, 85-89.

Kallel, F., Bettaieb, F., Khiari, R., García, A., Bras, J., & Chaabouni, S. E. (2016). Isolation and structural characterization of cellulose nanocrystals extracted from garlic straw residues. *Industrial Crops and Products*, *87*, 287-296.

Kamio, E., Takahashi, S., Noda, H., Fukuhara, C., & Okamura, T. (2008). Effect of heating rate on liquefaction of cellulose by hot compressed water. *Chemical Engineering Journal*, *137*, 328-338.

Kang, S., Wanapat, M., Pakdee, P., Pilajun, R., & Cherdthong, A. (2012). Effects of energy level and *Leucaena leucocephala* leaf meal as a protein source on rumen fermentation efficiency and digestibility in swamp buffalo. *Animal Feed Science and Technology*, *174*(3-4), 131-139.

Karimi, K., & Taherzadeh, M. J. (2016). A critical review on analysis in pretreatment of lignocelluloses : Degree of polymerization, adsorption/desorption, and accessibility. *Bioresource Technology*, *203*, 348-356.

Keffer, V. I., Turn, S. Q., Kinoshita, C. M., & Evans, D. E. (2009). Ethanol technical potential in Hawaii based on sugarcane, banagrass, *Eucalyptus*, and *Leucaena*. *Biomass and Bioenergy*, *33*(2), 247-254.

Kim, H. S., Kim, S., Kim, H. J., & Yang, H. S. (2006). Thermal properties of bio-flour-filled polyolefin composites with different compatibilizing agent type and content. *Thermochimica Acta*, *451*(1-2), 181-188.

Khamlue, R., Ounaroon, A., & Saelim, N. (2012). Purification and characterization of polysaccharides extracted from *Tremella fuciformis* and *Auricularia auricula*. e-proceeding 1st Mae Fah Luang University International Conference 2012, Thailand, 1-9.

Koocheki, a, Razavi, S. M. a, Milani, E., Moghadam, T. M., Abedini, M., Alamatiyan, S., & Izadkhah, S. (2007). Physical properties of watermelon seed as a function of moisture content and variety. *International Agrophysics*, *21*, 349-359.

Kopania, E., Wietecha, J., & Ciechańska, D. (2012). Studies on isolation of cellulose fibres from waste plant biomass. *Fibres and Textiles in Eastern Europe*, *96*, 167-172.

Kuboyama, K., Sasaki, N., Nakagome, Y., & Kataoka, M. (2005). Wet digestion. *Analytical Chemistry*, *360*, 184-191.

Kuhad, R. C., Gupta, R., Khasa, Y. P., & Singh, A. (2010). Bioethanol production from *Lantana camara* (red sage): Pretreatment, saccharification and fermentation. *Bioresource Technology*, *101*(21), 8348-8354.

Kumar, S., Dheeran, P., Singh, S. P., Mishra, I. M., & Adhikari, D. K. (2015). Kinetic studies of two-stage sulphuric acid hydrolysis of sugarcane bagasse. *Renewable Energy*, *83*, 850-858.

Kumar, A. K., & Sharma, S. (2017). Recent updates on different methods of pretreatment of lignocellulosic feedstocks: A review. *Bioresources and Bioprocessing*, *4*(7), 1-19.

Kushnir, E. Y., Autlov, S. A., & Bazarnova, N. G. (2015). Preparation of microcrystalline cellulose directly from wood under microwave radiation. *Russian Journal of Bioorganic Chemistry*, *41*(7), 713-718.

Lanzafame, P., Temi, D. M., Perathoner, S., Spadaro, A. N., & Centi, G. (2012). Direct conversion of cellulose to glucose and valuable intermediates in mild reaction conditions over solid acid catalysts. *Catalysis Today*, *179*(1), 178-184.

Le Normand, M., Moriana, R., & Ek, M. (2014). Isolation and characterization of cellulose nanocrystals from spruce bark in a biorefinery perspective. *Carbohydrate Polymers*, *111*, 979-987.

Lenihan, P., Orozco, a., O'Neill, E., Ahmad, M. N. M., Rooney, D. W., & Walker, G. M. (2010). Dilute acid hydrolysis of lignocellulosic biomass. *Chemical Engineering Journal*, *156*, 395-403.

Levis, S. R., & Deasy, P. B. (2001). Production and evaluation of size reduced grades of microcrystalline cellulose. *International Journal of Pharmaceutics*, *213*(1-2), 13-24.

Li, C., Zhang, Z., & Zhao, Z. K. (2009). Direct conversion of glucose and cellulose to 5-hydroxymethylfurfural in ionic liquid under microwave irradiation. *Tetrahedron Letters*, *50*(38), 5403-5405.

Li, F. H., Hu, H. J., Yao, R. S., Wang, H., & Li, M. M. (2012). Structure and saccharification of rice straw pretreated with microwave-assisted dilute lye. *Industrial and Engineering Chemistry Research*, *51*, 6270-6274.

Lin, N., & Dufresne, A. (2014). Nanocellulose in biomedicine: Current status and future prospect. *European Polymer Journal*, *59*, 302-325.

Lin, X., Fan, J., Wen, Q., Li, R., Jin, X., Wu, J., … Ying, H. (2013). Optimization and validation of a GC–FID method for the determination of acetone-butanol-ethanol fermentation products. *Journal of chromatographic science*, *52*(3), 264-270.

Lin, Y., Zhang, W., Li, C., Sakakibara, K., Tanaka, S., & Kong, H. (2012). Factors affecting ethanol fermentation using *Saccharomyces cerevisiae* BY4742. *Biomass and Bioenergy*, *47*, 395-401.

Liu, C., Huang, Y., Wang, X., Tai, Y., Liu, L., Sun, C., & Liu, H. (2018). Emergy analysis for transportation fuels produced from corn stover in China. *Journal of Cleaner Production*, *174*, 213-225.

Liu, Z., Li, L., Liu, C., & Xu, A. (2017). Saccharification of cellulose in the ionic liquids and glucose recovery. *Renewable Energy*, *106*, 99-102.

Liu, Z., Li, X., Xie, W., & Deng, H. (2017). Extraction, isolation and characterization of nanocrystalline cellulose from industrial kelp (*Laminaria japonica*) waste. *Carbohydrate Polymers*, *173*, 353-359.

López-Bellido, L., Wery, J., & López-Bellido, R. J. (2014). Energy crops: Prospects in the context of sustainable agriculture. *European Journal of Agronomy*, *60*, 1-12.

López, F., García, J. C., Pérez, a., García, M. M., Feria, M. J., & Tapias, R. (2010). *Leucaena diversifolia* a new raw material for paper production by soda-ethanol pulping process. *Chemical Engineering Research and Design*, *88*, 1-9.

López, F., García, M. M., Yánez, R., Tapias, R., Fernández, M., & Díaz, M. J. (2008). *Leucaena* species valoration for biomass and paper production in 1 and 2 year harvest. *Bioresource Technology*, *99*, 4846-4853.

López, F., Pérez, a., García, J. C., Feria, M. J., García, M. M., & Fernández, M. (2011). Cellulosic pulp from *Leucaena diversifolia* by soda-ethanol pulping process. *Chemical Engineering Journal*, *166*, 22-29.

Lu, Q., Cai, Z., Lin, F., Tang, L., Wang, S., & Huang, B. (2016). Extraction of cellulose nanocrystals with a high yield of 88% by simultaneous mechanochemical activation and phosphotungstic acid hydrolysis. *Sustainable Chemistry and Engineering*, *4*(4), 2165-2172.

Mandal, A., & Chakrabarty, D. (2011). Isolation of nanocellulose from waste sugarcane bagasse (SCB) and its characterization. *Carbohydrate Polymers*, *86*(3), 1291-1299.

Mani, S., Tabil, L. G., & Sokhansanj, S. (2004). Grinding performance and physical properties of wheat and barley straws, corn stover and switchgrass. *Biomass and Bioenergy*, *27*(4), 339-352.

Mannan, S., Fakhru'l-Razi, A., & Alam, M. Z. (2007). Optimization of process parameters for the bioconversion of activated sludge by *Penicillium corylophilum*, using response surface methodology. *Journal of Environmental Sciences*, *19*(1), 23-28.

Marett, J., Aning, A., & Foster, E. J. (2017). The isolation of cellulose nanocrystals from pistachio shells via acid hydrolysis. *Industrial Crops and Products*, *109*, 869-874.

Mariano, M., El Kissi, N., & Dufresne, A. (2014). Cellulose nanocrystals and related nanocomposites: Review of some properties and challenges. *Journal of Polymer Science Part B: Polymer Physics*, *52*(12), 791-806.

Martínez-Sanz, M., Lopez-Rubio, A., & Lagaron, J. M. (2011). Optimization of the nanofabrication by acid hydrolysis of bacterial cellulose nanowhiskers. *Carbohydrate Polymers*, *85*(1), 228-236.

Masuko, T., Minami, A., Iwasaki, N., Majima, T., Nishimura, S. I., & Lee, Y. C. (2005). Carbohydrate analysis by a phenol-sulfuric acid method in microplate format. *Analytical Biochemistry*, *339*(1), 69-72.

Magwaza, L. S., & Opara, U. L. (2015). Analytical methods for determination of sugars and sweetness of horticultural products-A review. *Scientia Horticulturae*, *184*, 179-192.

Meena Devi, V. N., Ariharan, V. N., & Nagendra Prasad, P. (2013). Nutritive value and potential uses of *Leucaena leucocephala* as biofuel - A mini review. *Research Journal of Pharmaceutical, Biological and Chemical Sciences*, *4*(1), 515-521.

Mendes, C. A. D. C., Ferreira, N. M. S., Furtado, C. R. G., & de Sousa, A. M. F. (2015). Isolation and characterization of nanocrystalline cellulose from corn husk. *Materials Letters*, *148*, 26-29.

Merci, A., Urbano, A., Grossmann, M. V. E., Tischer, C. a., & Mali, S. (2015). Properties of microcrystalline cellulose extracted from soybean hulls by reactive extrusion. *Food Research International*, *73*, 38-43.

Haafiz, M. K., Eichhorn, S. J., Hassan, A., & Jawaid, M. (2013). Isolation and characterization of microcrystalline cellulose from oil palm biomass residue. *Carbohydrate Polymers*, *93*(2), 628-634.

Mohamad, M., Wei, T. C., Mohammad, R., & Wei, L. J. (2017). Optimization of operating parameters by responsesurface methodology for malachite green dye removal using biochar prepared from eggshell. *Journal of Engineering and Applied Sciences*, *12*(11), 3621-3633.

Mohammadi, R., Mohammadifar, M. A., Mortazavian, A. M., Rouhi, M., Ghasemi, J. B., & Delshadian, Z. (2016). Extraction optimization of pepsin-soluble collagen from eggshell membrane by response surface methodology (RSM). *Food Chemistry*, *190*, 186-193.

Mondal, S. (2017). Preparation, properties and applications of nanocellulosic materials. *Carbohydrate Polymers*, *163*, 301-316.

Mood, S. H., Golfeshan, A. H., Tabatabaei, M., Jouzani, G. S., Najafi, G. H., Gholami, M., & Ardjmand, M. (2013). Lignocellulosic biomass to bioethanol, a comprehensive review with a focus on pretreatment. *Renewable and Sustainable Energy Reviews*, *27*, 77-93.

Morais, J. P. S., Rosa, M. D. F., De Souza Filho, M. D. S. M., Nascimento, L. D., Do Nascimento, D. M., & Cassales, A. R. (2013). Extraction and characterization of nanocellulose structures from raw cotton linter. *Carbohydrate Polymers*, *91*(1), 229-235.

Morales-delaRosa, S., Campos-Martin, J. M., & Fierro, J. L. G. (2012). High glucose yields from the hydrolysis of cellulose dissolved in ionic liquids. *Chemical Engineering Journal*, *181*, 538-541.

Morales-delaRosa, S., Campos-Martin, J. M., & Fierro, J. L. G. (2014). Optimization of the process of chemical hydrolysis of cellulose to glucose. *Cellulose*, *21*(4), 2397-2407.

Mosier, N., Wyman, C., Dale, B., Elander, R., Lee, Y. Y., Holtzapple, M., & Ladisch, M. (2005). Features of promising technologies for pretreatment of lignocellulosic biomass. *Bioresource Technology*, *96*, 673-686.

Mourabet, M., El Rhilassi, A., El Boujaady, H., Bennani-Ziatni, M., El Hamri, R., & Taitai, A. (2015). Removal of fluoride from aqueous solution by adsorption on hydroxyapatite (HAp) using response surface methodology. *Journal of Saudi Chemical Society*, *19*(6), 603-615.

Mu, C., Jiang, M., Zhu, J., Zhao, M., Zhu, S., & Zhou, Z. (2014). Isolation of cellulose from steam-exploded rice straw with aniline catalyzing dimethyl formamide aqueous solution. *Renewable Energy*, *63*, 324-329.

Nazir, M. S., Wahjoedi, B. A., Yussof, A. W., & Abdullah, M. A. (2013). Eco-friendly extraction and characterization of cellulose from oil palm empty fruit bunches. *BioResources*, *8*(2), 2161-2172

Mullen, B. F., & Gutteridge, R. C. (2002). Wood and biomass production of *Leucaena* in subtropical Australia. *Agroforestry Systems*, *55*, 195-205.

Mussatto, S. I., Dragone, G., Guimarães, P. M. R., Paulo, J., Silva, A., Carneiro, L. M., … Teixeira, J. A. (2010). Technological trends , global market , and challenges of bio-ethanol production. *Biotechnology Advances*, *28*(6), 817-830.

Nagar, P. (2014). Bioethanol, Butanol & Biodiesel From Crop Residue. *International Journal of Engineering & Science Research*, *4*(11), 812-819.

Nehdi, I. A., Sbihi, H., Tan, C. P., & Al-Resayes, S. I. (2014). *Leucaena leucocephala* (Lam.) de Wit seed oil: Characterization and uses. *Industrial Crops and Products*, *52*, 582-587.

Neto, W. P. F., Silvério, H. A., Dantas, N. O., & Pasquini, D. (2013). Extraction and characterization of cellulose nanocrystals from agro-industrial residue-soy hulls. *Industrial Crops and Products*, *42*, 480-488.

Ni, J., Wang, H., Chen, Y., She, Z., Na, H., & Zhu, J. (2013). A novel facile two-step method for producing glucose from cellulose. *Bioresource Technology*, *137*, 106-110.

Normaniza, O., Faisal, H. a., & Barakbah, S. S. (2008). Engineering properties of *Leucaena leucocephala* for prevention of slope failure. *Ecological Engineering*, *32*, 215-221.

Nuruddin, M., Chowdhury, A., Haque, S. A., Rahman, M., Farhad, S. F., Jahan, M. S., & Quaiyyum, A. (2011). Extraction and characterization of cellulose microfibrils from agricultural wastes in an integrated biorefinery initiative. *Biomaterials*, *3*, 5-6.

Nwokocha, L. M., & Williams, P. A. (2012). Rheological characterization of the galactomannan from *Leucaena leucocephala* seed. *Carbohydrate Polymers*, *90*(2), 833-838.

Oliveira, F. B. de, Bras, J., Pimenta, M. T. B., Curvelo, A. A. da S., & Belgacem, M. N. (2016). Production of cellulose nanocrystals from sugarcane bagasse fibers and pith. *Industrial Crops and Products*, *93*, 48–57.

Oliveira, L. S., & Franca, A. S. (2009). From solid biowastes to liquid biofuels. *Agricultural Wastes*, 265-290.

Orozco, A., Ahmad, M., Rooney, D., & Walker, G. (2007). Dilute acid hydrolysis of cellulose and cellulosic bio-waste using a microwave reactor system. *Process Safety and Environmental Protection*, *85*, 446-449.

Orozco, R. S., Hernández, P. B., Morales, G. R., Núñez, F. U., Villafuerte, J. O., Lugo, V. L., … Vázquez, P. C. (2014). Characterization of lignocellulosic fruit waste as an alternative feedstock for bioethanol production. *BioResources*, *9*(2), 1873-1885.

Othman, S. H. (2014). Bio-nanocomposite materials for food packaging applications : Types of biopolymer and nano-sized filler. *Italian Oral Surgery*, *2*, 296-303.

Palme, A., Theliander, H., & Brelid, H. (2016). Acid hydrolysis of cellulosic fibres: Comparison of bleached kraft pulp, dissolving pulps and cotton textile cellulose. *Carbohydrate Polymers*, *136*, 1281-1287.

Pandey, V. C., & Kumar, A. (2013). *Leucaena leucocephala*: An underutilized plant for pulp and paper production. *Genetic Resources and Crop Evolution*, *60*, 1165-1171.

Pang, J., Zheng, M., Sun, R., Song, L., Wang, A., Wang, X., & Zhang, T. (2015). Catalytic conversion of cellulosic biomass to ethylene glycol: Effects of inorganic impurities in biomass. *Bioresource Technology*, *175*, 424-429.

Panwal, J. H., Viruthagiri, T., & Baskar, G. (2011). Statistical modeling and optimization of enzymatic milk fat splitting by soybean lecithin using response surface methodology. *International Journal of Nutrition and Metabolism*, *3*, 50-57.

Parawira, W. (2010). Biodiesel production from *Jatropha curcas*: A review. *Scientific Research and Essays*, *5*(14), 1796-1808.

Park, S., Baker, J. O., Himmel, M. E., Parilla, P. A., & Johnson, D. K. (2010). Cellulose crystallinity index: Measurement techniques and their impact on interpreting cellulase performance. *Biotechnology for Biofuels*, *3*(1), 1-10.

Patel, S., Kothari, D., & Goyal, A. (2011). Enhancement of dextransucrase activity of *Pediococcus pentosaceus* mutant SPAm1 by response surface methodology. *Indian Journal of Biotechnology*, *10*(3), 346-351.

Payormhorm, J., Kangvansaichol, K., Reubroycharoen, P., Kuchonthara, P., & Hinchiranan, N. (2013). Pt/Al_2O_3-catalytic deoxygenation for upgrading of *Leucaena leucocephala*-pyrolysis oil. *Bioresource Technology*, *139*, 128-135.

Phaiboonsilpa, N., & Saka, S. (2011). Two-step hydrolysis of Japanese cedar as treated by semi-flow hot-compressed water with acetic acid. *Green Energy and Technology*, *66*, 142-146.

Phanthong, P., Guan, G., Ma, Y., Hao, X., & Abudula, A. (2016). Effect of ball milling on the production of nanocellulose using mild acid hydrolysis method. *Journal of the Taiwan Institute of Chemical Engineers*, *60*, 617-622.

Phisalaphong, M., Srirattana, N., & Tanthapanichakoon, W. (2006). Mathematical modeling to investigate temperature effect on kinetic parameters of ethanol fermentation. *Biochemical Engineering Journal*, *28*(1), 36-43.

Pius, A., Ekebafe, L., Ugbesia, S., & Pius, R. (2014). Modification of adhesive using cellulose micro-fiber (CMF) from melon seed shell. *American Journal of Polymer Science, 4*(4), 101-106.

Poletto, M., Júnior, H., & Zattera, A. (2014). Native cellulose: Structure, characterization and thermal properties. *Materials*, *7*(9), 6105-6119.

Popping, B., & Diaz-Amigo, C. (2014). The probability of obtaining: A correct and representative result in allergen analysis. *Agro Food Industry Hi-Tech, 25*, 421-442.

Prakash Maran, J., & Manikandan, S. (2012). Response surface modeling and optimization of process parameters for aqueous extraction of pigments from prickly pear (*Opuntia ficus-indica*) fruit. *Dyes and Pigments*, *95*(3), 465-472.

Punsuvon, V., Vaithanomsat, P., & Iiyama, K. (2008). Simultaneous production of α-cellulose and furfural from bagasse by steam explosion pretreatment. *Maejo International Journal of Science and Technology*, *2*(1), 182-191.

Qing, Q., Guo, Q., Zhou, L., Gao, X., Lu, X., & Zhang, Y. (2017). Comparison of alkaline and acid pretreatments for enzymatic hydrolysis of soybean hull and soybean straw to produce fermentable sugars. *Industrial Crops and Products*, *109*, 391-397.

Rabemanolontsoa, H., & Saka, S. (2016). Various pretreatments of lignocellulosics. *Bioresource Technology*, *199*, 83-91.

Ragland, K. W., Aerts, D. J., & Baker, A. J. (1991). Properties of wood for combustion analysis. *Bioresource Technology*, *37*, 161-168.

Rahim, N., Li, A. R., Kamarun, D., & Ahmad, M. R. (2017). Isolation and characterization of galactomannan from seed of *Leucaena leucocephala. Polymer Bulletin*, 1-11.

Rahimi Kord Sofla, M., Brown, R. J., Tsuzuki, T., & Rainey, T. J. (2016). A comparison of cellulose nanocrystals and cellulose nanofibres extracted from bagasse using acid and ball milling methods. *Advances in Natural Sciences: Nanoscience and Nanotechnology*, *7*(3), 1-9.

Rambabu, N., Panthapulakkal, S., Sain, M., & Dalai, A. K. (2016). Production of nanocellulose fibers from pinecone biomass: Evaluation and optimization of chemical and mechanical treatment conditions on mechanical properties of nanocellulose films. *Industrial Crops and Products*, *83*, 746-754.

Reales-Alfaro, J. G., Trujillo-Daza, L. T., Arzuaga-Lindado, G., Castaño-Peláez, H. I., & Polo-Córdoba, Á. D. (2013). Acid hydrolysis of water hyacinth to obtain fermentable sugars. *CT&F - Ciencia, Tecnologia y Futuro*, *5*(2), 101-112.

Reddy, J. P., & Rhim, J. (2014). Isolation and characterization of cellulose nanocrystals from garlic skin. *Materials Letters*, 3-6.

Ritter, G. J. (1929). Determination of alpha-cellulose. *Industrial & Engineering Chemistry Analytical Edition*, *1*(1), 52-54.

Roman, M., & Winter, W. T. (2004). Effect of sulfate groups from sulfuric acid hydrolysis on the thermal degradation behavior of bacterial cellulose. *Biomacromolecules*, *5*(5), 1671-1677.

Rosa, M. F., Medeiros, E. S., Malmonge, J. A., Gregorski, K. S., Wood, D. F., Mattoso, L. H. C., … Imam, S. H. (2010). Cellulose nanowhiskers from coconut husk fibers: Effect of preparation conditions on their thermal and morphological behavior. *Carbohydrate Polymers*, *81*(1), 83-92.

Rosa, S. M. L., Rehman, N., De Miranda, M. I. G., Nachtigall, S. M. B., & Bica, C. I. D. (2012). Chlorine-free extraction of cellulose from rice husk and whisker isolation. *Carbohydrate Polymers*, *87*(2), 1131-1138.

Santos, C. C., de Souza, W., Sant Anna, C., & Brienzo, M. (2018). Elephant grass leaves have lower recalcitrance to acid pretreatment than stems, with higher potential for ethanol production. *Industrial Crops and Products*, *111*, 193-200.

Sasaki, C., Sumimoto, K., Asada, C., & Nakamura, Y. (2012). Direct hydrolysis of cellulose to glucose using ultra-high temperature and pressure steam explosion. *Carbohydrate Polymers*, *89*(1), 298-301.

Sasikumar, E., & Viruthagiri, T. (2008). Optimization of process conditions using response surface methodology (RSM) for ethanol production from pretreated sugarcane bagasse: Kinetics and modeling. *BioEnergy Research*, *1*(3-4), 239-247.

Shokoohi, S., Tsigounis, K., Urmaza, L. M., & Perez, A. Z. (2016). The effect of stress due to sodium chloride exposure on the growth of *Saccharomyces cerevisiae*. *The Expedition*, *5*.

Saxena, R. C., Adhikari, D. K., & Goyal, H. B. (2009). Biomass-based energy fuel through biochemical routes: A review. *Renewable and Sustainable Energy Reviews*, *13*(1), 167-178.

Segal, L., Creely, J. J., Martin, A. E., & Conrad, C. M. (1959). An empirical method for estimating the degree of crystallinity of native cellulose using the x-ray diffractometer. *Textile Research Journal*, *29*(10), 786-794.

Seok, J., Lee, Y. Y., & Hyun, T. (2016). A review on alkaline pretreatment technology for bioconversion of lignocellulosic biomass. *Bioresource Technology*, *199*, 42-48.

Sethi, P., & Kulkarni, P. R. (1994). Chemical composition of *Leucaena leucocephala* seeds. *International Journal of Food Sciences and Nutrition*, *45*(1), 5-13.

Shah, N., Ul-Islam, M., Khattak, W. A., & Park, J. K. (2013). Overview of bacterial cellulose composites: A multipurpose advanced material. *Carbohydrate Polymers*, *98*(2), 1585-1598.

Shankar, S., & Rhim, J.-W. (2016). Preparation of nanocellulose from micro-crystalline cellulose: The effect on the performance and properties of agar-based composite films. *Carbohydrate Polymers*, *135*, 18-26.

Sharma, N., Kalra, K. L., Oberoi, H. S., & Bansal, S. (2007). Optimization of fermentation parameters for production of ethanol from kinnow waste and banana peels by simultaneous saccharification and fermentation. *Indian Journal of Microbiology*, *47*(4), 310-316.

Shin, H. K., Pyo Jeun, J., Bin Kim, H., & Hyun Kang, P. (2012). Isolation of cellulose fibers from kenaf using electron beam. *Radiation Physics and Chemistry*, *81*(8), 936-940.

Shirajuddin, S., Kamarun, D., Ismail, N. E., Abdul Wahab, M. S., Li, A. R., & Rahim, N. (2015). Extraction and characterization of galactomannan from seeds of *Leucaena leucocephala*. *Advanced Materials Research*, *1134*, 213-219.

Sindhu, R., Gnansounou, E., Binod, P., & Pandey, A. (2016). Bioconversion of sugarcane crop residue for value added products - An overview. *Renewable Energy*, *98*, 203-215.

Singh, M. K., Singh, J., Kumar, M., & Thakur, I. S. (2014). Novel lipase from *basidiomycetes Schizophyllum commune* ISTL04, produced by solid state fermentation of *Leucaena leucocephala* seeds. *Journal of Molecular Catalysis B: Enzymatic*, *110*, 92-99.

Singh, S., Kundu, S. S., Negi, A. S., Gupta, S. K., Singh, N. P., & Pachouri, V. C. (2002). *Leucaena* seeds as protein supplement in the rations of growing sheep. *Asian-Australasian Journal of Animal Sciences*, *15*(10), 1433-1438.

Siqueira, G., Abdillahi, H., Bras, J., & Dufresne, A. (2010). High reinforcing capability cellulose nanocrystals extracted from *Syngonanthus nitens* (Capim Dourado). *Cellulose*, *17*(2), 289-298.

Siqueira, G., Várnai, A., Ferraz, A., & Milagres, A. M. F. (2013). Enhancement of cellulose hydrolysis in sugarcane bagasse by the selective removal of lignin with sodium chlorite. *Applied Energy*, *102*, 399-402.

Skiba, E. A., Budaeva, V. V., Baibakova, O. V., Zolotukhin, V. N., & Sakovich, G. V. (2017). Dilute nitric-acid pretreatment of oat hulls for ethanol production. *Biochemical Engineering Journal*, *126*, 118-125.

Smyth, M., García, A., Rader, C., Foster, E. J., & Bras, J. (2017). Extraction and process analysis of high aspect ratio cellulose nanocrystals from corn (*Zea mays*) agricultural residue. *Industrial Crops and Products*, *108*, 257–266.

Soom, R. M., Aziz, A. A., Hassan, W. H. W., & Top, A. G. (2009). Solid-state characteristics of microcrystalline cellulose from oil palm empty fruit bunch fibre. *Journal of Oil Palm Research*, *21*, 613-620.

Sudamalla, P., Saravanan, P., & Matheswaran, M. (2012). Optimization of operating parameters using response surface methodology for adsorption of crystal violet by activated carbon prepared from mango kernel. *Sustainable Environmental Research*, *22*(1), 1-7.

Sudiyani, Y. (2009). Utilization of biomass waste empty fruit bunch fiber of palm oil for two sides of the same coin : Energy and environment. *Research Workshop on Sustainable Biofuel*, 4-5.

Sun, B., Peng, G., Duan, L., Xu, A., & Li, X. (2015). Pretreatment by NaOH swelling and then HCl regeneration to enhance the acid hydrolysis of cellulose to glucose. *Bioresource Technology*, *196*, 454-458.

Sun, J. X., Sun, X. F., Zhao, H., & Sun, R. C. (2004). Isolation and characterization of cellulose from sugarcane bagasse. *Polymer Degradation and Stability*, *84*(2), 331-339.

Sun, J. X., Xu, F., Sun, X. F., Xiao, B., & Sun, R. C. (2005). Physico-chemical and thermal characterization of cellulose from barley straw. *Polymer Degradation and Stability*, *88*(3), 521-531.

Sun, N., Liu, H., Sathitsuksanoh, N., Stavila, V., Sawant, M., Bonito, A., … Holmes, B. M. (2013). Production and extraction of sugars from switchgrass hydrolyzed in ionic liquids. *Biotechnology for Biofuels*, *6*(1), 39.

Sun, S., Sun, S., Cao, X., & Sun, R. (2016). The role of pretreatment in improving the enzymatic hydrolysis of lignocellulosic materials. *Bioresource Technology*, *199*, 49-58.

Sun, X. F., Sun, R. C., Su, Y., & Sun, J. X. (2004). Comparative study of crude and purified cellulose from wheat straw. *Journal of Agricultural and Food Chemistry*, *52*(4), 839-847.

Sun, Y., & Cheng, J. (2002). Hydrolysis of lignocellulosic materials for ethanol production: A review. *Bioresource Technology*, *83*, 1-11.

Taherzadeh, M. J., & Karimi, K. (2008). Pretreatment of lignocellulosic wastes to improve ethanol and biogas production: A review. *International Journal of Molecular Sciences, 9*(9), 1621-1651.

Taherzadeh, M. J., & Karimi, K. (2015). Acid-based hydrolysis processes for ethanol from lignocellulosic materials: A review. *Bioresources*, *2*, 472-499.

Tesfaw, A., & Assefa, F. (2014). Current trends in bioethanol production by *Saccharomyces cerevisiae*: substrate, inhibitor reduction, growth variables, coculture, and immobilization. *International Scholarly Research Notices*, 1-11.

Thakur, V. K., Thakur, M. K., & Gupta, R. K. (2014). Review: Raw natural fiber-based polymer composites. *International Journal of Polymer Analysis and Characterization*, *19*(3), 256-271.

Thiagarajan, J., Srividhya, P. K., & Rajasakeran, E. (2013). A review of thermo-chemical energy conversion process of non-edible seed cakes. *Journal of Energy Bioscience*, *4*(2), 7-15.

Thiripura Sundari, M., & Ramesh, A. (2012). Isolation and characterization of cellulose nanofibers from the aquatic weed water hyacinth - *Eichhornia crassipes. Carbohydrate Polymers*, *87*(2), 1701-1705.

Thoorens, G., Krier, F., Leclercq, B., Carlin, B., & Evrard, B. (2014). Microcrystalline cellulose, a direct compression binder in a quality by design environment-A review. *International Journal of Pharmaceutics*, *473*(1-2), 64-72.

Tibolla, H., Pelissari, F. M., & Menegalli, F. C. (2014). Cellulose nanofibers produced from banana peel by chemical and enzymatic treatment. *LWT - Food Science and Technology*, *59*(2P2), 1311-1318.

Tibolla, H., Pelissari, F. M., Rodrigues, M. I., & Menegalli, F. C. (2017). Cellulose nanofibers produced from banana peel by enzymatic treatment: Study of process conditions. *Industrial Crops and Products*, *95*, 664-674.

Torget, R. W., Kim, J. S., & Lee, Y. Y. (2000). Fundamental aspects of dilute acid hydrolysis/fractionation kinetics of hardwood carbohydrates: Cellulose hydrolysis. *Industrial and Engineering Chemistry Research*, *39*(8), 2817-2825.

Trache, D., Donnot, A., Khimeche, K., Benelmir, R., & Brosse, N. (2014). Physico-chemical properties and thermal stability of microcrystalline cellulose isolated from alfa fibres. *Carbohydrate Polymers*, *104*(1), 223-230.

Trache, D., Hussin, M. H., Hui Chuin, C. T., Sabar, S., Fazita, M. R. N., Taiwo, O. F. A., … Haafiz, M. K. M. (2016). Microcrystalline cellulose: Isolation, characterization and bio-composites application - A review. *International Journal of Biological Macromolecules*, *93*, 789-804.

Turhan, I., Bialka, K. L., Demirci, A., & Karhan, M. (2010). Ethanol production from carob extract by using *Saccharomyces cerevisiae*. *Bioresource Technology*, *101*(14), 5290-5296.

Uesu, N. Y., Pineda, E. a G., & Hechenleitner, a. a W. (2000). Microcrystalline cellulose from soybean husk: Effects of solvent treatments on its properties as acetylsalicylic acid carrier. *International Journal of Pharmaceutics*, *206*(1-2), 85-96.

Uncu, O. N., & Cekmecelioglu, D. (2011). Cost-effective approach to ethanol production and optimization by response surface methodology. *Waste Management*, *31*(4), 636-643.

Vasconcelos, N. F., Feitosa, J. P. A., da Gama, F. M. P., Morais, J. P. S., Andrade, F. K., de Souza Filho, M. de S. M., & Rosa, M. de F. (2017). Bacterial cellulose nanocrystals produced under different hydrolysis conditions: Properties and morphological features. *Carbohydrate Polymers*, *155*, 425-431.

Vassilev, S. V., Baxter, D., Andersen, L. K., & Vassileva, C. G. (2010). An overview of the chemical composition of biomass. *Fuel*, *89*(5), 913-933.

Verma, P. R. P., & Razdan, B. (2002). Studies on *Leucaena leucocephala* seed gum : Rheological properties. *Jurnal of Scientific & Industrial Research*, *61*, 437-443.

Wahab, R., Mustafa, M. T., Sudin, M., Mohamed, A., Rahman, S., Samsi, H. W., & Khalid, I. (2013). Extractives, holocellulose, α-cellulose, lignin and ash contents in cultivated tropical bamboo *Gigantochloa brang*, *G. levis*, *G. scortechinii* and *G. wrayi*. *Current Research Journal of Biological Sciences*, *5*(6), 266-272.

Wang, D., Shang, S. Bin, Song, Z. Q., & Lee, M. K. (2010). Evaluation of microcrystalline cellulose prepared from kenaf fibers. *Journal of Industrial and Engineering Chemistry*, *16*(1), 152-156.

Wang, R. Ã., Ji, Y., Melikoglu, M., Koutinas, A., & Webb, C. (2006). Optimization of innovative ethanol production from wheat by response surface methodology. *Process Safety and Environmental Protection, 85*, 404-412.

Wang, Y., Song, H., Peng, L., Zhang, Q., & Yao, S. (2014). Recent developments in the catalytic conversion of cellulose. *Biotechnology & Biotechnological Equipment*, *28*(6), 981-988.

Wang, Z., Yao, Z. J., Zhou, J., & Zhang, Y. (2017). Reuse of waste cotton cloth for the extraction of cellulose nanocrystals. *Carbohydrate Polymers*, *157*, 945-952.

Watkins, D., Nuruddin, M., Hosur, M., Tcherbi-Narteh, A., & Jeelani, S. (2015). Extraction and characterization of lignin from different biomass resources. *Journal of Materials Research and Technology*, *4*(1), 26-32.

Wijaya, Y. P., Putra, R. D. D., Widyaya, V. T., Ha, J. M., Suh, D. J., & Kim, C. S. (2014). Comparative study on two-step concentrated acid hydrolysis for the extraction of sugars from lignocellulosic biomass. *Bioresource Technology*, *164*, 221-231.

Wise, L. E., Murphy, M. & D'addieco, A. A. (1946). Chlorite holocellulose: Its fractionation and bearing on summative wood analysis and on studies on the hemicelluloses. *Paper Trade Journal*, *122*(2), 35-43.

Wyman, C. E., Spindler, D. D., & Grohmann, K. (1992). Simultaneous saccharification and fermentation of several lignocellulosic feedstocks to fuel ethanol. *Biomass and Bioenergy*, *3*(5), 301-307.

Xiang, L. Y., Mohammed, M. A., & Samsu Baharuddin, A. (2016). Characterisation of microcrystalline cellulose from oil palm fibres for food applications. *Carbohydrate Polymers*, *148*, 11-20.

Xie, J., Hse, C. Y., De Hoop, C. F., Hu, T., Qi, J., & Shupe, T. F. (2016). Isolation and characterization of cellulose nanofibers from bamboo using microwave liquefaction combined with chemical treatment and ultrasonication. *Carbohydrate Polymers*, *151*, 725-734.

Xiros, C., Topakas, E., & Christakopoulos, P. (2013). Hydrolysis and fermentation for cellulosic ethanol production. *Wiley Interdisciplinary Reviews: Energy and Environment*, *2*(6), 633-654.

Xu, J., Cheng, J. J., Sharma-shivappa, R. R., & Burns, J. C. (2010). Lime pretreatment of switchgrass at mild temperatures for ethanol production. *Bioresource Technology*, *101*(8), 2900-2903.

Yang, H., Yan, R., Chen, H., Lee, D. H., & Zheng, C. (2007). Characteristics of hemicellulose, cellulose and lignin pyrolysis. *Fuel*, *86*, 1781-1788.

Yang, H., Yan, R., Chen, H., Zheng, C., Lee, D. H., & Liang, D. T. (2006). In-depth investigation of biomass pyrolysis based on three major components: Hemicelluloses, cellulose and lignin. *Energy and Fuels*, *20*(17), 388-393.

Yeung, P. K. K., Wong, F. T. W., & Wong, J. T. Y. (2002). Mimosine, the allelochemical from the leguminous tree *Leucaena leucocephala,* selectively enhances cell proliferation in dinoflagellates. *Applied and Environmental Microbiology*, *68*(10), 5160-5163.

Yoon, S. Y., Han, S. H., & Shin, S. J. (2014). The effect of hemicelluloses and lignin on acid hydrolysis of cellulose. *Energy*, *77*, 19-24.

Zabed, H., Sahu, J. N., Suely, A., Boyce, A. N., & Faruq, G. (2017). Bioethanol production from renewable sources : Current perspectives and technological progress. *Renewable and Sustainable Energy Reviews*, *71*, 475-501.

Zayed, M. Z., Sallam, S. M. A., & Shetta, N. D. (2018). Review article on *Leucaena leucocephala* as one of the miracle timber trees. *International Journal of Pharmacy and Pharmaceutical Sciences*, *10*(1), 1-7.

Zhang, L. hui, Li, D., Wang, L. jun, Wang, T. peng, Zhang, L., Chen, X. D., & Mao, Z. huai. (2008). Effect of steam explosion on biodegradation of lignin in wheat straw. *Bioresource Technology*, *99*(17), 8512-8515.

Zhao, H., Kwak, J. H., Conrad Zhang, Z., Brown, H. M., Arey, B. W., & Holladay, J. E. (2007). Studying cellulose fiber structure by SEM, XRD, NMR and acid hydrolysis. *Carbohydrate Polymers*, *68*(2), 235-241.

Zhao, H., Kwak, J. H., Wang, Y., Franz, J. A., White, J. M., & Holladay, J. E. (2005). Effects of crystallinity on dilute acid hydrolysis of cellulose by cellulose ball-milling. *Energy Fuels*, *20*(2), 807-811.

Zhu, S., Wu, Y., Yu, Z., Liao, J., & Zhang, Y. (2005). Pretreatment by microwave/alkali of rice straw and its enzymic hydrolysis. *Process Biochemistry*, *40*, 3082-3086.

Zhuo, K., Du, Q., Bai, G., Wang, C., Chen, Y., & Wang, J. (2015). Hydrolysis of cellulose catalyzed by novel acidic ionic liquids. *Carbohydrate Polymers*, *115*, 49-53.

LIST OF PUBLICATIONS AND PAPER PRESENTED

Published articles/publications:

Husin, M., Rahim, N., Ahmad, M.R., Romli, A.Z., & Ilham, Z. (2019). Hydrolysis of microcrystalline cellulose isolated from waste seeds of *Leucaena leucocephala* for glucose production. *Malaysian Journal of Fundamental and Applied Sciences*, *15*(2), 200-205.

Husin, M., Li, A.R., Ramli, N., Romli, A.Z., Hakimi, M.I., & Ilham, Z. (2017). Preparation and characterization of cellulose and microcrystalline cellulose isolated from waste *Leucaena leucocephala* seeds. *International Journal of Advanced and Applied Sciences*, *4*(3), 51-58.

Presentation:

Husin, M., Man, S., Ayob, M.K.M, & Ilham, Z. (2016). Effect of boiling reaction time on the FTIR pattern of cellulose isolated from energy biomass *Leucaena leuocochephala* seeds. *International Sustainable Technology, Energy & Civilization Conference – ISTECC 2016* (2nd Kyoto University South East Asian Forum), 13 February 2016. Puri Pujangga Hotel, Bangi.